

Investigation of the electrical characteristics of  
GaAsP light-emitting diodes (LED's) under conditions  
of mechanical stress

A Thesis submitted for the degree of Doctor of Philosophy

by

Arthur Max Lea

Department of Physics, Brunel University

July 1986

**BEST COPY**

**AVAILABLE**

Poor text in the original  
thesis.

## ACKNOWLEDGEMENTS

I wish to express my thanks to my employers, the Inner London Education Authority, for the generous research facilities, including relaxation time from my teaching duties, which have been afforded to me at South London College (formerly Norwood Technical College); to them and to the Governors, the former Principal and my colleagues, all of whom have in different ways given me their warmest support, I am deeply grateful. In particular I would like to single out for special mention Dr J. Ballard, formerly Vice Principal of South London College, and Mr E. Begg, the present Vice Principal, for their help and encouragement.

Finally, my deepest gratitude is to my Supervisor, Dr W. Fulop, of the Department of Physics, Brunel University, for having suggested the research topic in the first place and for his patient help and advice over many years.

Physical Sciences Department,

South London College.

## ABSTRACT

The main line pursued is the mechanical stressing of light-emitting diodes (LED's) by pressing on the surface with spherically rounded sapphire probes ranging from 100  $\mu\text{m}$  to 500  $\mu\text{m}$  radius of curvature and with forces up to 50 grams weight on the largest probe, care being taken not to exceed the elastic limit of the material, which is estimated to be about  $1.4 \times 10^9$  pascals (14,000 atmospheres) at the central bottom point of the probe. With the diode under forward bias a very wide range of current is covered - from 10 mA to about 100  $\mu\text{A}$  in the light-emitting region and from 100  $\mu\text{A}$  to 100 nA in the generation/recombination region - and across the whole range a small decrease in current of about 1 per cent or less is observed.

The classical theory of the distribution of stress by a spherical probe has been investigated by a modern computer technique, and by integration of the stress over the whole of the junction interface it is shown that the decrease in

current can be ascribed to the increase in band gap of the semiconductor that is brought about by the axial component of pressure stress at right angles to the interface.

With the larger currents in the light-emitting region a further decrease in current of the order of 1 per cent or less can be ascribed to heat conduction from the warm surface of the diode to the probe, thereby lowering the temperature of the interface. Finally, the electrical characteristics of the diode under reverse bias have been investigated, with incident light playing an important role; in the absence of light the extremely small currents ( $10^{-12}$  to  $10^{-10}$  amp) are consistent with thermal generation of carriers similar to the generation/recombination mechanism for very low currents in the forward direction.

---

## CONTENTS

	pages
ACKNOWLEDGEMENTS	—
ABSTRACT	—
1 INTRODUCTION	1-5
2 REVIEW OF THE PRESENT RESEARCH	6-14
3 DIODE UNDER REVERSE BIAS	15-26
(a) Capacitance Measurements	15-17
(b) Electrical Characteristics and the Effect of Light	17-21
(c) Current-Voltage Characteristics	21-26
4 DIODE UNDER FORWARD BIAS	27-33
(a) Current-Voltage Characteristics	27-30
(b) d.c. and a.c. Resisance	31-33
5 STRESS UNDER A PROBE OF SPHERICAL SURFACE	34-45
(a) Simple Theory of Stress	34-37
(b) Estimate of Elastic Limit	37-42
(c) Depth of Junction Interface	42-44
(d) Variation of Stress with Depth	44-45
6 ELECTRICAL MEASUREMENTS	46-58
(a) Preliminary Investigations	46-53
(b) Electrical Changes under Varying Stress	53-58
7 DISTRIBUTION OF STRESS OVER JUNCTION INTERFACE	59-88
(a) Advanced Theory of Stress	59-69
(b) Spectral Shift Experiment of Dr S Konidaris	70-77
(c) Effect of Pressure on Diode Current	77-84
(d) Effect of the Uniaxial Stress Component $p_z$	84-88

	pages
8 TEMPERATURE EFFECT	89-105
(a) Theoretical Temperature Coefficient	89-91
(b) Measurement of Temperature Coefficient	91-93
(c) Estimate of Working Temperature	93-96
(d) Heat Flow Hypothesis	97-105
9 FINAL EXPERIMENTAL STAGES	106-121
(a) Re-assessment of Early Measurements	106-113
(b) Further Electrical Measurements under Stress	113-121
10 REVIEW OF PAST WORK	122-131
11 CONCLUSION	132-138
<hr/>	
APPENDIX A: Method of Applying Stress	139-151
APPENDIX B: Current-Voltage Characteristics of the Diode	152-153
APPENDIX C: Change of Characteristics with Stress	154-157
APPENDIX D: Change of Characteristics with Temperature	158-161
APPENDIX E: Circuitry and Galvanometer Deflection	162-169
REFERENCES	170-172

---

## 1 INTRODUCTION

This research topic was first suggested in 1976 by Dr. W. Fulop, of the Department of Physics, Brunel University, as a continuation of previous work done under his supervision at Brunel by Dr. S. Konidaris, one of the main features of this latter research being summed up in a paper by Fulop and Konidaris entitled "The influence of anisotropic stress on the electrical characteristics of GaAs<sub>1-x</sub>P<sub>x</sub> diodes" <sup>(1)</sup>, x being about 0.4. In this work Konidaris used an extremely sharp diamond probe with a radius of curvature at the tip of 25  $\mu\text{m}$  (he also used 12.5  $\mu\text{m}$ ) and pressed it onto the centre of a light-emitting diode (LED) with forces ranging from 1 to 10 grams. The choice of such a fine probe would seem to be based on previous investigations of a similar nature that had been done in the United States <sup>(2,3,4)</sup> and in Japan <sup>(5,6)</sup> on silicon and germanium diodes, and with a force of 10 grams such a probe enabled enormously high pressures of about  $6 \times 10^9$  pascals ( $6 \times 10^{10}$  dynes  $\text{cm}^{-2}$  or 60,000 atmospheres) to be exerted in a very localised region at



the centre of contact on the diode surface. A stress as great as this certainly exceeded the elastic limit of the materials involved, and tiny spots of permanent damage were observed by all the workers involved in their experiments.

The research by Konidaris with a 25  $\mu\text{m}$  diamond probe showed that within a range of current from 5 nA to about 10  $\mu\text{A}$ , ie in the generation-recombination (GR) region of the diode where there is current but no light, there was a stress-induced increase in current that was dependent exponentially on force, but that in the light-emitting (LE) region up to a maximum working current of about 10 mA there was no effect. Obviously the use of a very fine probe involved a distribution of stress which was highly anisotropic in that the stress would diminish very rapidly with radial distance from the point of contact, and the hypothesis advanced<sup>(1)</sup> for explaining the observed effects is very much bound up in this anisotropy.

At the same time, Konidaris did some further work with a glass probe of large radius (1.2 mm) and a force of 300

grams, and though he was unable to detect any change of current, either in the GR or in the LE region, he was successful in measuring a small spectral shift in the emitted light<sup>(7)</sup>, his technique involving the ingenious feature that a glass probe enabled him to collect the light which was given off from the diode surface that was under stress. In this case, despite the large force, the shallow curvature of the probe ensured that the stress was not highly anisotropic in that the pressure distribution gently decreased with distance from the centre of contact and could be considered to be uniaxial; also, with such curvature the stress was somewhat below the elastic limit of the material so that no damage was expected, nor was seen, to be done to the diode.

The choice by Fulop and Konidaris of a GaAs/P diode was interesting for two reasons: first, it enabled the permanent damage to be easily seen as very small "black spots" where the LED no longer emitted light; and secondly, by the early years of the 1970 decade red-emitting LEDs were being manufactured in very large

quantities mainly for the rapidly expanding market of pocket calculators. Subsequently, of course, such calculators have tended to use liquid crystal displays, but it is still true that LEDs are very widely used in industry (eg for instrument panel displays) and any information on their behaviour could have a significant impact on their manufacture and use. Thus a thorough investigation of the stress effect might have a 'spin off' in that a device such as a transducer might emerge; such hopes for a viable transducer have been expressed by C. A. Hogarth as far back as 1970 in connection with research on heterojunctions<sup>(8)</sup>.

Thus in 1976 the stage was set for the line of enquiry presented in this thesis. Three prominent features stood out:-

(i) Only two sizes of probe had been used on GaAs/P diodes, namely 25  $\mu\text{m}$  (ignoring the 12.5  $\mu\text{m}$ ) and 1.2 mm radius, and consequently the range of stress was sharply contrasted between extremely high anisotropic values and a lower uniaxial one.

(ii) There were two regions of the LED to be explored under forward bias, the LE and GR respectively, and in addition there was plenty of scope for filling in with a wide variety of probes and forces, preferably arranged so that the maximum pressure never exceeded the elastic limit since all the workers agreed that it was the non-damaging stress which was presumed to account for the various effects observed.

(iii) The range of currents to be investigated in the device was fairly wide - at least four orders of magnitude from 10 mA to 1  $\mu$ A and possibly further.

## 2 REVIEW OF THE PRESENT RESEARCH

At the outset it was agreed by Brunel University that the present research could be done on a part-time basis at South London College (formerly Norwood Technical College), a college of further education of the Inner London Education Authority, where the author is a full-time member of the teaching staff. The resources for fundamental research at South London College are extremely limited in that very little money is available for purchasing equipment outside the educational range, and the few technicians available are employed for general-purpose duties so that they are not expected to have specialized skills and do not have any sophisticated workshops. Despite this, it was envisaged that elaborate facilities would not be necessary and that the research could be undertaken provided that accommodation was available; in this latter respect the College was able to supply generous bench space in a large room that was used only by the physics staff (for the development of teaching aids and the preparation of examination

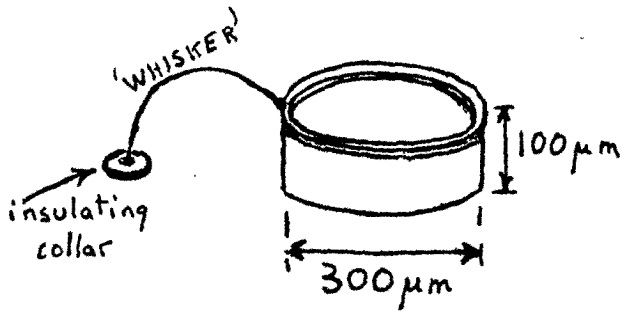


Fig.1

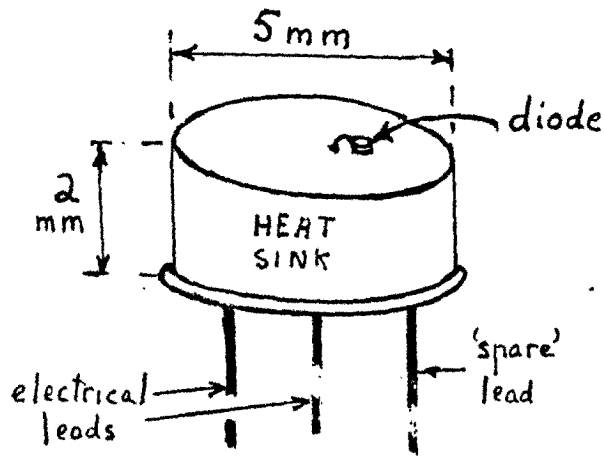


Fig.2

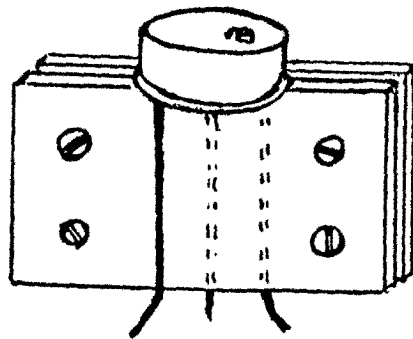


Fig.3

practicals etc.).

In the first instance fresh diodes had to be obtained, since the previous batch had nearly all been used up. These were of a special experimental pattern, with an exposed top surface, and were kindly supplied early in 1977 by Standard Telecommunication Laboratories Ltd., of Harlow, Essex; they were of the same type as had been used by Konidaris, who has given a fairly detailed account of their manufacture<sup>(1,7)</sup>. The main features of the diodes are shown in Figs 1 and 2, from which it can be seen that they were comparatively small, being about 300  $\mu\text{m}$  (or 0.3 mm) in diameter and 100  $\mu\text{m}$  deep, with a narrow aluminium ring around the rim (Fig. 1); the junction interface lay at a very shallow depth, about 1.3  $\mu\text{m}$  below the top surface. Each diode was mounted on a heat sink consisting of an alloy cap about 5 mm in diameter and 2 mm deep with three stout leads fixed into the base of the cap (Fig. 2). Only two of the leads were in electrical operation; the third one was a dummy but nevertheless proved to be useful for mechanically holding the diode

(Fig. 3).

Early on in the research, before work on stressing the diodes was properly under way, the electrical characteristics of the diodes under reverse bias were investigated. Capacitance measurements enabled the band gap of the GaAs/P material to be determined, and excellent agreement was obtained with the value determined by Konidaris in connection with his spectroscopic work<sup>(7)</sup>. At the same time the reverse bias current - voltage characteristics under varying conditions of ambient light were investigated and some interesting (though not unexpected) conclusions were reached. However, in the absence of light the results were substantially different from similar experiments performed by Konidaris with his earlier batch of diodes<sup>(9)</sup>, and various suggestions are advanced to account for this.

Simultaneously with the ordering of the LEDs diamond probes of 25, 50 and 75  $\mu\text{m}$  radius were bought<sup>(10)</sup>, but later on it was found that this range was far too limited and that probes of much greater radius would be necessary.



At this stage (early in 1979) it was realized that large diamond probes would be too expensive, and so a change was made to sapphire which, although less hard than diamond, has proved to be a very successful material. Six sapphire probes were bought<sup>(10)</sup> covering a range from 100 to 1000  $\mu\text{m}$  (or 1 mm) thus almost matching in size with the glass probe of 1.2 mm as used by Konidaris.

In parallel with these activities, a fairly elaborate structure (made of the toy construction material "Meccano"), with suitable viewing by two low-power microscopes, was designed and built so that a diode could be held in place and stressed with an accurately positioned probe under a wide range of forces from 0.001 to more than 100 grams, if necessary. At the same time, because the stresses were deliberately kept low, it became apparent that a Wheatstone bridge network would be necessary for observing the very small electrical changes of 1 per cent or less that were involved; this was done by measurement of the out-of-balance current across the bridge galvanometer. After preliminary readings had been

made with the most sensitive galvanometer available in South London College, it was eventually necessary to buy in a very expensive special one, a "Levell" meter, Type TM 9BP (see Section 3(c), p.21, for description), so that measurements down to a few picoamps could be made.

All this took a number of years and it was not until about 1980 that a pattern of results emerged which proved to be difficult to reconcile with the findings of previous workers, particularly since the current change under stress always proved to be a decrease and not an increase. A considerable amount of time was spent investigating the theory of elastic deformation under stress by a spherically tipped probe, a theory which was originated by the famous Heinrich Hertz in 1881. By means of a modern computer program it was possible to calculate the stress below the surface in the region of the junction interface, and the results are interesting in that they do not seem to have been calculated in this way before and represent original research; however they do not supply a complete explanation for the electrical changes that were observed

under varying stress.

A further stumbling block arose in that during the first few years of the research the conventional reading of the well-known journals and abstracts revealed very few references which were of much relevance. In recent years it has been possible to extend the literature search much more thoroughly over a wide range by means of the computer facilities that are available in the Brunel University Library, namely a search by DIALOG Information Services, Inc, through the files of "INSPEC Database". A number of papers have been discovered which have some bearing on the research undertaken by the author; most of these papers are by workers in overseas countries. In general it is probably true to say that the imposition of stress on a diode by means of a loaded probe has not been pursued by any other worker since the time of Konidaris and his predecessors in the United States and Japan.

In the research outlined in this thesis one of the conclusions is that the imposition of pressure by a loaded probe widens the band gap of GaAs/P and thus shortens the

wavelength of the emitted light in the LE region; this theory has already been considered at length by the previous workers (1-7) and for the most part they discount it. Nevertheless in this research it is reckoned to be valid and mainly explains the experimental observations. This does not necessarily conflict with the results of the previous workers since they all used very fine probes of radius  $25 \mu\text{m}$  (and less) so that, as has already been stated, the pressure distribution was highly anisotropic. In particular, Fulop and Konidaris<sup>(1)</sup> have advanced the theory that in their experiments the pressure causes elastic energy  $E(r)$  to be stored up,  $r$  being the radial distance from the central point of contact of the probe, and that the controlling parameter is the gradient  $dE/dr$ . Thus effectively the increase in current that was observed by Konidaris (in the GR but none in the LE region) can be ascribed to the pressure gradient  $dp/dr$  rather than the pressure  $p$ .

However, when Konidaris performed a spectroscopic experiment with a glass probe of very broad curvature<sup>(7)</sup>

his results were different; no current change was observed, but the small decrease in wavelength of the emitted light that he measured was explained as being directly due to the increase in band gap brought about by pressure  $p$ . This ties in well with another experiment by Share<sup>(11)</sup> who, shortly after Konidaris, reported the results of similar work in which uniaxial stress was applied across the whole surface of an LED by means of a heavily loaded anvil; a decrease in wavelength was obtained which for the most part was ascribed to an increase of band gap with pressure. Share also observed a marked decrease in current (in the LE region), an effect which would be expected if the band gap were to be widened; this is significant in that it differs from the experiments of previous workers using fine probes, but is in accordance with the present research which has been mainly conducted with probes of broad curvature.

Nevertheless the present research indicates that some other effect must also be bringing about a decrease in current, and this shows up markedly when the forces on the

probe are very low. In order to account for this a theory is proposed whereby heat conduction from the diode to the probe also plays a role, particularly in the LE region where the current is producing a significant rise in the temperature of the diode. Thus the final outcome of the present research is not one that had been anticipated at the onset, and as regards the feasibility of designing a transducer that is largely independent of the temperature the outlook is not promising.

The above is a summary of how the research has developed over the years. The subsequent sections will deal with individual aspects of the work and do not necessarily follow a strict chronological sequence, although in general the pattern is the one along which the various lines of research were pursued.

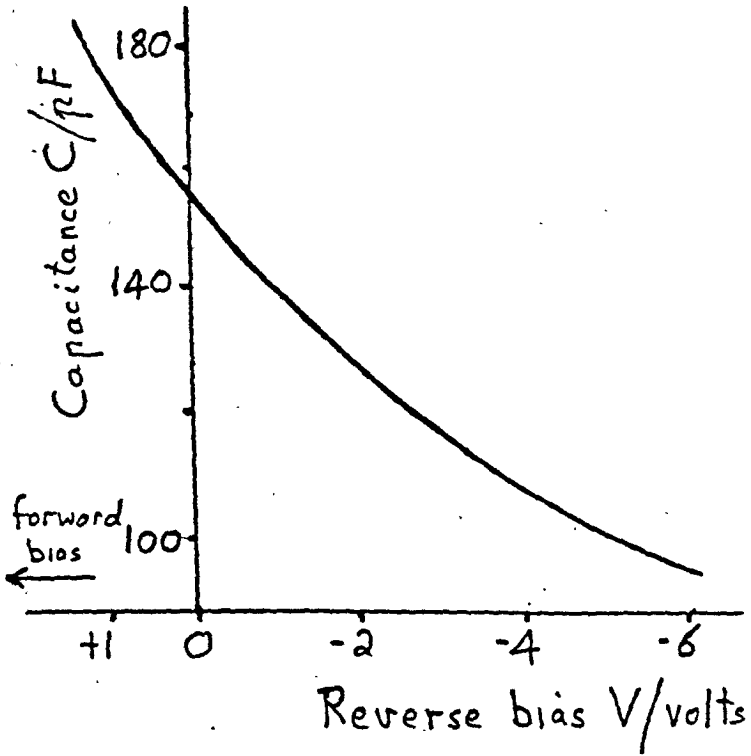


Fig.4

### 3 DIODE UNDER REVERSE BIAS

#### (a) Capacitance measurements

Early in 1976, while waiting for fresh diodes and for probes of larger radius, an opportunity arose to measure the capacitance of an LED with apparatus that was not being used at Brunel University (it had just been released by a research student and was about to be taken up by another one). The LED was from the batch originally supplied to Konidaris and was the only one that had not been used; consequently it was free from any defect that might have been imposed by severe stress etc. The apparatus was a "Brookdeal" phase sensitive detector (Type 411) with a reference unit (Type 422) and amplifier (Type 452) and gave a read-out of capacitance versus reverse voltage onto an X-Y plotter. The curve obtained (Fig 4) was extremely smooth and the axes were also drawn by the plotter, the calibration being obtained against a standard decade capacitor box and a battery and "AVO" voltmeter respectively.

From the spectral shift measurements of Konidaris it



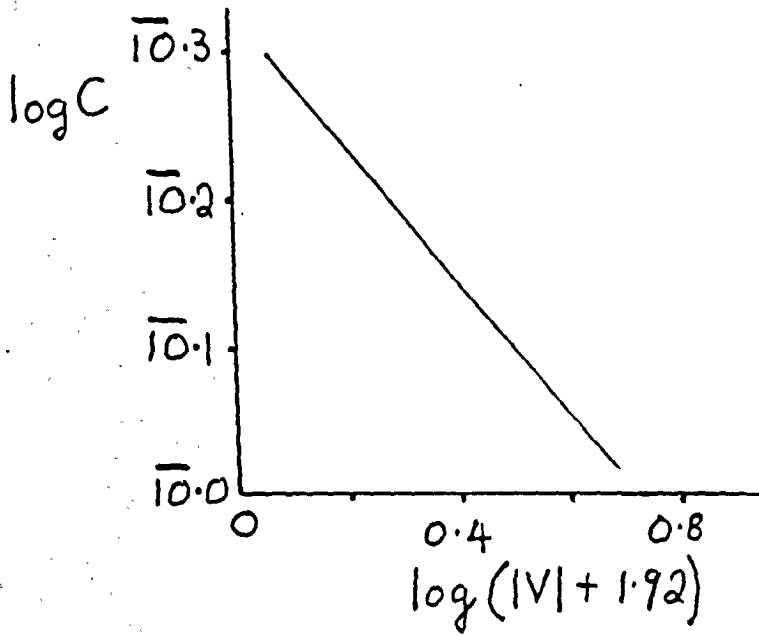


FIG.5

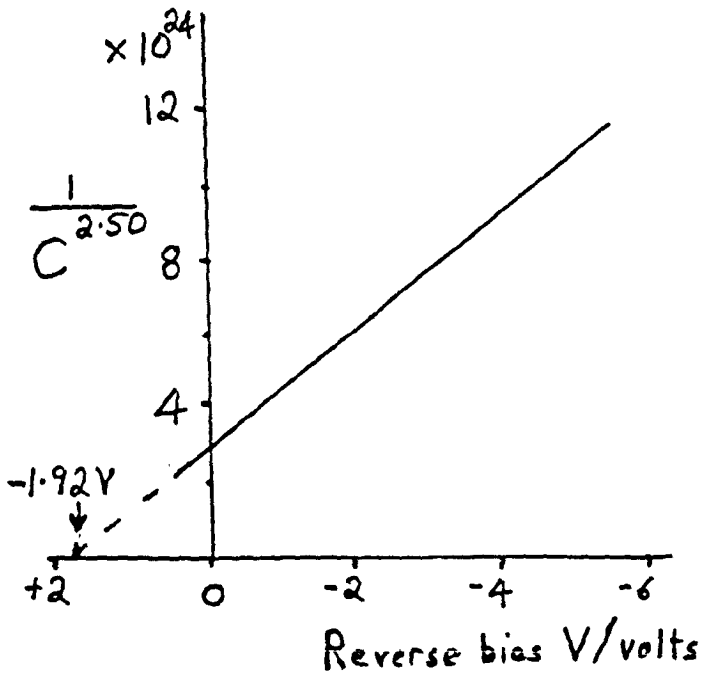


FIG.6

was known that the wavelength of light emitted was 0.6470  $\mu\text{m}$  (to four-figure accuracy) for a particular diode, though of course this could vary slightly with another LED; the band gap should therefore be  $1.241/0.6470 = 1.91(8)$  eV. On this basis it can be assumed that the relation for the capacitance  $C$  should be:-  $C^n$  varies as  $(V + 1.92)$  and that a graph of  $\log C$  against  $\log(V + 1.92)$  should be a straight line. This in fact proved to be the case (Fig 5), and a deviation of 0.02 volt on the value of 1.92 gave a detectable departure from a straight line. The slope of  $-1/2.50$  indicates the value of  $n$ , and the subsequent graph (Fig 6) again gave a very good straight line of intercept 1.92 volts. In general  $\log C$  varies as  $\log(V + V_D)$  where  $V_D$  is the 'built-in' potential, but in the case of the highly doped diode it can be assumed that  $V_D = E_G/q$  where  $E_G$  is the band gap energy.

This result for the value of the band gap was not only satisfying in that it gave very close agreement with Konidaris's spectral work, but subsequently it has been found necessary to know the value in order to make

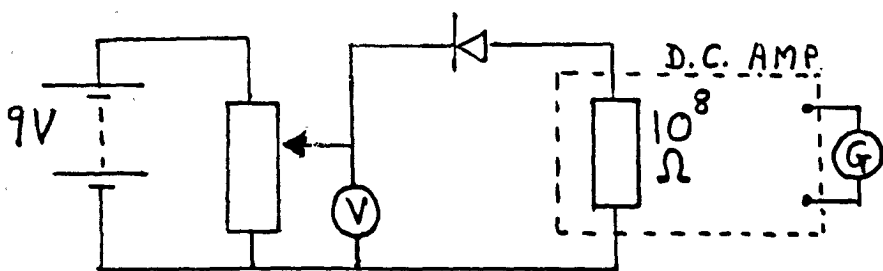


Fig.7

a theoretical calculation of the temperature variation of the LED (as described in Section 8).

(b) Theoretical characteristics and the effect of light

By 1978 when a certain amount of exploratory work on stressing diodes under forward bias had already been done, it was decided to investigate what effects such a stress would have, if any, on the electrical characteristics under reverse bias.

The circuit (Fig 7) used a "Griffin" d.c. amplifier electrometer for measuring the current. This is a simple piece of apparatus, widely used in physics education, and effectively measures the potential difference (up to a maximum of one volt across a high-impedance resistor built into the instrument so that a resistance of  $10^8$  ohms gives a full-scale deflection on a milliammeter at 10 nA input); allowance has to be made for a drop in p.d. of a fraction of a volt across the instrument. Bringing the probe very close to the top surface of the diode, but without actually touching it, resulted in a significant decrease in current; however no further change was observable

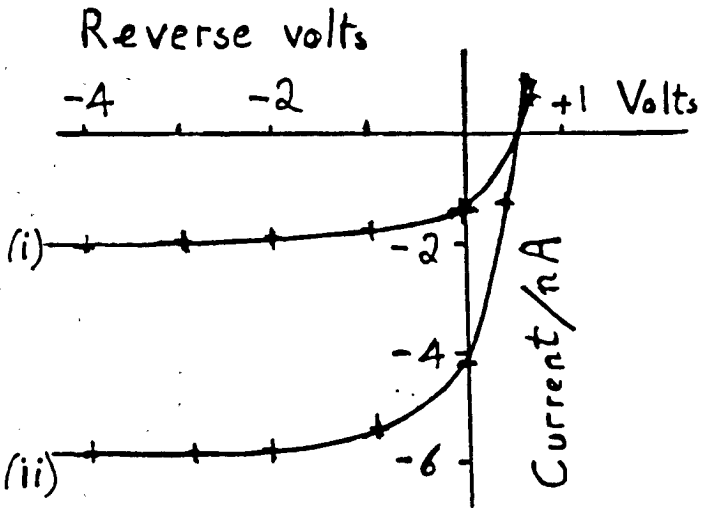


Fig.8

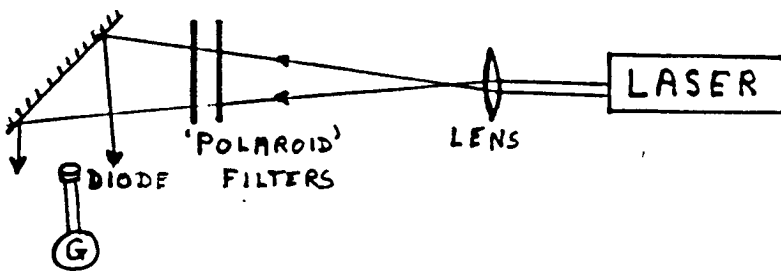


Fig.9

after contact had been made and pressure applied. At first sight an explanation of this might be that the proximity of the probe could be a capacitance effect, but this can be discounted by the fact that the circuit is entirely d.c. It was soon realised that the true explanation was a shadowing effect :- a considerable amount of the ambient light was blotted out by the probe and its metal holder. This was confirmed by the relatively crude measurements made under varying lighting conditions as shown in Fig 8:- curve (i) under normal fluorescent lighting of the laboratory (corresponding approximately to daylight conditions); and curve (ii) with much greater illumination, namely a 60-watt bulb in a typical reading-lamp reflector shining directly downwards onto the diode at a distance of half a metre.

At this stage it was decided to test the effect of light intensity under more controlled conditions. In an otherwise dark laboratory the unbiased diode was illuminated by laser light, as shown in Fig 9, and the reverse potential thereby built up by the light was

measured on a galvanometer that was not particularly sensitive but was the best one that was available at the time - namely a "Galvamp" with full-scale reading of 90  $\mu\text{V}$  or 90 nA (1000 ohm resistance).

The intensity of the laser light was controlled by rotating a "Polaroid" filter relative to another one; starting in the crossed position, if the angle between the filters is  $\theta$ , then the amplitude is reduced by a factor  $\sin \theta$  and the intensity by  $\sin^2 \theta$  (eg at  $45^\circ$  the intensity is a half). The angle was measured by mounting one of the filters on a rotating holder made of "Meccano" with a low-gear drive such that two revolutions of a handle were equivalent to  $3^\circ$ . The laser was a simple helium-neon type of very low power (sufficiently low for it to be permitted in a classroom and demonstrated to students) and emitted reddish unpolarised light of wavelength  $0.6238 \mu\text{m}$ ; thus the wavelength was shorter than that of the LED ( $0.6470 \mu\text{m}$ ) and there was no problem with absorption of the photons emitted by the laser. It was necessary to spread the laser beam with a lens since otherwise the light intensity

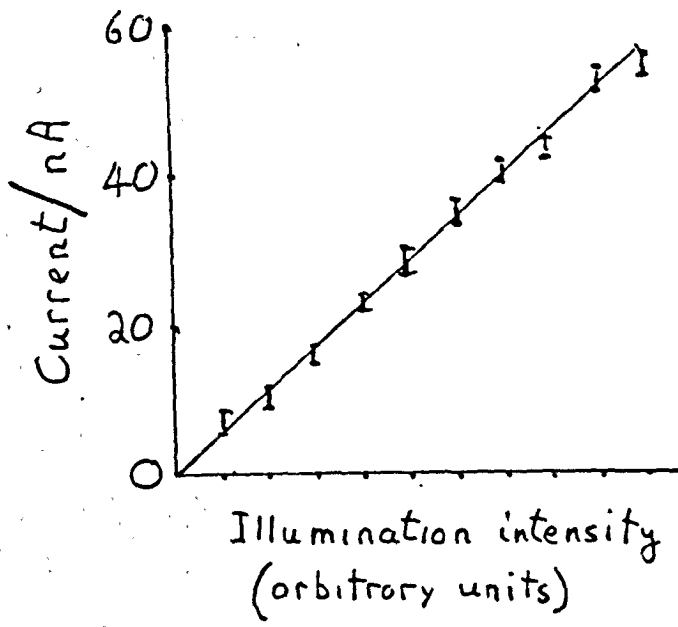


Fig.10

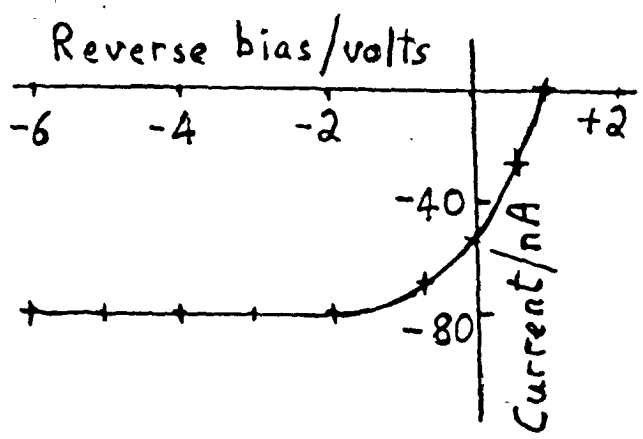


Fig.11



would have been rather high, and in addition there were marked striations in the beam; these striations together with the scratches and irregularities in the "Polaroid" filters produced fluctuations in the electrical readings but, by spreading the beam and by shifting the filters laterally so as to obtain the maximum electrical output for each angular position, a remarkably consistent set of readings was obtained (Fig 10).

As can be seen from Fig 10 the electrical output is undoubtedly linear with luminous intensity. With only one "Polaroid" filter in position (kept fixed) and the laser beam still spread by a lens, reverse-bias characteristics were measured, using the "Galvamp" as the current meter, and this gave the graph shown in Fig 11. The maximum of 80 nA rose to 250 nA when the "Polaroid" filter was removed.

Finally, the reverse-bias characteristics were measured with the LED in a light-tight box so that it was in total darkness, the circuit used being the same as in Fig 7 except that the fixed resistor on the "Griffin" d.c. amplifier/electrometer was changed to  $10^{10}$  ohms, giving a

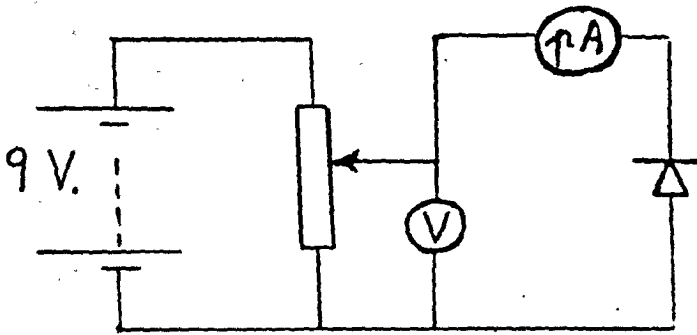


Fig.12

full-scale deflection of 100 pA. It was observed that after exposure to light, there was a pronounced delay of several seconds before the LED settled down, but even then the readings were not at all steady. The most noteworthy feature of the readings was that the range of current was 0 to 50 pA, which is vastly different from that recorded by Konidaris, and further comment on this is reserved for the following sub-section

(c) Current-voltage characteristics in the absence of light

By late 1980, when a high-class galvanometer had become available (the "Levell" meter already referred to in Section 2, p.10), the reverse-bias measurements on an LED in a light-tight box were repeated, using the circuit of Fig 12 in which the voltage was read by an AVO. The Levell meter was used in the 15-0-15, 50-0-50 and 150-0-150 picoamp ranges, each range having an input resistance of  $10^6$  ohms so that the maximum voltage drop across the instrument was 0.15mV at 150pA. Two main difficulties arose:- (i) Due to the presence of contact voltages and/or thermoelectric emf's, the 9-volt battery had to

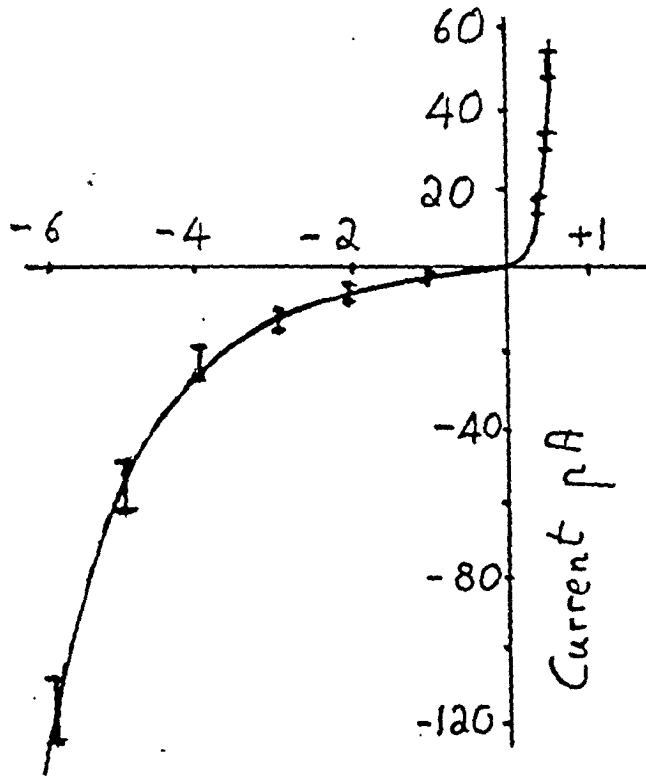


Fig.13

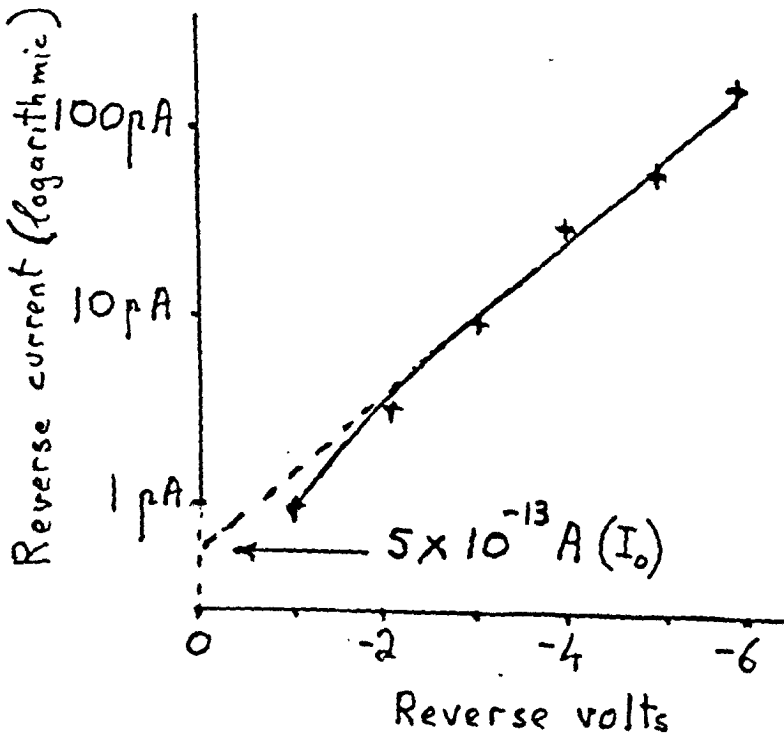


Fig.14

respectively. A number of diodes were tested and they all gave values of  $I_0$  ranging between  $10^{-13}$  and  $10^{-12}$  amp with  $K$  approximately 1 volt.

Besides the remarkably close fit to an exponential the outstanding feature of these measurements is the enormous departure from those of Konidaris<sup>(1,7)</sup>, who recorded an approximate exponential ranging from about  $10^{-8}$  amp at -1 volt to  $10^{-6}$  amp at -6 volts, compared with the currents in Fig 14 which are approximately  $10^{-12}$  to  $10^{-10}$  amp for the same voltage scale. Konidaris postulates a tunnelling process and (to quote) "...rule(s) out the possibility of GR currents in the reverse direction, which can be theoretically estimated to be about at least 3-4 orders of magnitude lower than our experimental values.." Obviously in the present research the mechanism would indeed appear to be one of generation/recombination; ie reverse saturation currents are brought about by the thermal generation of carriers in the same manner as they occur in the low-voltage region of forward bias.

Of course the mechanism in the forward direction must

be somewhat different from that of the reverse direction, as can be seen in Fig 13 by the shape of the exponential curve in the positive quarter of the graph compared with that in the negative quarter. In the next section the forward characteristic is studied in detail, and in the relation  $I = I_0 \exp(V/K)$  the values of  $I_0$  and  $K$  are about  $10^{-15}$  amp and 0.05 volt ( $2kT/q$ ) respectively; this quantifies the difference between the forward and reverse directions.

At the time of the above measurements the diodes under test were not the same as those supplied to Konidaris, but nevertheless they were made up to similar specifications by Standard Telecommunication Laboratories, Ltd, and under forward bias (see next section) had virtually identical characteristics. The naïve possibility that Konidaris worked under conditions of ambient light can be dismissed since, among other things, he was looking for (and found) very weak light under reverse bias<sup>(12)</sup>, and he also implies (without specifically stating it) that he was measuring in darkness. A possible explanation is that

he inadvertently damaged his diodes either by very severe mechanical stress with his 25  $\mu\text{m}$  probe (assuming that he made his measurements after, and not before, stressing his devices) or, as is more likely, by electrical stress with much higher reverse voltages than he actually records on his graphs; thus unwanted leakage or 'break through' currents flowed which swamped the very small currents that would otherwise have been recorded with unblemished devices. Another possibility which has been suggested<sup>(13)</sup> is that the diodes supplied for the present research were prepared sometime later and that in the intervening years the 'clean up' in the manufacturing process had been considerably improved.

It is apparent that the above aspect of the electrical behaviour of the LED under reverse bias could be profitably explored further. Obviously the line to be pursued would be one of temperature variation, and in particular the characteristic at a liquid nitrogen temperature might very well yield interesting results. However, in view of the limited resources available to the present worker and

the fact that the main purpose of the research was to investigate the behaviour of the diode under mechanical stress, the reverse bias characteristics were not explored any further.

When the above measurements were being taken no electrical change with mechanical stress could be detected; but in view of the very small change in current observed under forward bias, as recorded in Section 6, and the necessity for sensitive circuits to measure this variation, it is not surprising that it was impossible to detect any effect under reverse bias (if indeed there was any).



#### 4 DIODE UNDER FORWARD BIAS

##### (a) Current-Voltage Characteristics

In order to establish the range of the light-emitting (LE) region and the transition to the generation-recombination (GR) region of the diodes supplied, their current-voltage (I-V) characteristics were measured. There was an additional reason for doing this in that the inverse slope  $dV/dI$  of the characteristic measures the a.c. (or differential) resistance  $R_{ac}$  as distinct from the d.c. resistance  $R_{dc}$  given by  $V/I$ . Thus subsequently, when a small electrical change took place (for example, by applying stress with a probe or due to a small alteration in temperature) the change could either be measured as a small voltage  $\Delta V$  or as a small current  $\Delta I$ . Knowing the value of  $R_{ac}$  at the appropriate point on the characteristic it was easy to convert from voltage to current change, or vice versa, by the relation  $\Delta V = R_{ac} \Delta I$ . The justification for this relation is explained in detail in Appendix B.

Over the ten-million-fold range of current from 1 nA

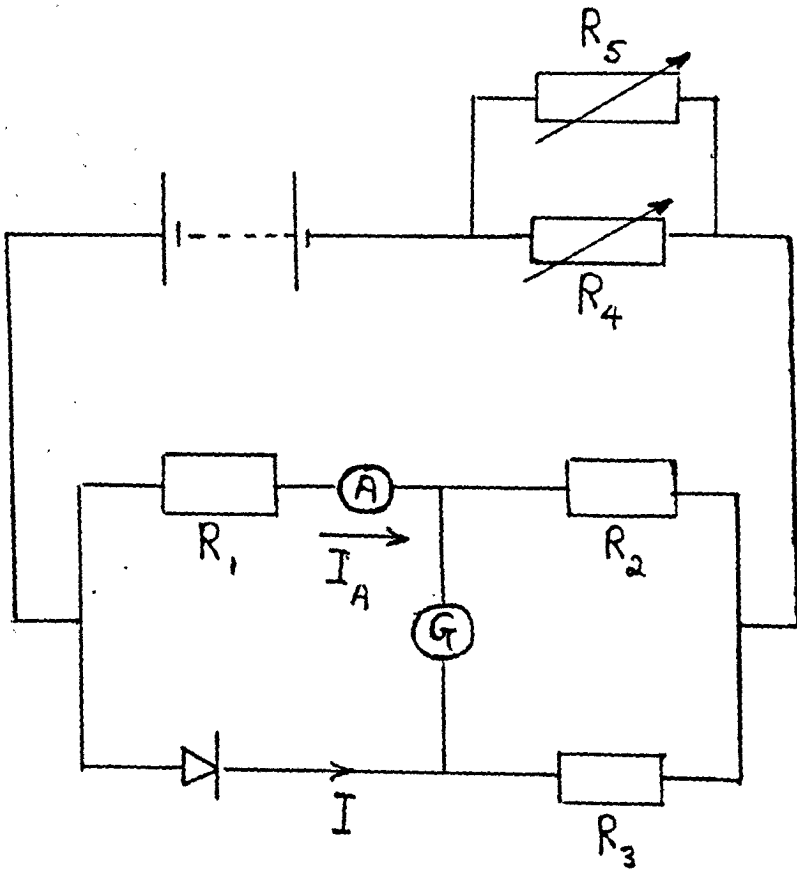


Fig.15

to 10 mA the corresponding voltage range is 0.9 to 1.6 V and so, in principle, an accurate measurement of voltage by means of a potentiometer and standard cell would appear to be necessary. In practice however it was found that, with a microammeter of fairly dependable calibration and three resistance boxes going up in decades to 1 megohm, a Wheatstone bridge was an excellent circuit that was easy to adjust and gave consistently good readings. This was the method used in the early years when the best galvanometers available had a modest sensitivity of a bit less than 1 nA. The circuit is shown in Fig 15, the three resistance boxes being  $R_1, R_2$  and  $R_3$ ;  $R_4$  was used in low range as a rheostat and  $R_5$  in high range as a fine control on  $R_4$ . It is easily seen that  $V = R_1 I_A$  (ignoring the p.d. across the ammeter) and that  $I = R_2 I_A / R_3$ . Since  $R_2 / R_3$  can be varied from more than 1000/1 to less than 1/1000 the current range of 10 mA down to 1 nA can be accommodated on a single instrument, namely a microammeter that is always set at its full-scale reading of 10  $\mu$ A.

A typical set of values obtained in mid-1978 is shown

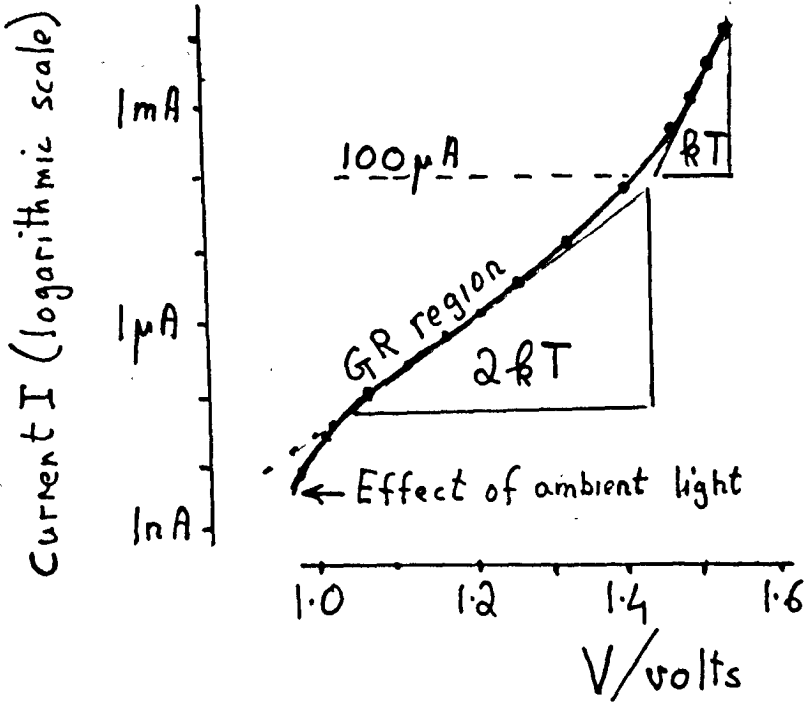


Fig.16

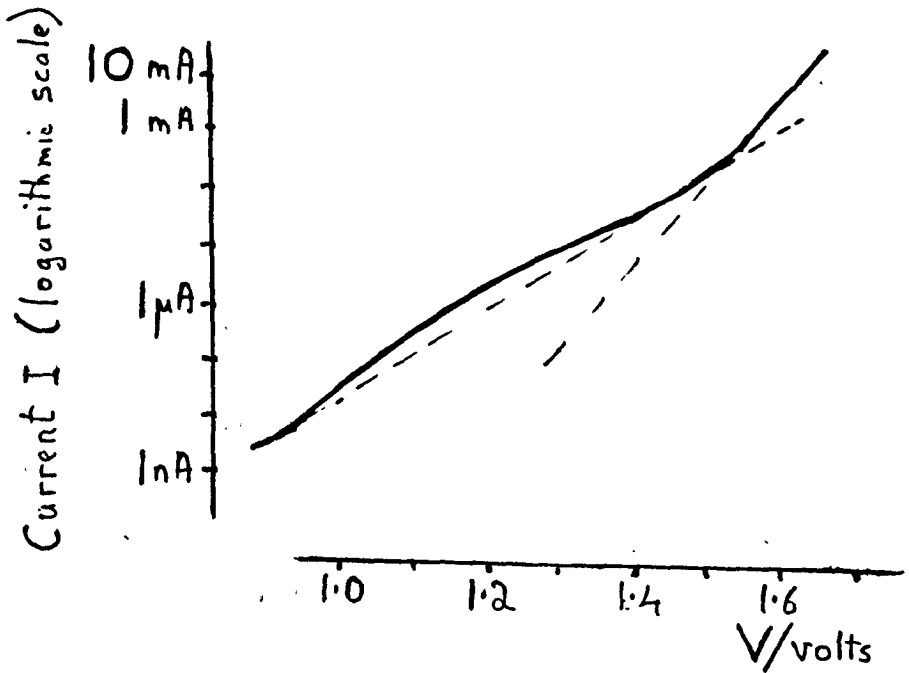


Fig.17

in Fig 16. The general relation for an LED is:-

$I = I_0 \exp[(qV/nkT - 1)]$ ; however measurement shows that

$I_0$  is approximately  $10^{-15}$  amp (see Appendix B) and there-

fore for currents substantially greater than this the -1

term can be neglected. Hence on the basis of an approx-

imate relation  $I = I_0 \exp(qV/nkT)$  and assuming that at

room temperature  $kT = 25$  meV, the inverse of the slopes

in Fig 16 gives the values as  $nkT$  as follows:-

in the GR region  $nkT = 52.(1)$  meV =  $2kT$  (approximately),

in the LE region  $nkT = 32.(6)$  meV =  $kT$  (approximately).

The transition takes place at about  $100 \mu A$ . It is to be

noted that at about  $10nA$  ambient light plays a significant

role, and for currents less than this the device must be

kept in the dark. Although the above values are somewhat

different from those of Konidaris, who quotes  $60$  meV,  $20$

meV and  $20 \mu A$  respectively for a particular diode<sup>(1)</sup>, the

disagreement is not significant since the variation for

diodes from the same batch was quite considerable. Thus

another diode gave  $57$  meV,  $40$  meV and a transition of  $10$

$\mu A$ , while yet another showed a curious 'hump' in the GR

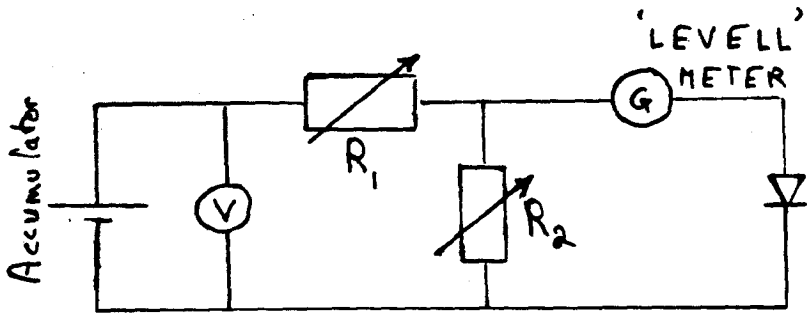


Fig.18

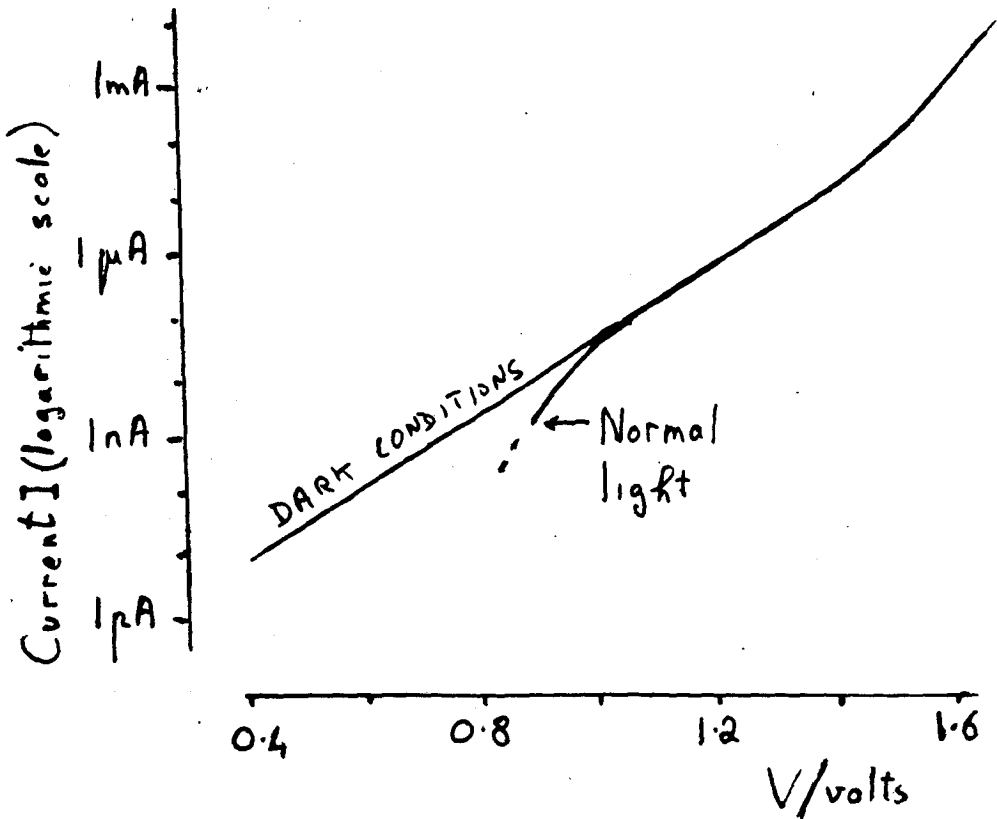


Fig.19

region (Fig 17). In Section 8 (c) p.96 a suggestion is made as to why  $kT$  in the LE range could be somewhat larger than the theoretical 25 meV.

Towards the end of 1980 when the very sensitive "Levell" meter was available it was possible to measure the characteristics by means of a more straightforward circuit (Fig 18) in which the voltage was determined by the fraction  $R_2/(R_1 + R_2)$  of the "AVO" reading of the constant value of the accumulator and the current could be recorded directly on the "Levell" meter down to 10 pA, a very small correction being allowed for the p.d. across the meter. The graph is shown in Fig 19, and it can be seen that the GR part is remarkably straight (ie an exponential relation) right down to the lowest current, provided that ambient light is excluded.

The main conclusion is that, though the general relation is of the form  $I = I_0 \exp(qV/nkT)$  with  $n$  approximately 1 in the LE and 2 in the GR region, the value of  $n$  varies considerably from one LED to another and so does the transition point of 10 to 100  $\mu A$ , despite the fact

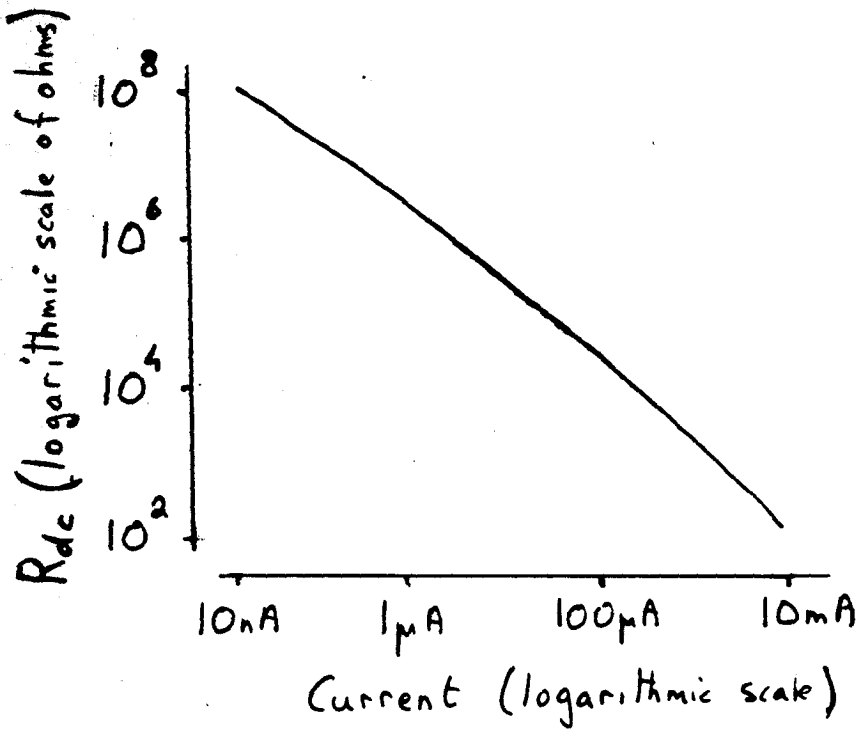


Fig.20

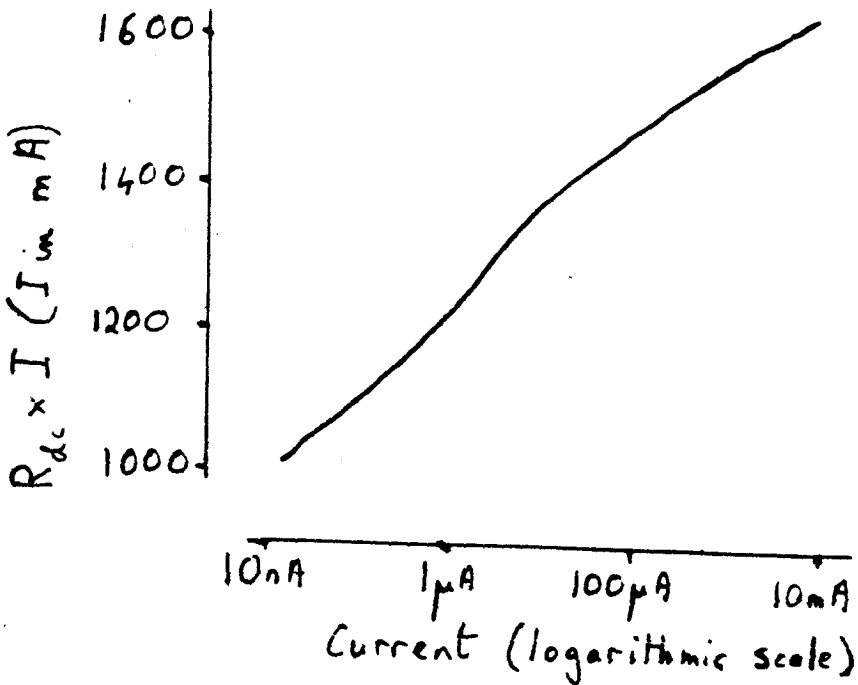


Fig.21



that the diodes were all from the same batch.

(b) d.c. and a.c. Resistance

As pointed out at the beginning of this section, in dealing with the measurement of small electrical changes under pressure from a probe etc., it is necessary to know the a.c. resistance  $R_{ac}$  of the LED's at any point on the characteristic. It is interesting to compare  $R_{ac}$  with the d.c. resistance  $R_{dc}$ ; this latter can be determined from an accurate graph of the characteristic by which the values of  $V$  and  $I$  can be read off directly and the d.c. resistance  $V/I$  calculated. Because of the enormous range a logarithmic presentation is necessary, and Fig 20 shows the values of  $R_{dc}$  obtained from the characteristic of Fig 19. Since the voltage changes very slowly the variation of  $R_{dc}$  is roughly inversely proportional to current, and an alternative presentation is given in Fig 21 in which the product  $R_{dc} \times I$  ( $I$  being in mA) is plotted against  $\log I$ ; this latter shows up the transition between the LE and GR regions with slightly more contrast.

Turning now to the more important quantity namely  $R_{ac}$ ,

Facing  
p.32

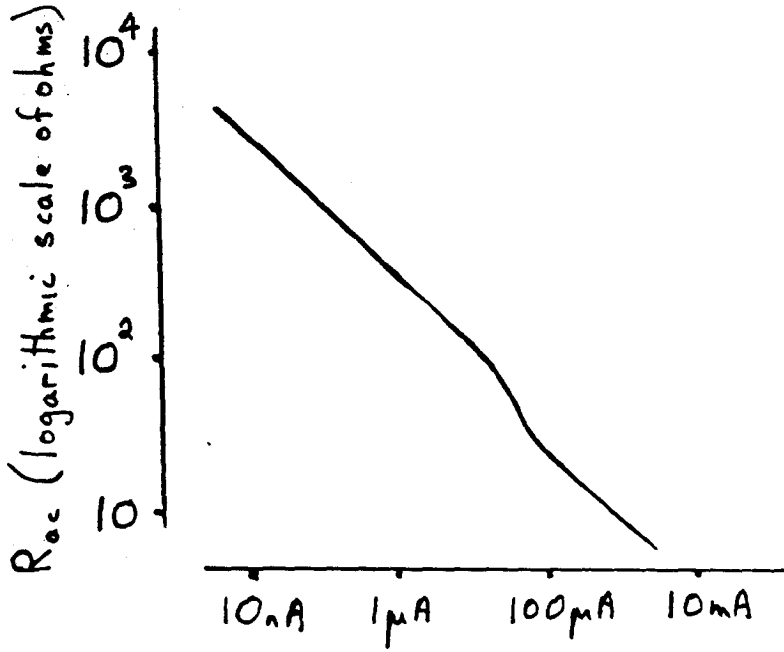


Fig.22

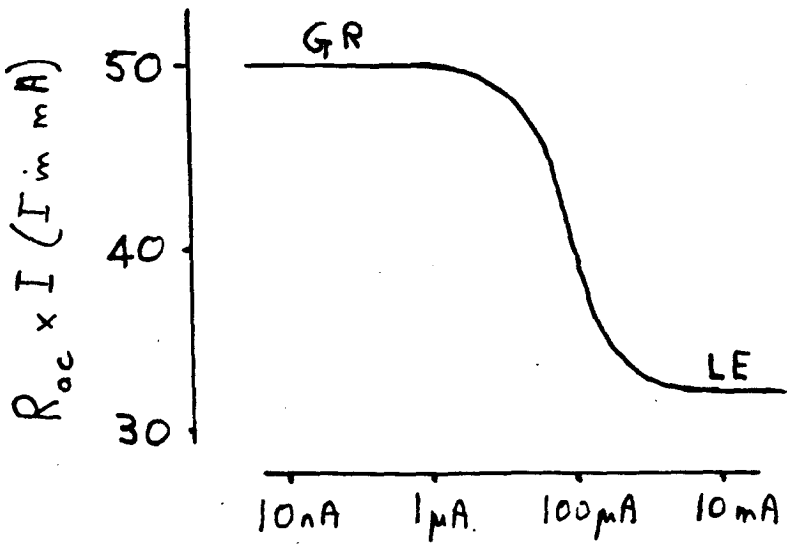


Fig.23

there is the relation  $I = I_0 \exp(qV/nkT)$  and by differentiation

$$\frac{dI}{I} = \frac{q}{nkT} dV \quad \text{so that } R_{ac} = \frac{dV}{dI} = \frac{1}{I} \frac{nkT}{q}$$

Thus by measurement of  $nkT/q$  from the slopes of the LE and GR regions respectively,  $R_{ac}$  can be readily calculated. The strictly logarithmic graph is shown in Fig 22, and the alternative presentation in Fig 23; in the latter diagram the contrast of  $R_{ac} \times I$  between the LE and GR regions is very marked and, unlike the corresponding diagram for  $R_{dc}$ , the transition can be readily seen. The main feature of the two sorts of graphs is that in general the d.c. resistance is very roughly thirty times greater than the a.c. resistance.

The increase in value of  $n$  from approximately 1 to 2 as one proceeds from the LE to the GR region is an important feature since the calculation of the percentage current change  $\Delta I/I$  from the reading of the voltage change  $\Delta V$  involves the factor  $1/n$ . Although the measurements of the I-V characteristics were made fairly

early on in the research, it was not until the later stages that the significance of the  $1/n$  factor was fully realised, and all the experimental readings taken in the GR region had to be subsequently amended by a factor of about a half when calculating the percentage change.

Facing  
p.34

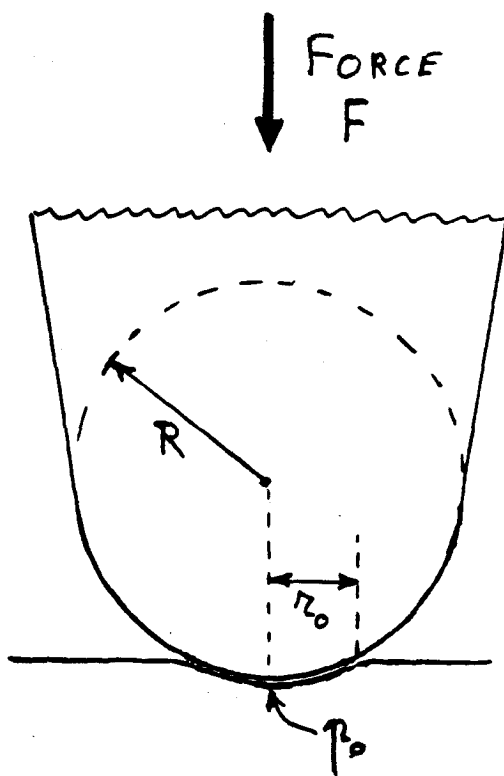


Fig.24

## 5 STRESS UNDER A PROBE OF SPHERICAL SURFACE

### (a) Simple theory of stress

A good deal of numerical work on the problem of a spherical surface pressing down on a flat infinite plane was reported in the 1920's (14,15), but a most useful reference has proved to be an engineering text-book of more recent years by Lipson and Juvinall (16) in which stress by both ball and roller bearings is discussed. The rounded tip of a diamond or sapphire probe pressing onto the flat surface of an LED presents the same geometrical configuration as for a spherical ball (Fig 24), the important parameters being the force  $F$  on the probe, the pressure  $p_0$  at the centre of contact, the radius  $r_0$  of the indented surface of contact, and the radius of curvature  $R$  of the probe. Lipson and Juvinall quote:

$$p_0 = \frac{1}{\pi} \left( \frac{6F}{R^2 \Delta^2} \right)^{1/3} \quad \text{and} \quad r_0 = \left( \frac{3}{4} FR \Delta \right)^{1/3}$$

$$\text{where } \Delta = \frac{1 - \sigma_1^2}{E_1} + \frac{1 - \sigma_2^2}{E_2}$$

$\sigma_1$  and  $\sigma_2$  are Poisson's ratio, and  $E_1$  and  $E_2$  are Young's

modulus for the two respective materials in contact.

Straightaway there arises a difficulty as to the value of  $\sigma$  and  $E$  for  $\text{GaAs}_{0.6}\text{P}_{0.4}$  since a standard reference (17) only quotes for GaAs, namely  $0.37$  and  $8.5 \times 10^{10}$  newtons metre<sup>-2</sup> (or  $8.5 \times 10^{11}$  dynes cm<sup>-2</sup>). Also there are a number of forms of diamond, but the corresponding values for diamond can be taken as approximately  $0.3$  and  $8 \times 10^{11}$  N m<sup>-2</sup> (18). It is easy to see that when inserting numerical values into the expression  $(1 - \sigma^2)$  the two values of Poisson's ratio are not critical; in addition, since diamond is about ten times harder than the semiconductor, most of the deformation takes place in the LED surface and the value of Young's modulus for diamond is of secondary importance. Hence a good approximation can be made whereby  $\Delta$  reduces to  $0.960/E$  in which  $E$  is Young's modulus for the semiconductor material. The two basic relations for  $p_0$  and  $r_0$  then become

$$p_0 = 0.59(FE^2/R^2)^{1/3} \quad \text{and} \quad r_0 = 0.89(FR/E)^{1/3}.$$

From this a third relation emerges, namely  $p_0/r_0 = 0.66E/R$ . There is a further useful relation involving the

average pressure  $p_{av}$  over the area of contact  $r_o$ . Since  $p_{av} = F/\pi r^2$ , it can easily be shown from the two basic relations for  $p_o$  and  $r_o$  that  $p_{av} = \frac{2}{3} p_o$ .

As an example of the above relations, calculation shows that for a force of 1 gram on a 25  $\mu\text{m}$  probe  $p_o$  is nearly  $3 \times 10^9$  Pa (30,000 atm) or about  $6 \times 10^9$  Pa for a 10 gm force, and for a 300 gm force on a glass stylus of radius 1.2 mm (as used by Konidaris)  $p_o$  is about  $0.8 \times 10^9$  Pa (8,000 atm), allowance being made in this latter case for the deformation being about equally spread between the glass and semiconductor.

Turning now to a sapphire probe, the situation is not very different from diamond despite the fact that Young's modulus for sapphire is about  $4.3 \times 10^{11}$  N m<sup>-2</sup> or  $4.4 \times 10^6$  kg cm<sup>-2</sup>, as quoted by the suppliers of the probes<sup>(10)</sup>, which is approximately half the value for diamond. Most of the deformation still takes place in the softer semiconductor material, and the appropriate relations are:-

$$p_o = 0.56 (FE^2/R^2)^{1/3}, \quad r_o = 0.92 (FR/E)^{1/3} \quad \text{and} \quad p_o/r_o = 0.61E/R$$

where, as before,  $E$  is Young's modulus for the semi-



conductor material ( $8.5 \times 10^{10} \text{ N m}^{-2}$ ). Thus the change from diamond to sapphire scarcely makes any difference.

(b) Estimate of the elastic limit

During the early part of the research three LED's were severely damaged trying out different stresses. The damage could easily be seen as a 'black spot' in the bright red surface of the diode, ie where the junction interface, which lies just below the surface, had been so severely stressed that it no longer emitted any light in that region. In fact several dozen tests were made with diamond probes of radius 25, 50 and 75  $\mu\text{m}$  because it was easy to shift the position of the probe to a new place and make another black spot; a diode was only finally discarded when its surface was literally covered in black spots.

After stress had been imposed by a force of a few grams on the probe of 25  $\mu\text{m}$  radius, mechanical damage to the surface could be observed when the diode was illuminated by strong white light at an oblique angle and viewed at normal incidence with a low-power microscope.

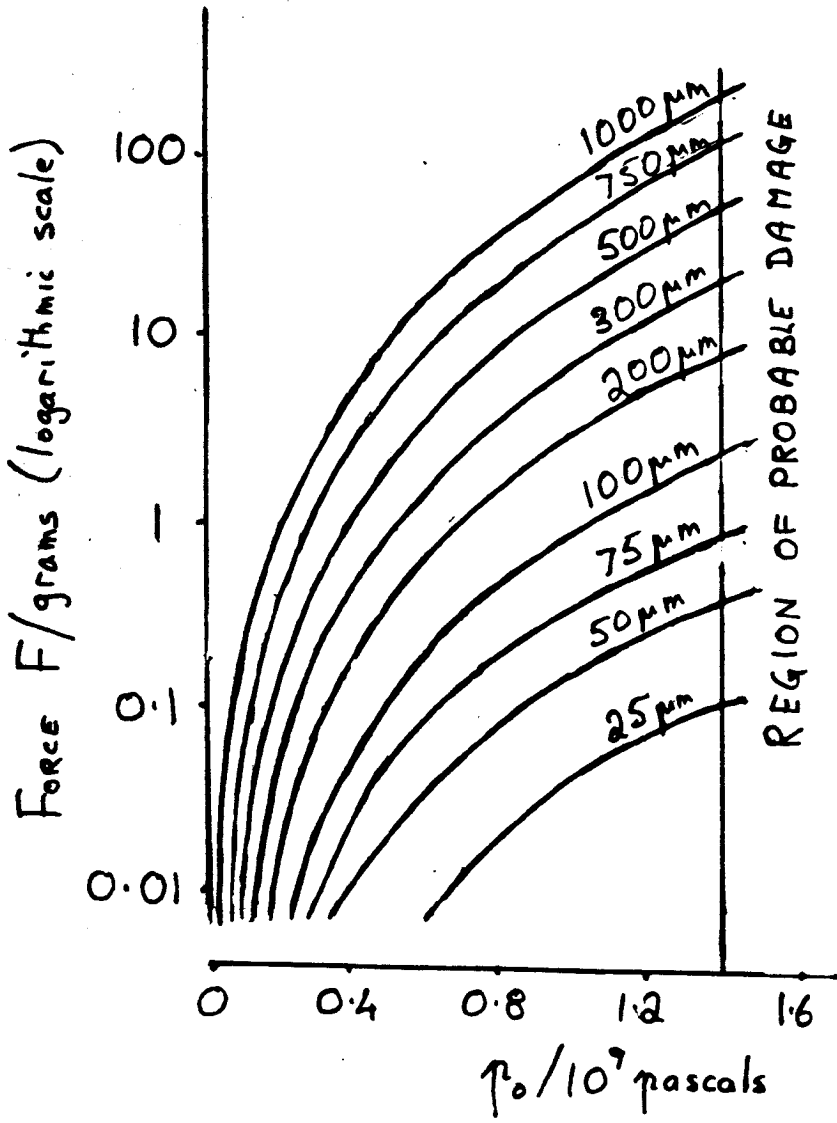


Fig.25

The damage appeared to be a shallow cratering of the surface with slight splintering in the crater, not unlike the larger effect on a glass block as reported further on in this section.

As a result of these tests an empirical criterion was reached fairly early on in the research whereby the elastic limit was judged to be about  $1.4 \times 10^9$  Pa (as calculated from  $p_0$ ) although subsequent evidence by other workers (19) suggests that even this may be too high. In fact one paper from the Soviet Union (20) maintains that degradation of GaAs may begin to take place at a stress as low as  $3 \times 10^8$  Pa. Nevertheless, if one accepts  $1.4 \times 10^9$  Pa as being a not unreasonable upper limit, one can see that it is a stress which is much lower than that imposed by other workers since it corresponds to a force of 0.1 gram on a 25  $\mu\text{m}$  probe or 1 gram on a 75  $\mu\text{m}$  one.

In order to determine the pressure exerted by a particular force on one of the probes the set of curves shown in the graph of Fig 25 was constructed; the three smaller probes of radius 25 to 75  $\mu\text{m}$  are diamond, and the

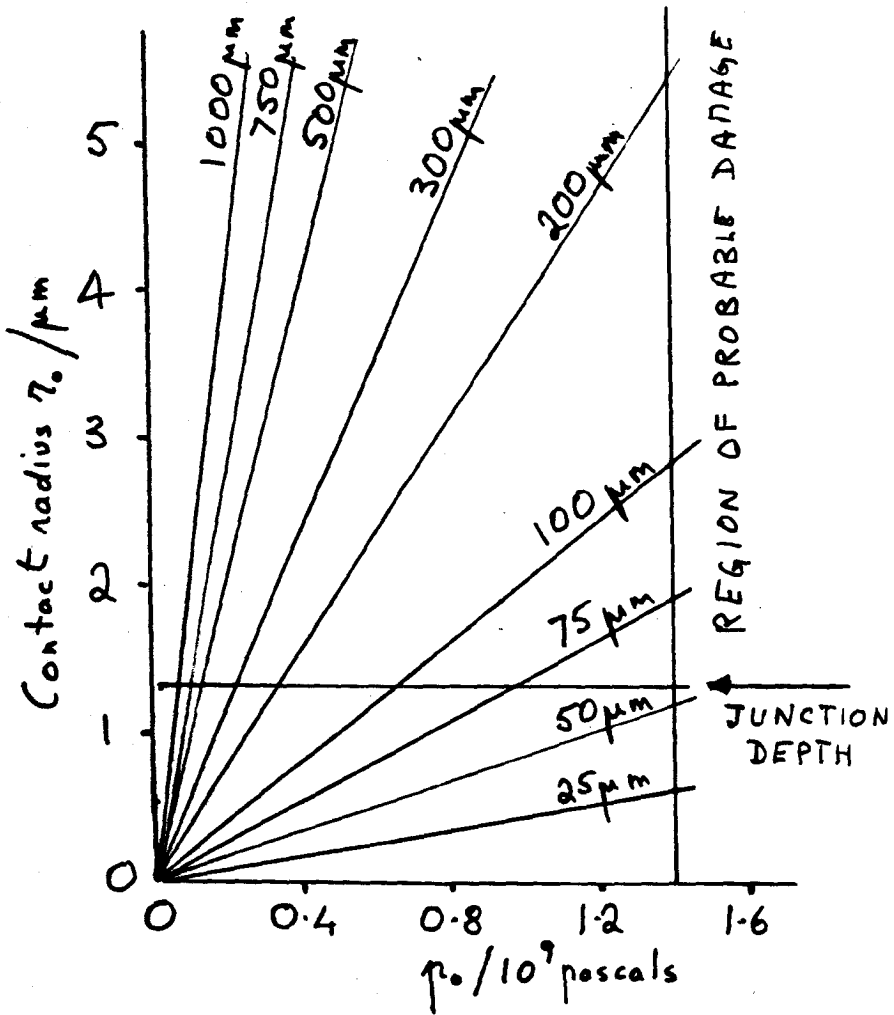


Fig.26

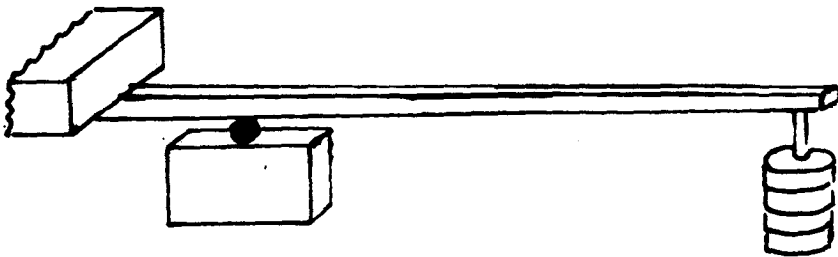


Fig.27

six larger ones from 100 to 1000  $\mu\text{m}$  are sapphire. A feature of these curves is that even a fairly small force of 0.01 gram can cause quite a considerable pressure, although the area of contact is of course very small. The radius  $r_0$  of this contact area can be read from the straight-line graphs of Fig 26, and if the corresponding force is required then the  $p_0$  value can be converted to  $F$  from Fig 25. Initially it was necessary to know the value of  $r_0$  when assessing how it compared with the depth of the junction below the diode surface, quoted as 1.3  $\mu\text{m}$  by the manufacturers (see next sub-section). Subsequently it has been found that the value of  $r_0$  is also required for the calculation of heat flow to the probe as discussed in Section 8(d).

Finally, in order to check on a likely value of the elastic limit a large-scale experiment was designed as follows. A laboratory glass block of dimensions 11 by 6 by 2 cm was laid on its long narrow side and loaded with a steel ball bearing (Fig 27); with a maximum weight of 10 kg and a lever ratio of about 8 a force of 80 kg could be

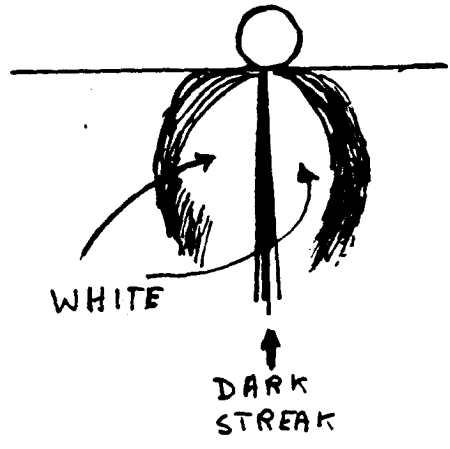


Fig.28

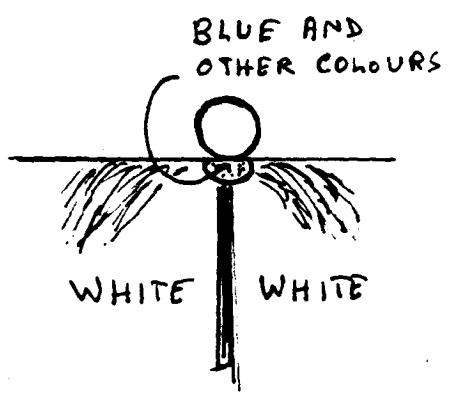


Fig.29

applied, and balls of radius 23, 16, 9, 6 and 4 mm were tried out. At the same time crossed "Polaroid" filters were placed on either side of the large face of the block, and by looking along a line at right angles to the large face photoelastic strain patterns were observed; the illumination was intensified by placing a bright light shielded with tissue paper behind the block so that the lamp was viewed through the filters. In the patterns that were observed darkness indicated very little strain whereas white or other colours were obviously due to a double-refraction interference effect brought about by strain. In practice the patterns did not vary very much over a wide range of sizes of balls and forces; with the large ball of 23 mm radius and a relatively small force of 4 kg on the ball the appearance was as shown in Fig 28; increasing the force up to 80 kg caused the whiteness to become brighter and extend almost throughout the block, and at the same time there was a small semicircle of bright colours immediately under the point of contact (Fig 29). The effects were more or less the same with the

smaller balls and also when the glass block was substituted by a "Perspex" one.

As regards permanent damage to the face of the block, this was only observed in the case of maximum stress, namely 80 kg on the 4 mm ball (but not with the 6 mm one), and showed up as definite splintering of the surface to a radius of about half a millimetre or less; it was visible to the naked eye and was studied in more detail with a hand lens and also a low-power microscope. Using a value of  $2.1 \times 10^{11} \text{ N m}^{-2}$  for Young's modulus of steel and 0.27 for Poisson's ratio<sup>(21)</sup> and corresponding values of  $7.1 \times 10^{10} \text{ N m}^{-2}$  and 0.25 for glass<sup>(22)</sup>, the equations quoted in sub-section (a) must be amended to  $p_0 = 0.50(FE^2/R^2)^{1/3}$  and  $r_0 = 0.98(FR/E)^{1/3}$ , ie not very different from those for diamond or sapphire on the diode. Calculation shows that the damaging stress  $p_0$  must be about  $3.1 \times 10^9 \text{ Pa}$  and the radius  $r_0$  about 0.35 mm. In considering different materials a better indication of elastic limit is probably given by strain rather than stress, and the strain that damaged the glass was 4.36 per cent. This figure can be compared



Facing  
p.42

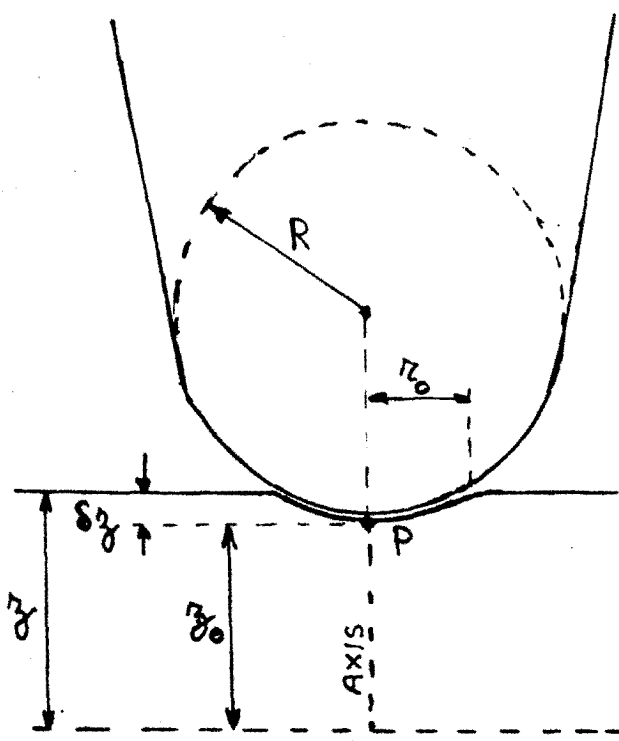


Fig.30

with a force of 1 gram on a 25  $\mu\text{m}$  diamond probe which also causes damage and for which the stress is  $2.9 \times 10^9 \text{ N m}^{-2}$ ,  $r_0$  is 1.29  $\mu\text{m}$  and the strain is 3.4 per cent.

(c) Depth of the junction interface

At this point it is appropriate to discuss the difficulty that is involved in defining any general depth  $z$  below the flat surface of the diode when that surface is deformed by pressure from a spherical probe. In Fig 30 it can be seen that  $z$  reduces to  $z_0$  when the depth is measured from the centre of contact P down the axis of the probe; this is a detail that seems to have been completely ignored in all the many literature references that have been consulted regarding the problem of pressure exerted by a spherical probe on a plane surface.

If  $z - z_0 = \delta z$ , then provided  $\delta z \ll 2R$  the well-known approximation for the 'spherometer' can be used:

$$\delta z = \frac{r_0^2}{2R} = \left(\frac{r_0}{R}\right)^2 \frac{R}{2}$$

However in the relations quoted at the end of part (a) of this section (p.36) it can be seen that:

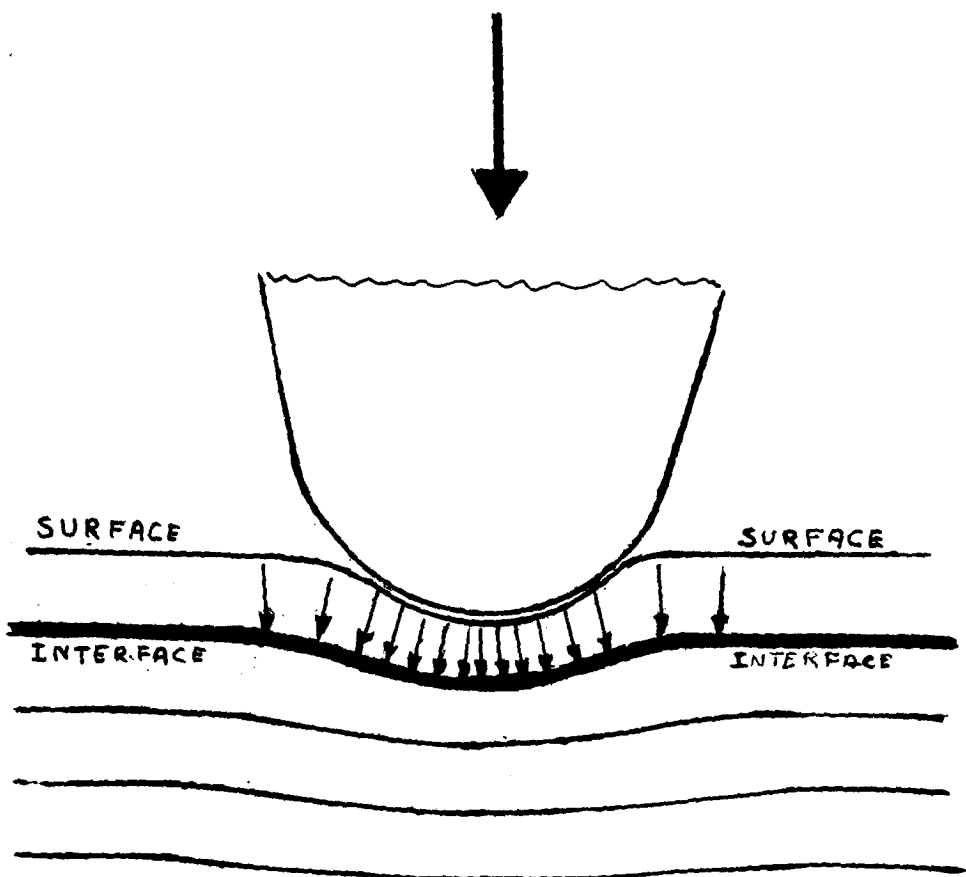


Fig.31

$$\frac{r_0}{R} = \frac{p_0}{0.61E} \quad \text{and therefore} \quad \delta z = \frac{p_0^2 R}{0.744 E^2}$$

Thus the greatest value of  $\delta z$  to be considered occurs when the probe of largest curvature exerts a maximum limiting stress  $p_0$  of  $1.4 \times 10^9$  Pa, and in fact the largest probe used in this research (and the one that was mainly used) had a curvature of radius  $500 \mu\text{m}$ . Substitution in the appropriate formulae gives  $\delta z = 0.18 \mu\text{m}$  and  $r_0 = 13.5 \mu\text{m}$ . Since the electrical measurements relate to the pressure effects taking place within the junction interface at a depth of  $1.3 \mu\text{m}$ , the value of  $0.18 \mu\text{m}$  represents a 14 per cent difference, and at first sight this would appear to be a serious matter.

Nevertheless, in the calculations of the ensuing sections the discrepancy is neglected for three reasons. (i) The relatively shallow interface will itself be somewhat deformed by the compressive forces extending below the probe (Fig 31), and therefore a considerable fraction of the  $\delta z$  error will be cancelled out. (ii) As is explained in subsequent sections, when one integrates

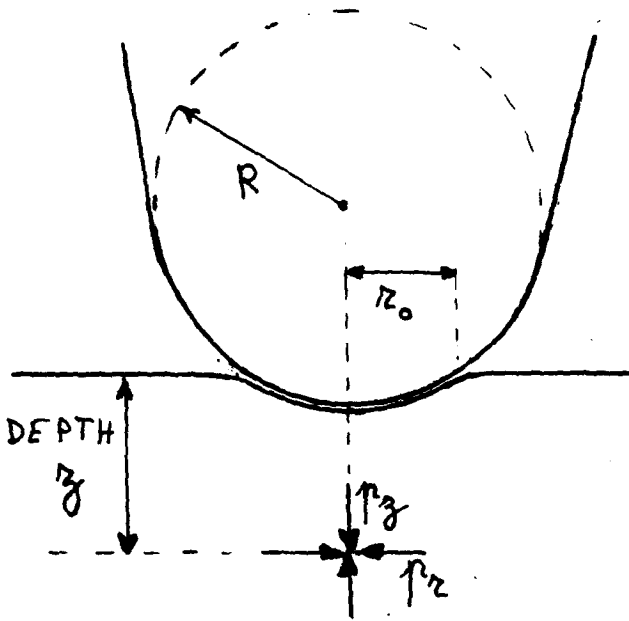


Fig.32

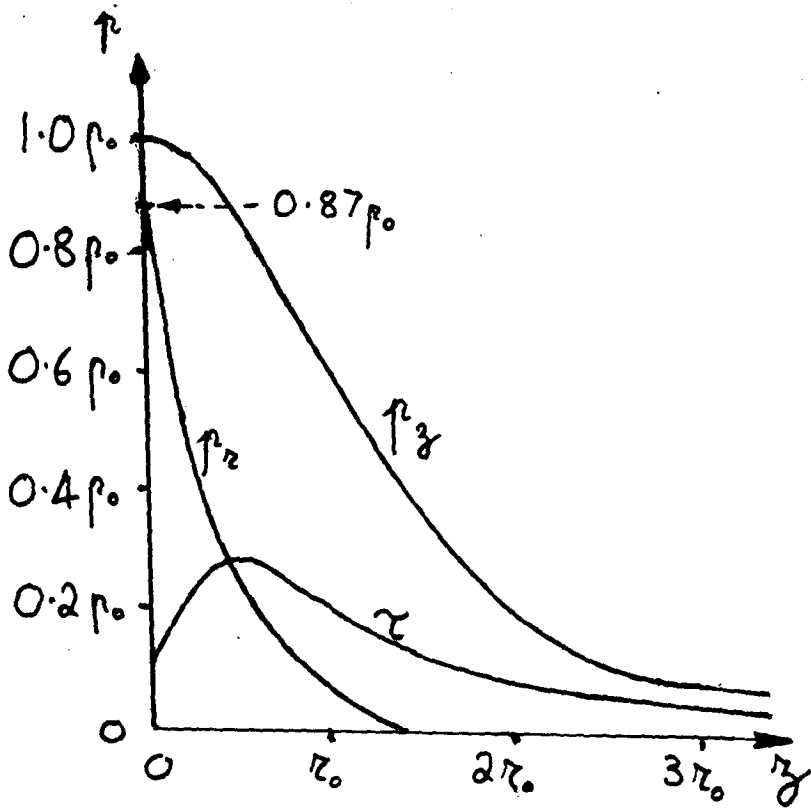


Fig.33

over the whole of the junction interface the contribution of an area of narrow radius about the axis is small compared with the much larger surrounding area in which, as one proceeds outwards to  $r_0 = 13.5 \mu\text{m}$  and beyond, the  $\delta z$  error reduces to zero. (iii) For probes of smaller radius, or for pressures less than the elastic limit, the value of  $\delta z$  is correspondingly reduced to less than 14 per cent of the junction depth, as can be seen from the the formula  $\delta z = p_0^2 R / 0.774 E^2$ .

(d) Variation of stress with depth

In addition to an evaluation of the maximum surface pressure  $p_0$  and the contact radius  $r_0$ , the text-book of Lipson and Juvinall also considers the effects at an axial depth  $z$  immediately below the central contact point (Fig 32); the axial compressive component  $p_z$  and the inward radial pressure  $p_r$ , together with the shearing stress  $\tau$ , are plotted out as shown in Fig 33.

From the values of  $r_0$  shown in Fig 26 it can be seen that for the sharp probes of 25 and 50  $\mu\text{m}$  radius the junction depth exceeds the value of  $r_0$  so that even

though the surface stress might be very damaging it could well be less than the elastic limit at the junction interface. Nevertheless it is probably very unwise to splinter the surface of the LED since this will lead to uncertain conditions if the probe is subsequently applied to the cratered area.

An interesting feature of Fig 33 is that there is a considerable shear stress which rises steeply with depth to a maximum at  $0.4r_0$  before tailing off. Again, this might be of significance for a very sharp probe but not for ones of larger radius. Although the possibility has been considered that it might be shear stress rather than pressure stress which causes electrical change in the diode, this idea has been abandoned since no such change consistent with the rise of stress with depth has been observed.

## 6 ELECTRICAL MEASUREMENTS

### (a) Preliminary investigations

On applying stress with a diamond probe of radius 25  $\mu\text{m}$  and forces ranging from 1 to 10 grams Konidaris observed a reversible increase in current within the GR range of 5 nA to 10  $\mu\text{A}$ , but reported that there was no change above this in the LE region. With a glass probe of large radius (1.2 mm) and a force of 300 grams he reported that again there was no electrical effect in the LE region, but there was a small spectral shift in the light output. With the probe of radius 25  $\mu\text{m}$  the current changes  $\Delta I$  in the GR region were comparatively large, of the order of 10 per cent or more, the percentage being independent of the diode current but markedly dependent on the force  $F$ ; the form of the relationship was

$$\Delta I \propto \exp(F/F_0), \text{ where } F_0 \text{ is a constant.}$$

In the present research these observations were initially repeated with a crude arrangement for applying similar forces on a 25  $\mu\text{m}$  probe and with a 1  $\mu\text{A}$  meter at three-quarters full-scale deflection; the positive change



Facing  
p.47

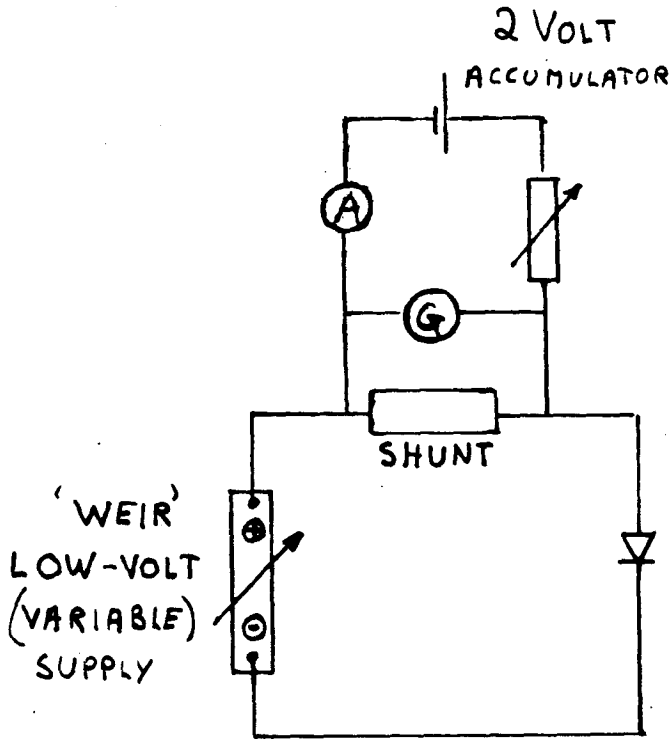


Fig.34. Constant voltage circuit

in the GR region did in fact take place, but the effect seemed to be only partially reversible and the "black spot" damage was very prominent. On the other hand a force of 1 gram on a diamond probe of radius 75  $\mu\text{m}$  did not cause any permanent damage and at the same time produced a very small decrease in the microammeter deflection. Thus  $\Delta I$  was the opposite way round; ie it was negative. For the most part the deflection was so small (less than 1 per cent) that a pocket lens was required for accurate observation; nevertheless it seemed to be perfectly reversible. With the same small stress of a 1 gram force on the 75  $\mu\text{m}$  probe a very small change in current also occurred in the LE region with a milliammeter set near the full-scale deflection of 1 mA, as it had done in the GR region with meters going up to 1  $\mu\text{A}$  (and 10  $\mu\text{A}$ ).

At this point the mechanical stage described in Appendix A was built so that much smaller forces of 100-10 mgm could be applied, and at the same time a circuit (Fig 34) was designed whereby the current through the diode could be balanced out giving a zero reading on a sensitive

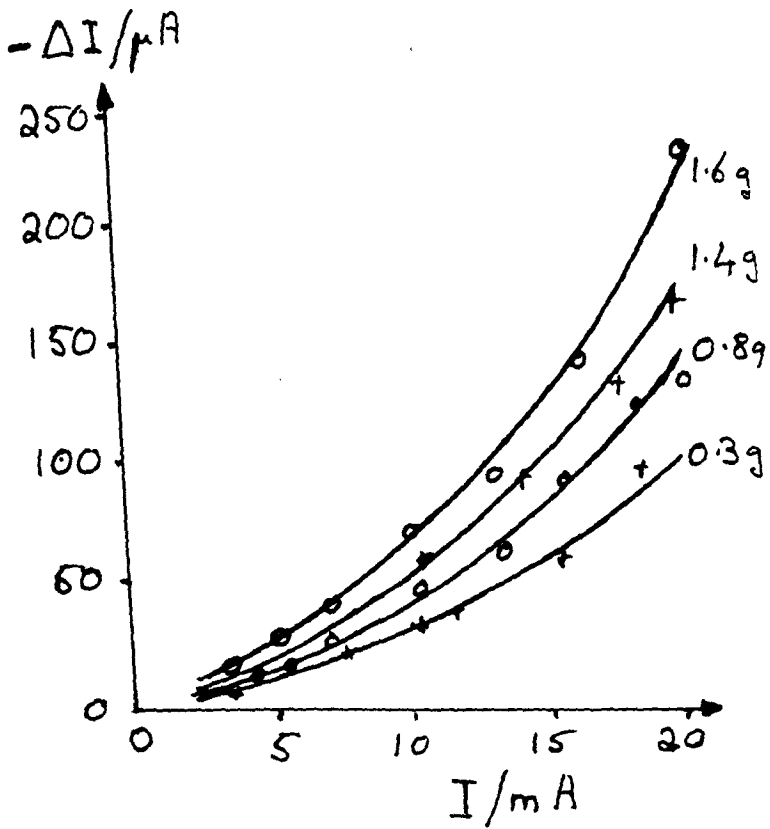


Fig.35. 75  $\mu m$  diamond probe

galvanometer; thus any small change in current when applying stress showed up directly as a large galvo deflection. For the most part readings were taken in the LE region of about 0.1 - 10 mA, the problem of sensitivity being very much less at higher currents; also it was in this region that no electrical change with stress had previously been recorded. All three diamond probes were used, but since the largest probe of radius 75  $\mu\text{m}$  gave the highest electrical change, most of the readings were taken with this. Typical results for four forces are indicated in Fig 35; the force of 1.6 gram was probably above the elastic limit but it did not seem to affect the electrical performance. Analysis showed the curves to be parabolic, ie  $-\Delta I$  varies as  $I^2$  for a given force.

The important conclusion drawn at this stage was that the change of current was negative and that it was reversible on removal of the stress. The galvanometer showed an instantaneous deflection on application of stress, this deflection being followed by a slow drift in the opposite direction; at the time (mid-1979) this drift

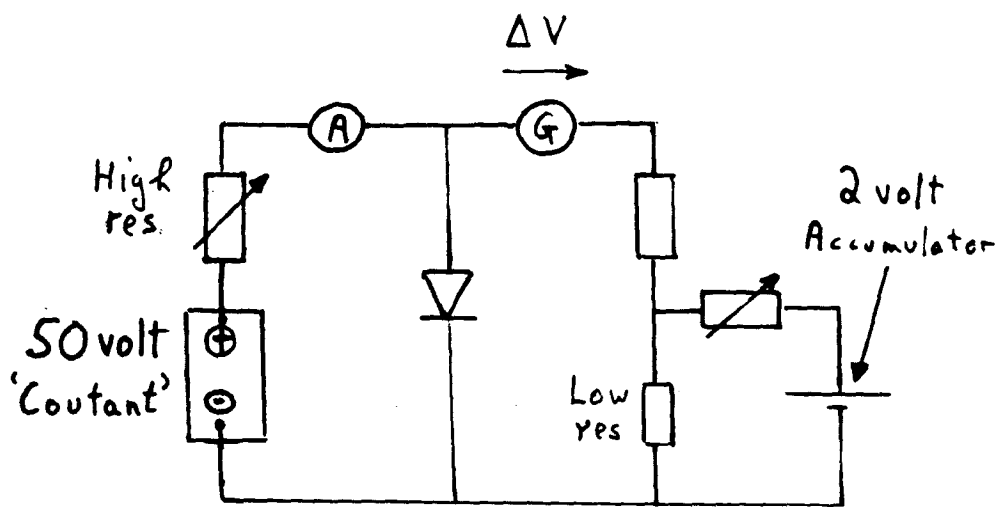


Fig.36. Constant current circuit

was recognised as being a temperature effect and was recorded as such (23), but its full significance was not realised at this stage. However, when the drift had ceased the circuit could be adjusted to give zero on the galvanometer, and then removal of the stress gave a deflection that was the reverse of the original one.

The circuit of Fig 34 shown on p.47 ensured that the voltage across the diode was kept constant and the current change measured directly. The main practical difficulty was that any adjustment in the diode current was extremely tedious since, a very small variation in voltage caused a large current change. Consequently an alternative circuit was devised (Fig 36) in which the current through the diode was kept constant and any effect due to stress was recorded as a voltage change on the galvanometer. In this latter circuit the constant current was ensured by having a comparatively large voltage supply ("Coutant", 50 volts) in series with a very high resistance and the diode; the balancing was obtained by means of a low-voltage supply on the other side of the circuit. The results for the same

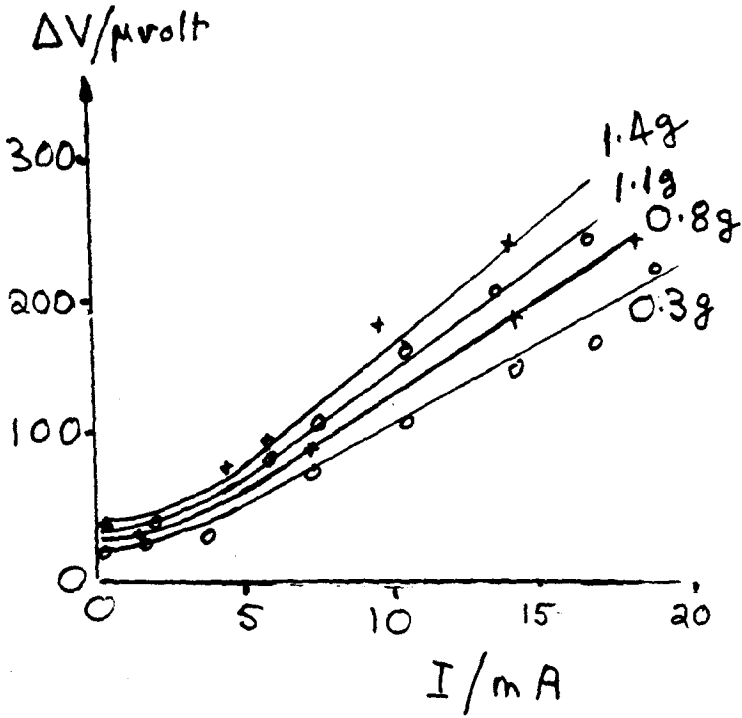


Fig.37. 75  $\mu$ m diamond probe

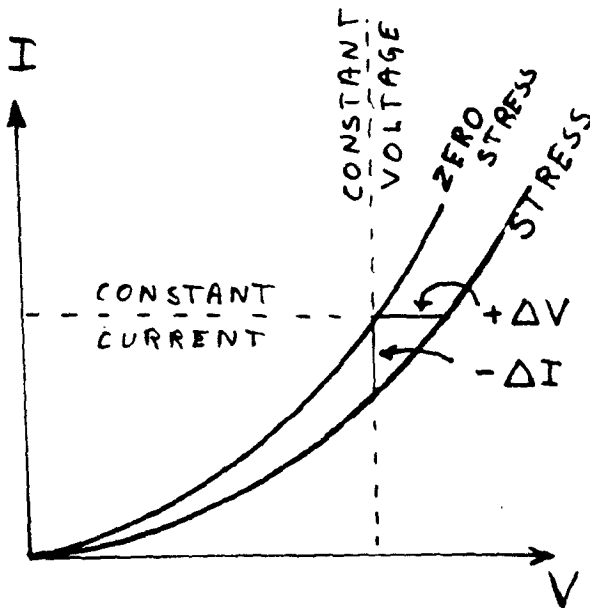


Fig.38

forces on the same probe and diode are shown in Fig 37. In both circuits of Figs 34 and 36 the galvanometer was an electronic chopper-type "Galvamp" of full-scale deflection 90 nA or 90  $\mu$ V (1000 ohms resistance); in the former case its sensitivity was adjusted by a shunt, which was very inconvenient, and in the latter by the much more easy method of a series resistance (a further reason for preferring the 'constant current' circuit).

A number of results emerge from drawing a comparison between the graphs of Figs 35 and 37. First, the current change  $\Delta I$  with stress is negative, but this shows up in the circuit of Fig 36 as a positive voltage change  $\Delta V$ . This can be explained by reference to Fig 38. The current-voltage relationship as described in Section 4 (a) is essentially an exponential curve; if the corresponding curve under stress is similar but very slightly displaced then a negative  $-\Delta I$  at a constant voltage would correspond to a positive  $\Delta V$  at a constant current, and the relation between them, namely  $\Delta V/|\Delta I|$ , equals the a.c. resistance  $R_{ac}$ .



Since  $I = I_0 \exp(qV/nkT)$  then  $\frac{dI}{I} = \frac{q}{nkT} dV$ .

Thus for a linear relation when  $\Delta V$  varies as  $I$  for a given stress (Fig 37) the corresponding relation for  $-\Delta I$  should be  $-\Delta I/I$  varies as  $I$ , or  $-\Delta I$  as  $I^2$ , ie a parabolic dependence as shown in Fig 35. The numerical agreement is also satisfactory; for example, from Figs 35 and 37 at  $I = 13 \text{ mA}$ ,  $-\Delta I = 100 \text{ } \mu\text{A}$  and  $\Delta V = 250 \text{ } \mu\text{V}$ . Thus the ratio of 2.5 ohms is consistent with the value of  $dV/dI$  as found from the characteristic of Fig 19:-  $nkT = 0.0326 \text{ eV}$  so that at  $I = 13 \text{ mA}$   $R_{ac} = 0.0326 / (13 \times 10^{-3}) = 2.5 \text{ ohms}$ .

This matter of the conversion of  $\Delta V$  from a constant current situation to the equivalent  $\Delta I$  that would be obtained if the diode were under a constant voltage is so crucial to all the experimental readings recorded in this research that it is considered in greater detail in Appendix C; also to be considered is the approximation involved in assuming a simple relation of the form  $I = I_0 \exp(qV/nkT)$ , and this is discussed in Appendix B.

Finally, in addition to the preliminary measurements

Facing  
p.52

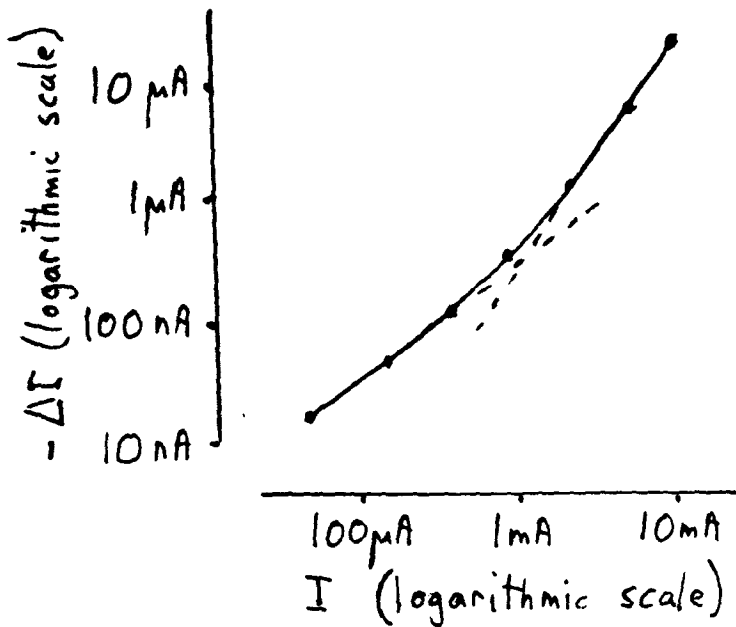


Fig.39. 0.8 gram on 75  $\mu\text{m}$  diamond probe;  
 $P_0 = 1.3 \times 10^4$  atm.

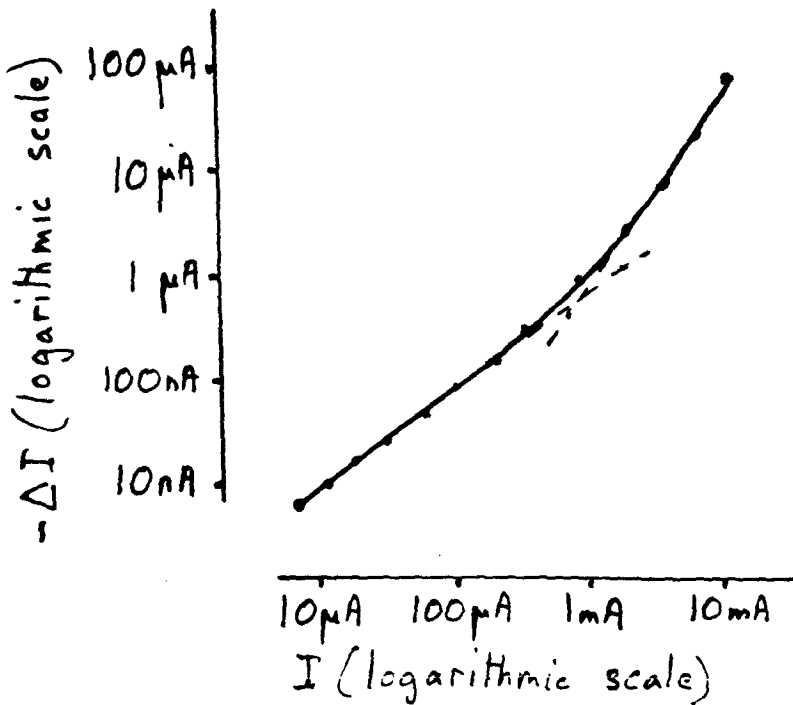


Fig. 40. 3.0 grams on 200  $\mu\text{m}$  sapphire probe;  
 $P_0 = 0.98 \times 10^4$  atm.

in the LE region as recorded above, further measurements were taken in the GR region using the constant current circuit of Fig 36. These became progressively more difficult to make because, as the current was reduced, so random fluctuations on the galvanometer became more pronounced; the moment stress was applied a quick assessment had to be made of the galvanometer deflection before it wandered off the scale. Repeated readings with averaging were necessary. However, when plotted on a logarithmic scale as shown in Figs 39 and 40 the following consistent pattern emerged: whereas in the LE region the slope is  $2.0 \pm 0.1$  (ie the parabolic relation observed in Fig 35), in the GR region the slope is  $1.0 \pm 0.1$ . Thus in the GR region  $\Delta I$  is still negative and reversible, but the dependence on the current is less than that prevailing in the LE region, the transition point being approximately the same as that observed in the current -voltage characteristics of the diode.

In connection with these two graphs it should be noted that they were originally reported<sup>(23)</sup> with the slope

in the GR region somewhat flatter. However later on, as explained in Appendix B, it was realised that, in calculating the current change from the galvanometer deflection, allowance had not been made for the increase in the a.c. resistance  $R_{ac}$  of the diode in going from the LE to the GR region.

(b) Electrical changes under varying stress

As already stated in Section 2, it was early in 1979 when a range of sapphire probes going up to a radius of curvature of 1000  $\mu\text{m}$  was acquired. At the same time it was realised that the circuit of Fig 36, whereby  $\Delta V$  was measured in a constant current situation, was in reality not very different from a conventional Wheatstone bridge and that it could be modified into this latter form using only one constant-voltage supply.

The basic technique was to balance the bridge initially and then to record the voltage  $V_G$  of the deflection that was registered on a sensitive galvanometer when the diode was stressed by a force  $F$  applied to a particular probe. Further details of the bridge are given

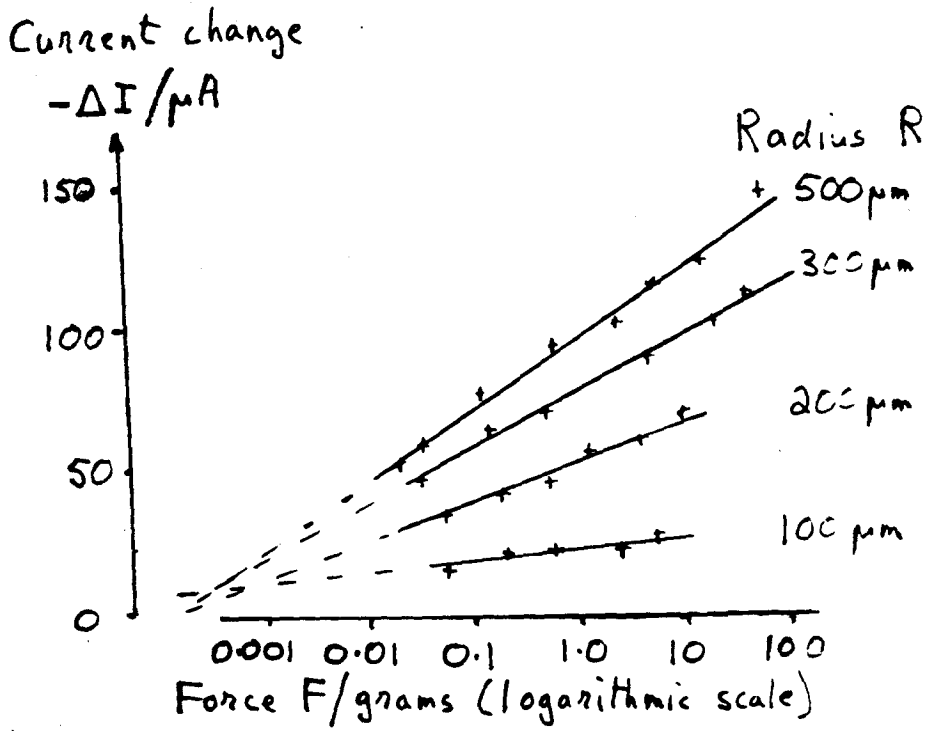


Fig.41. I = 1 mA; LE region

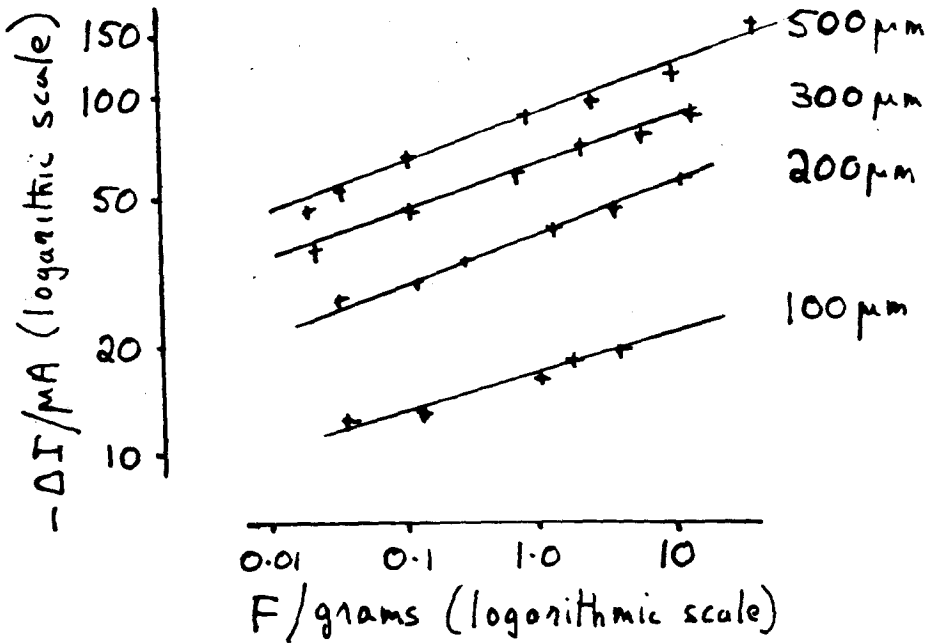


Fig.42. I = 1 mA; LE region

in Appendix E. For the most part the current was adjusted to approximately 10 mA, 1 mA, 100  $\mu$ A and 10  $\mu$ A with an intermediate reading of about 3.16 in each decade (ie a logarithmic half-way step). This method was adopted because it was far easier to adjust the current than to change a force or probe. By proceeding in this way and loading each probe with an appropriate range of forces (taking care not to exceed the elastic limit), it became possible to select the data so that the current change could be tabulated over a range of forces and probes for a fixed current. The pattern that emerged was fairly consistent, and an example is shown in Fig 41, the diode current being a constant 1 mA throughout, ie in the LE region.

From Fig 41 there appears to be an empirical relation of the form  $-\Delta I \propto \log F$ , and although at the time (in 1979) it was thought that this might be of some significance on subsequent consideration it has been deemed to be of no consequence. Another possibility is suggested by the log-log graphs of Fig 42, and from the slopes an alternative empirical relation emerges, namely

Facing  
p.55

Current change  
 $-\Delta I/\mu A$

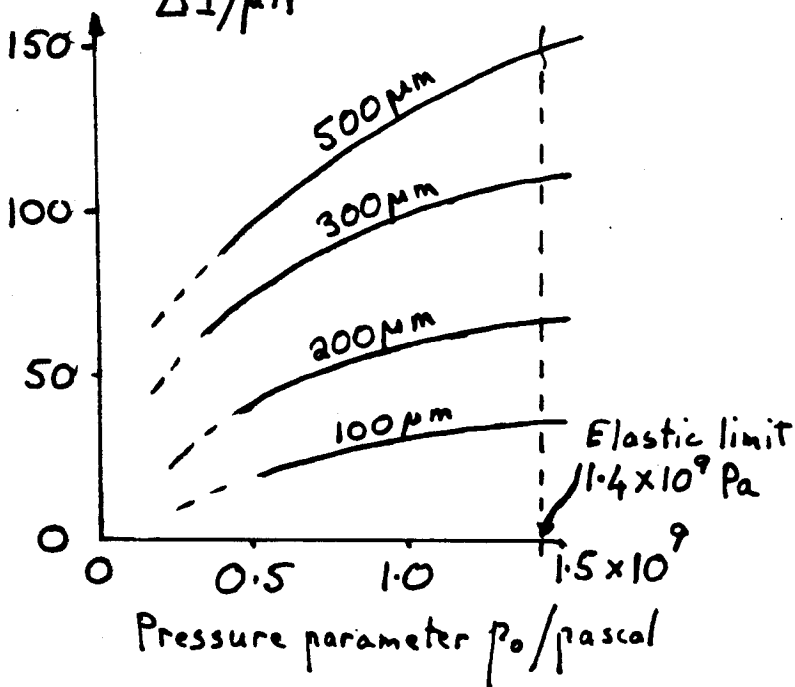


Fig.43

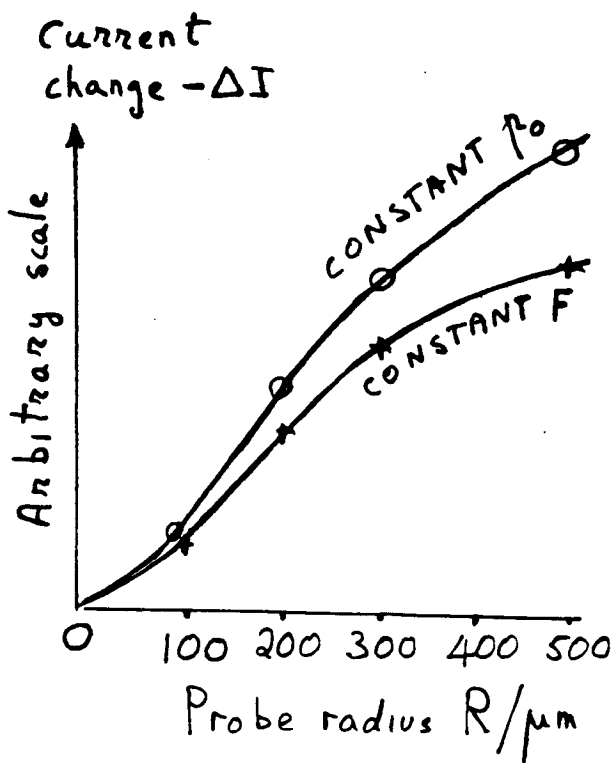


Fig.44

$-\Delta I \propto F^{0.12}$ ; this too has been discarded as being of no significance.

From Section 5(a) it can be seen that there is a basic relation  $F \propto p_0^3 R^2$ , where  $p_0$  is the maximum pressure under a probe of radius  $R$ , and Fig 25 (p.38) shows a series of curves for determining the relation between these parameters. Using this diagram the force  $F$  can be converted into the stress parameter  $p_0$ , and the curves for the current change  $-\Delta I$  versus  $p_0$  were constructed as shown in Fig 43; because of the theoretical relation  $F \propto p_0^3$  and the empirical relation given above, the curves are approximately  $-\Delta I \propto p_0^{0.36}$ .

Finally a graph of  $\Delta I$  (for the given current of 1 mA) versus the probe radius  $R$  was constructed for constant  $F$  and constant  $p_0$  (Fig 44), from which it can be seen that there is a rough linearity for constant  $p_0$ . During the time all the above readings were taken, the two largest probes of radius 750 and 1000  $\mu\text{m}$  respectively were not used because of the fear that they might break the fine wire connecting the diode to the heat sink (as explained



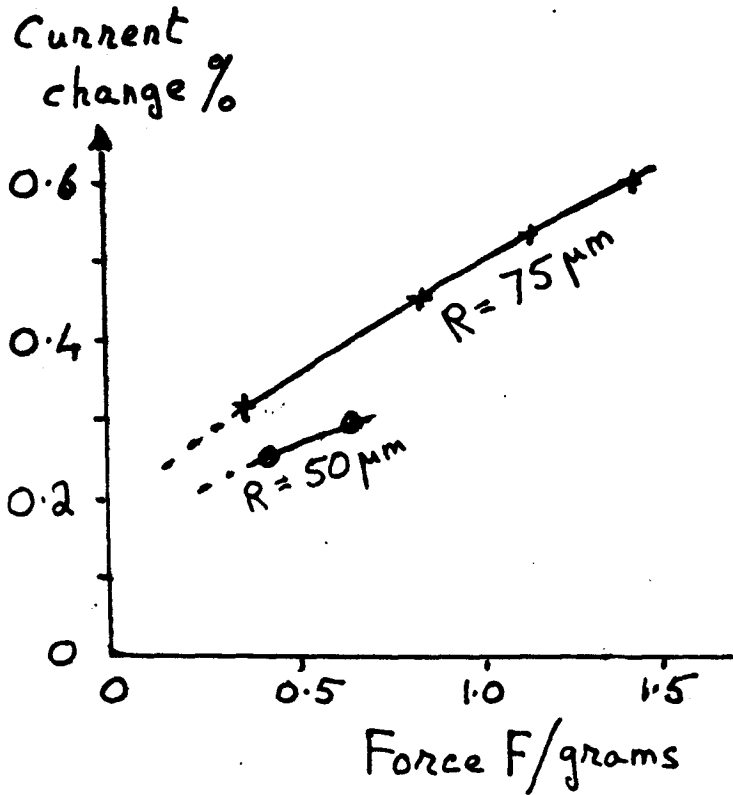


Fig.45. I = 10 mA (LE region)

in Appendix A, p.150).

When the above results first emerged no satisfactory explanation for them could be advanced; in particular the difficulty of reconciling the empirical relations of Figs 41, 42 or 43 with the approximate linearity of Fig 44 was especially awkward. Indeed the problem had already shown up as early as 1977 with the readings of Fig 35. If one takes a fixed current, say 10 mA, and plots  $-\Delta I$  against force  $F$  a graph such as Fig 45 is obtained; also shown are a couple of readings for the 50  $\mu\text{m}$  probe. The problem can be posed as follows: Why are the curves heading towards a large intercept on the  $-\Delta I$  axis? Surely at zero force  $-\Delta I$  must also be zero. Returning to Fig 41, it had been anticipated that a relation of the form  $-\Delta I \propto F$  might have emerged or even an exponential the other way round, namely  $-\Delta I \propto \exp F$ ; this latter was the form that Konidaris found although, of course, his  $\Delta I$  was positive.

Thus for some time the results obtained remained a mystery. Fulop and Konidaris <sup>(1)</sup> had originally pointed out in connection with the latter's observations that the

important aspect was not the damaging, though very localised, stress immediately under the probe but the highly anisotropic distribution over the diode; this stress would decrease very rapidly with distance from the centre and therefore would soon be well within the elastic limit, but at the same time it would cover the whole of the junction interface and hence should have a relatively large overall effect on the electrical performance. However, their theory did not include any detailed analysis of how this stress might in fact vary, and so it was decided to pursue classical elastic theory as described in the next section.

In the meantime, because a sensitive experimental arrangement had been devised, it was decided to investigate whether a moderately strong magnetic field would affect the performance of the LED. The diode was orientated in various directions between the poles of a permanent, horse-shoe magnet, the field strength between the poles being approximately 0.16 tesla (or 1600 gauss) as measured on a 'gaussmeter'. The technique was to bring

up the magnet abruptly across the diode, but no significant deflection on the galvanometer was observed.

## 7 DISTRIBUTION OF STRESS OVER THE JUNCTION INTERFACE

### (a) Advanced theory of stress

Up to this point the numerical value of stress has only been considered at the central point of contact between probe and diode and at a depth vertically below this. Obviously, if stress is going to have an overall effect on the electrical performance of an LED, one must consider how it is distributed throughout the junction interface. A classical paper that contains all the basic equations for making this calculation is one by S. Fuchs (24) published in 1913, an involved piece of applied mathematics that is not made any easier by being written in difficult German. Fuchs acknowledges his sources as being first and foremost the famous Heinrich Hertz, who made a start on the problem in 1881 (25), and also other workers at the beginning of this century.

The equations given below are the ones set out by Fuchs except that the symbols have been changed to conform with those of Section 5. Fuchs starts by considering the radius  $r_0$  of the contact area between probe and flat

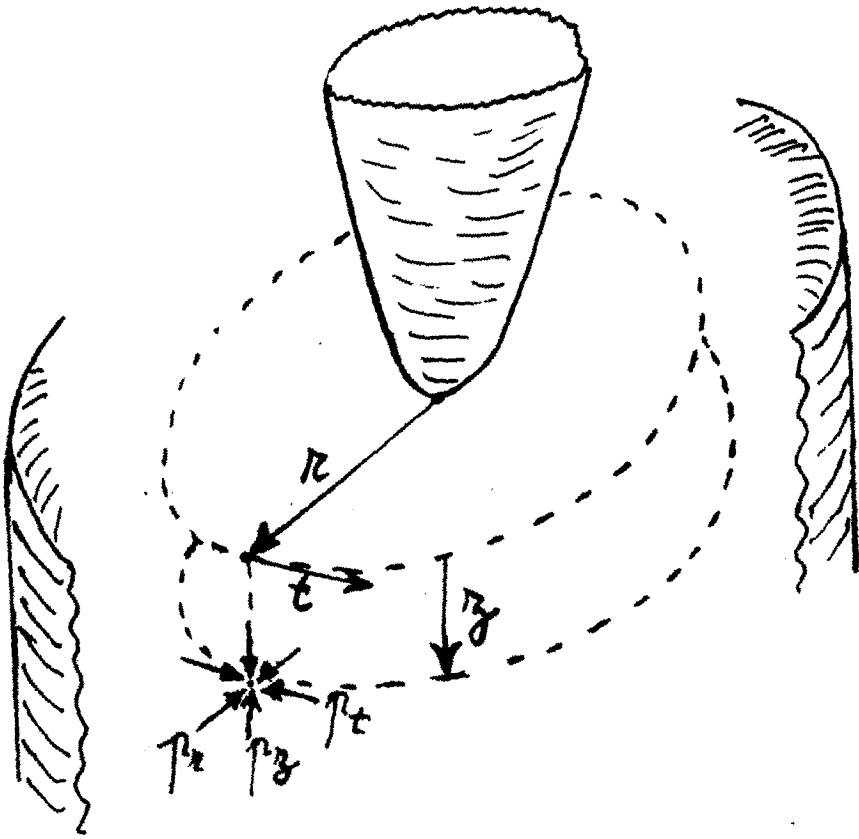


Fig.46

surface and deduces the average pressure  $p_{av}$  exerted by a force  $F$  over the area  $\pi r_o^2$ . He then defines a pressure  $p_o$  from  $p_o = \frac{3}{2} p_{av}$  which turns out to be the same  $p_o$  as given in Section 5. He also quotes relations for  $p_o$  and  $r_o$  in terms of the force, the radius of the spherical body, Poisson's ratio  $\sigma$  and Young's modulus  $E$  for the materials, all of which are again the same as given in Section 5.

The Fuchs theory then deals with the general situation of the radial, tangential and depth pressure  $p_r$ ,  $p_t$  and  $p_z$  at a point within the material on a radius  $r$  and at a depth  $z$  (Fig 46). Using a further parameter  $u$  defined as

$$u^2 = \frac{1}{2} \left\{ r^2 + z^2 - r_o^2 + \left[ (r^2 + z^2 - r_o^2)^2 + 4r_o^2 z^2 \right]^{1/2} \right\}$$

Fuchs quotes the stresses as follows

$$p_r = -p_o \left\{ \frac{(1-2\sigma)}{3} \left( \frac{r_o}{r} \right)^2 \left[ 1 - \left( \frac{z}{u} \right)^3 \right] + \left( \frac{z}{u} \right)^3 \left[ \frac{r_o^2 u^2}{u^4 + r_o^2 z^2} \right] + \frac{z}{u} \left[ \frac{(1-\sigma)u^2}{r_o^2 + u^2} + (1+\sigma) \frac{u}{r_o} \tan^{-1} \left( \frac{r_o}{u} \right) - 2 \right] \right\}$$

$$p_t = p_o \left\{ \frac{(1-2\sigma)}{3} \left( \frac{r_o}{r} \right)^2 \left[ 1 - \left( \frac{z}{u} \right)^3 \right] + \frac{z}{u} \left[ 2\sigma + \frac{(1+\sigma)u^2}{r_o^2 + u^2} - (1+\sigma) \frac{u}{r_o} \tan^{-1} \left( \frac{r_o}{u} \right) \right] \right\}$$

$$p_z = p_o \left( \frac{z}{u} \right)^3 \left[ \frac{r_o^2 u^2}{u^4 + r_o^2} \right]$$

These equations appear at first sight to be rather formidable, and no doubt in 1922 when Prof. W.B. Morton and L.J.Close, of Queen's University, Belfast, produced numerical results for different angular directions in space, which they published as sets of curves (14), the calculations were extremely laborious. Other workers in more recent years have also produced sets of curves (26), but none of them is in a form that is particularly useful for the present research in which the value of the stress at a particular depth, namely along the plane of the junction interface, is required.

However, with modern computer facilities complicated numerical calculations are no longer a problem. The Fuchs equations were converted into a numerical, non-dimensional form by expressing the distances  $r$ ,  $z$  and  $u$  in terms of the contact radius  $r_o$ , and the stresses as a fraction of the pressure term  $p_o$ . Then it was relatively straightforward to devise a program in BASIC and obtain tabulated



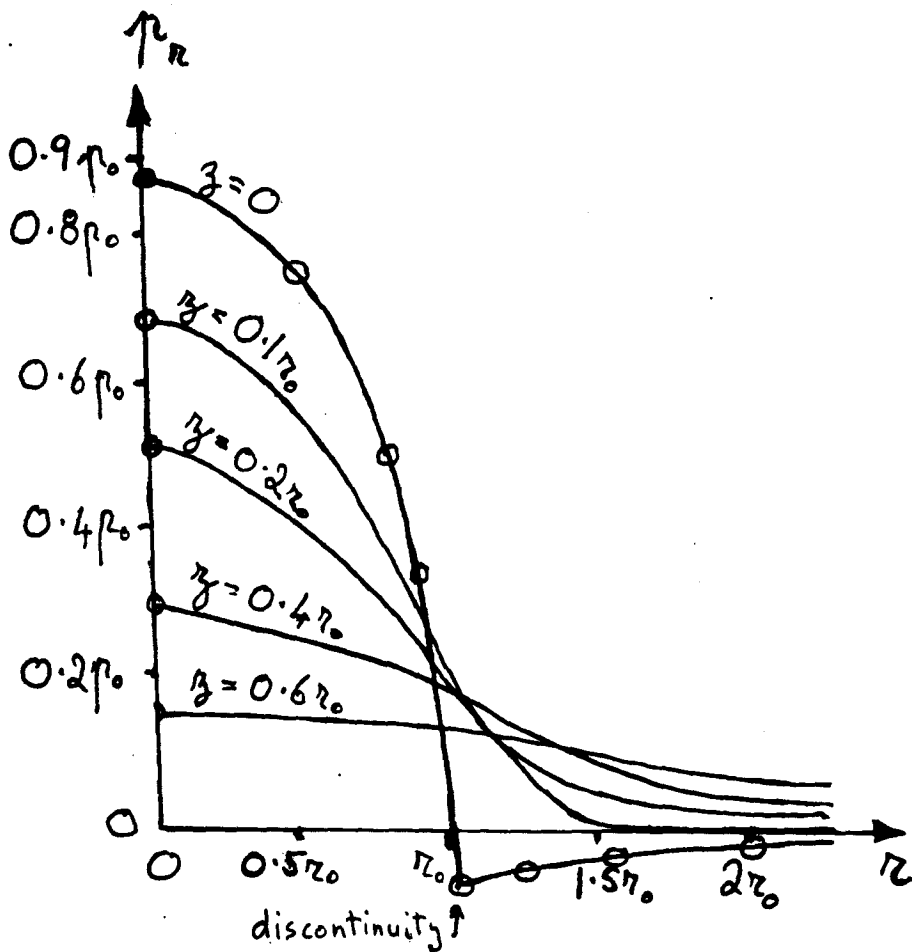


Fig.47. P.T.O. for Figs.48 and 49

values on the PRIME computer facility of South London College. From the computer print-out numerical values of  $p_r$ ,  $p_t$  and  $p_z$  for a number of depths  $z$  have been selected, and these are shown in Figs 47, 48 and 49; throughout the calculations, Poissons's ratio has been taken to be 0.37.

Since the computer will not handle special cases when  $z = 0$  or  $r = 0$  (and even putting  $z = 0.001 r_0$  etc) is not feasible because of difficulties in the solution of the quadratic in  $u$ ), the equations were reduced to simplified forms in these special circumstances. Thus when  $z \rightarrow 0$  there are two possibilities, the first being for values of  $r < r_0$  (ie under the probe); in this case  $u \rightarrow 0$  and the pressure stresses reduce to

$$p_r = p_0 \left\{ \left[ 1 - \left( \frac{r}{r_0} \right)^2 \right]^{1/2} - 0.0867 \left( \frac{r}{r_0} \right)^2 \left[ 1 - \left( 1 - \left( \frac{r}{r_0} \right)^2 \right)^{3/2} \right] \right\}$$

$$p_t = p_0 \left\{ 0.74 \left[ 1 - \left( \frac{r}{r_0} \right)^2 \right]^{1/2} + 0.0867 \left( \frac{r}{r_0} \right)^2 \left[ 1 - \left( 1 - \left( \frac{r}{r_0} \right)^2 \right)^{3/2} \right] \right\}$$

$$p_z = p_0 \left[ 1 - \left( \frac{r}{r_0} \right)^2 \right]^{1/2}$$

In the very special case of  $r = 0$ ,  $z = 0$  (ie at the

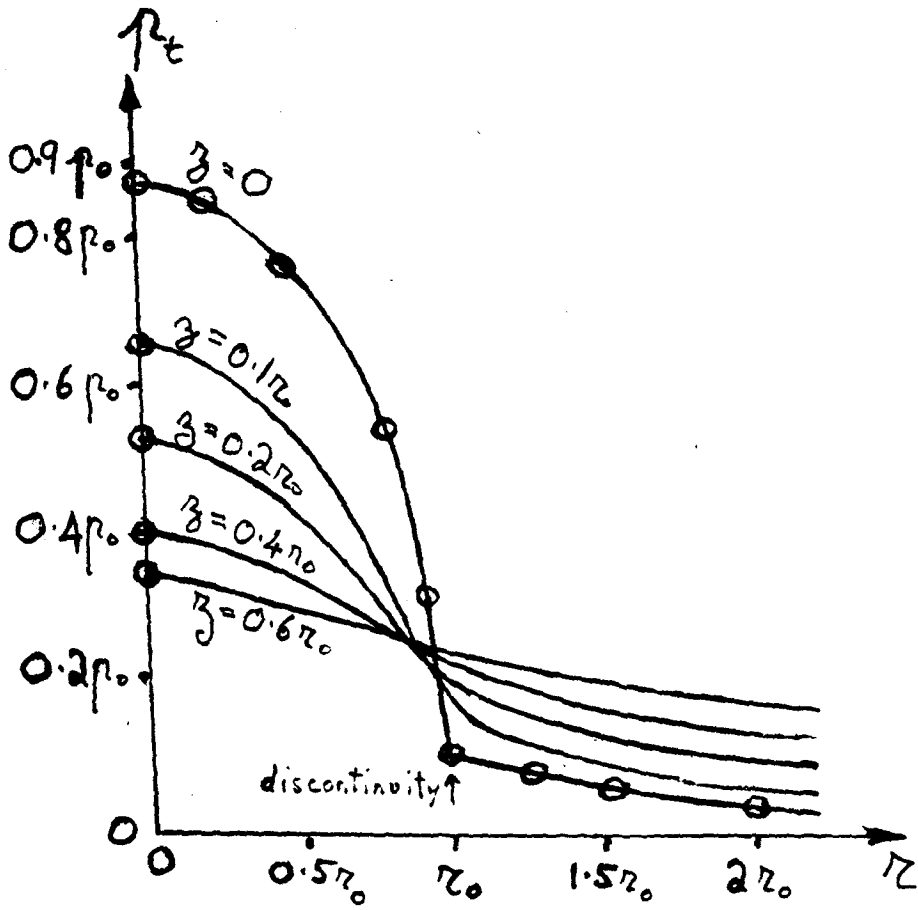


Fig.48. P.T.O. for Fig.49

central point of contact of the probe)  $p_r = p_o (1 - 0.13)$   
 $= 0.87p_o$  and  $p_t = p_o (0.74 + 0.13) = 0.87p_o$ ; thus  $p_r$  and  
 $p_t$  both reduce to the same value of  $0.87p_o$ , and in addit-  
 ion  $p_z$  reduces to  $p_o$ . These values fit in well with the  
 computer derived curves of Figs 47, 48 and 49.

The second possibility for  $z = 0$  is for values of  
 $r \geq r_o$  (ie outside the probe contact area) when  $u^2 \rightarrow$   
 $(r^2 - r_o^2)$ ; then the pressure components become

$$p_r = -0.067p_o (r_o/r)^2, \quad -p_r = p_t \quad \text{and} \quad p_z = 0$$

These results are also very satisfactory in as much as the  
 sum  $p_r + p_t + p_z = 0$ . As explained later on in this  
 section the total pressure is the algebraic (and not the  
 vectorial) sum of the components so that, as might be  
 expected, for the top surface of the diode which is not in  
 contact with the probe the stress is zero. Also, in this  
 region the radial component  $p_r$  is negative and therefore  
 indicates a stretching rather than compression; this too  
 is to be expected.

From all the above simplified equations numerical  
 values were easily determined on a pocket calculator, and

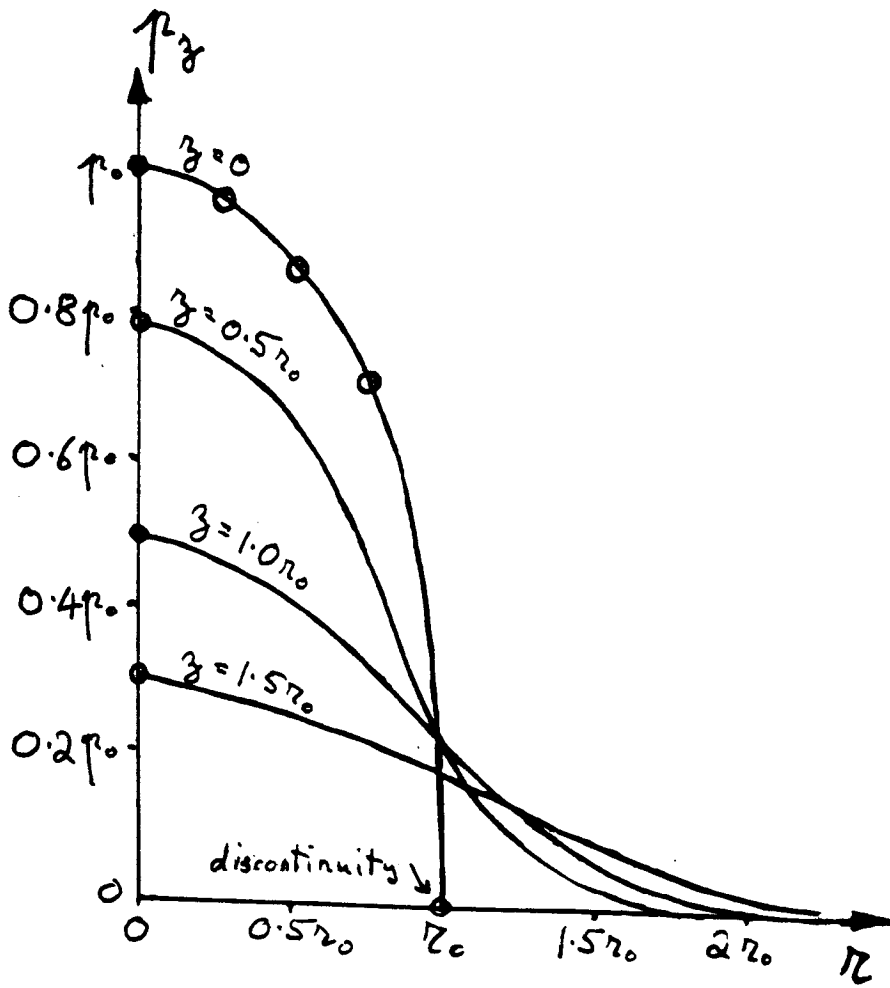


Fig.49. P.T.O. for Fig.50

they are shown as circled points  $\odot$  on the graphs; the fact that the points tie in with the curves derived from the computer greatly increases confidence that the latter correctly interpret the Fuchs equations.

For the special case when  $r \rightarrow 0$ , then  $u \rightarrow z$  and

$$p_r = p_o \left[ \frac{0.87r_o^2 + 1.37z^2}{r_o^2 + z^2} - 1.37 \frac{z}{r_o} \tan^{-1} \left( \frac{r_o}{z} \right) \right]$$

$$p_t = p_o \left[ \frac{0.87r_o^2 + 2.11z^2}{r_o^2 + z^2} - 1.37 \frac{z}{r_o} \tan^{-1} \left( \frac{r_o}{z} \right) \right]$$

$$p_z = p_o \left( \frac{r_o^2}{r_o^2 + z^2} \right)$$

Taking the values of  $p_r$  and  $p_z$  at  $r = 0$  the variation of pressure with depth down the vertical axis of contact can be determined and plotted graphically as shown in Fig 50; this proves to be the same as that quoted by Lipson and Juvinall, as discussed in Section 5 (see Fig 33, p.44), and also agrees with a corresponding diagram by Morton and Close, allowance being made in each case for a slight difference in Poisson's ratio. Both pairs of workers point out the obvious fact that down the central axis  $p_r$  and  $p_t$  must be identical, and the only disturbing

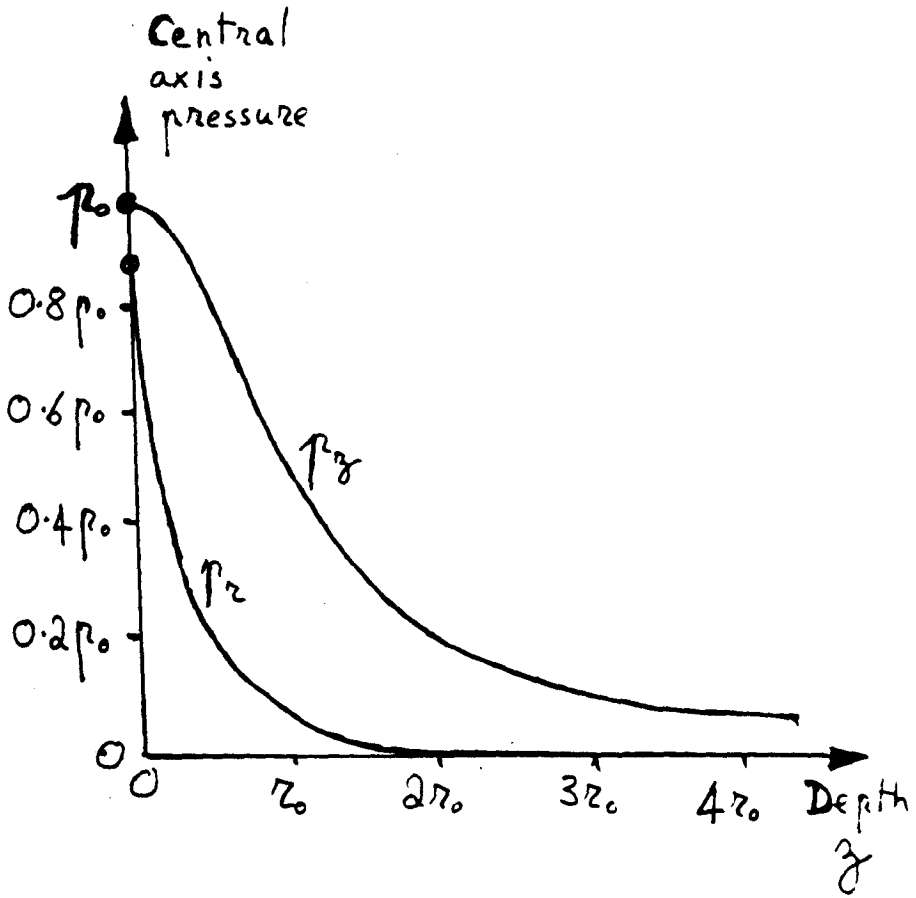


Fig.50

feature that emerges from the present research is that, if one starts from the original Fuchs equations, this does not appear to be the case for large values of  $z$  although it is true at shallow depths. Thus in the above simplified equations for  $r = 0$ , when  $z$  approaches infinity  $p_r$  and  $p_z$  tend to zero but  $p_t$  tends to  $2\sigma p_0$  (or  $0.74 p_0$ ), and this latter obviously cannot be true.

The immediate conclusion to be made is that there is something wrong with the Fuchs equation for  $p_t$ . One makes this statement with a great deal of diffidence in view of the fact that distinguished workers quoted in the references acknowledge Fuchs as their source and yet make no comment on this apparent inconsistency. Morton and Close point out that Fuchs "carried out a laborious process of arithmetical integration" and that other workers adopted a different approach and yet arrived at the same result. There arises the possibility that approximations are involved which only work satisfactorily at shallow depths. Indeed it may well be that specialists in this field already know about this and that one has



failed to examine the relevant literature. The line taken in the present research is that the computer curves for  $p_x$  and  $p_z$  are almost certainly correct and that, although the anomalous behaviour of  $p_t$  is worrying in that it appears to go astray at large values of  $z$ , it is satisfactory at the shallow depths and up to the large radial distances with which the present research is concerned.

Bearing this in mind, it was decided to explore what part pressure might play in the behaviour of an LED under stress. One possibility was that  $p_z$ , the stress at right angles to the junction interface, could be the relevant factor; an alternative could be the total effective pressure acting throughout the interface, (ignoring the complication that the medium is a crystal and treating it as if it were a simple isotropic solid). In the present research a decision was initially made in favour of the latter approach in view of the fact that other workers (3,7) had tried to tie in their readings with previously published results for the change in band gap  $E_G$  of various semiconductors under large hydrostatic

pressure; in particular Konidaris <sup>(7)</sup> performed the very interesting experiment on an LED which is discussed in the next sub-section.

According to classical elasticity theory <sup>(27)</sup>, if  $E$  is Young's modulus and  $\sigma$  Poisson's ratio, then the strains  $e_r$ ,  $e_t$  and  $e_z$  brought about by stress  $p_r$ ,  $p_t$  and  $p_z$  are

$$e_r = [p_r - \sigma(p_t + p_z)]/E$$

$$e_t = [p_t - \sigma(p_z + p_r)]/E$$

$$e_z = [p_z - \sigma(p_r + p_t)]/E$$

By the same theory these strains are scalar quantities that can be added together to give a 'dilatation' or volume strain  $dV/V$ . Therefore adding the above equations gives

$$dV/V = (p_r + p_t + p_z) (1 - 2\sigma)/E$$

However, hydrostatic pressure  $p_{hyd}$  and the resulting dilatation are related by the bulk modulus of elasticity  $K$  whereby

$$p_{hyd} = K dV/V$$

Again, from classical theory there is the following relation between  $E$  and  $K$ , namely  $E = 3K (1 - 2\sigma)$ .

Combining the above gives the effective hydrostatic pressure  $p_{hyd}$  as

$$p_{hyd} = (p_r + p_t + p_z)/3.$$

Given this somewhat surprisingly simple result, which is quoted by Ridner and Braun<sup>(3)</sup>, one can inspect the original Fuchs equations and note that in adding them together one pair of brackets cancels out and another pair adds up. The result is a less complex relation

$$P_{hyd} = \frac{P_r + P_t + P_z}{3} = \frac{2p_0}{3} \left[ \frac{z}{u} \left( 1 + \sigma + \left( \frac{\sigma u^2}{r_0^2 + u^2} \right) - \frac{z}{r_0} (1 + \sigma) \tan^{-1} \left( \frac{r_0}{u} \right) \right] \right]$$

In the special case when  $z \rightarrow 0$  and  $r < r_0$ , ie the surface of the diode in contact with the probe, this reduces to

$$P_{hyd} = 0.913 p_0 \left[ 1 - \left( \frac{r}{r_0} \right)^2 \right]^{1/2}$$

In the other special case when  $r \rightarrow 0$ , ie down the central axis of contact, this reduces to

$$P_{hyd} = \frac{1}{3} p_0 \left[ \frac{2.74 r_0^2 + 3.48 z^2}{r_0^2 + z^2} - 2.74 \frac{z}{r_0} \tan^{-1} \left( \frac{r_0}{z} \right) \right]$$

As in the previous cases, sets of curves for different values of  $z$  were obtained by processing the general equation for  $P_{hyd}$  on the PRIME computer, and some of these curves are shown overleaf in Fig 51. For the case

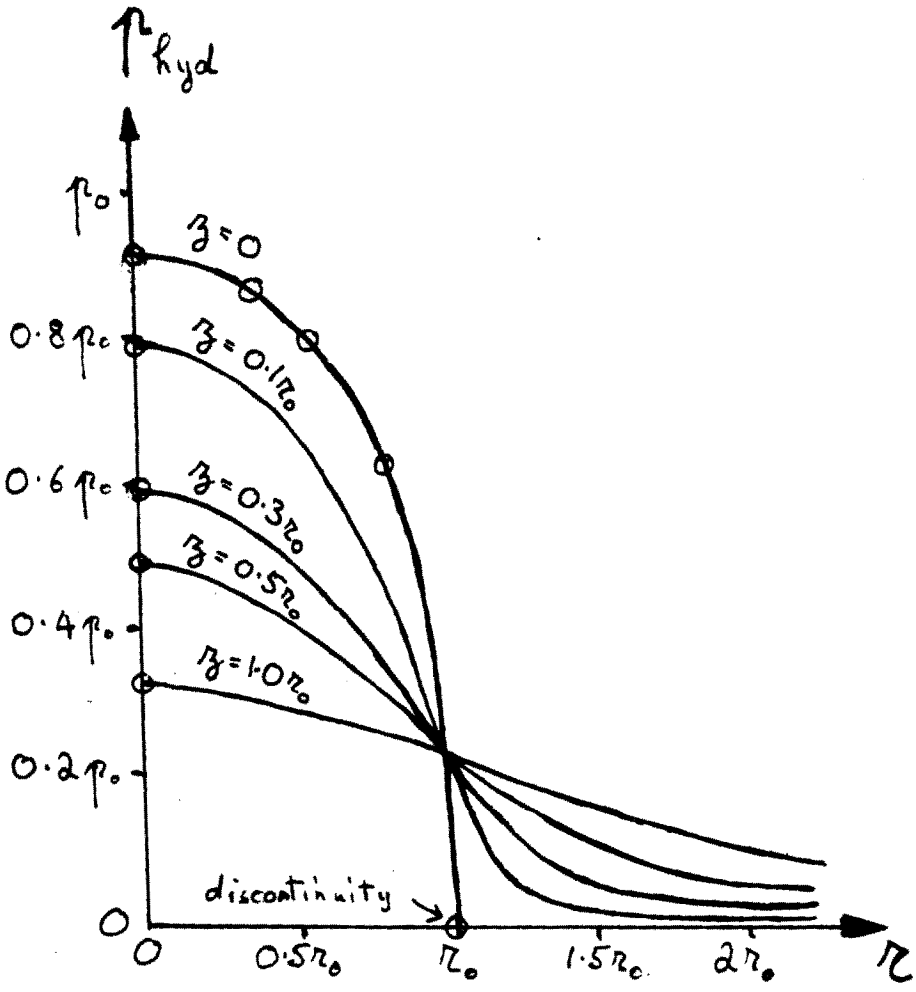


Fig.51

of  $r = 0$  and  $z = 0$  the special simplified equations were used and the readings (shown as  $\Theta$ ) were obtained with the aid of a pocket calculator. A prominent feature of the results is that outside the probe contact area the pressure at the surface of the diode ( $z = 0$ ) is zero, a result which is to be expected. Also, it is to be noticed that the overall appearance presents a pattern which is more continuous for a wide range of  $r$  and  $z$  than do the corresponding graphs of  $p_r$ ,  $p_t$  and  $p_z$ ; an example of this is that the  $p_{hyd}$  curves all cross one another almost exactly at a single point. Since  $p_{hyd}$  is a measure of the total stress in the material at any point, perhaps it is not surprising that the curves give a more realistic impression than the individual components that go to make up this stress. Detailed discussion of the application of the curves is given in the following two sub-sections.

(b) Spectral shift experiment of Dr S. Konidaris

For this experiment (7) Konidaris pressed a glass probe of large radius of curvature (1.2 mm) against an LED with forces ranging up to 300 grams. The light emitted by the

diode was collected by the glass probe acting as a lens, and by a sensitive spectrometer technique a slight decrease in wavelength was measured, the shift being proportional to the force. Since the direct band gap for GaAs/P is known to have a positive pressure coefficient  $dE_G/dp$  of  $11 \times 10^{-6}$  eV atmosphere<sup>-1</sup> when subjected to hydrostatic pressure (28), Konidaris suggested that the spectral change could very well be due to an increase in  $E_G$  brought about by the "near uniaxial stress" exerted by the probe thereby causing pressure along the junction interface. In addition he measured a slight decrease in the light output of the LED, and this would be consistent with an increase in  $E_G$  and hence a reduction in the current that is associated with the production of light. This theory is probably correct, although without any detailed knowledge of the pressure distribution it is difficult to verify it with any precision.

Konidaris argued that, with a force of 300 grams, the observed decrease of 0.60 nm in the wavelength of 647 nm was the equivalent of an increase of 1.74 meV in the  $E_G$  of

1.92 eV and that with a pressure coefficient of  $11 \times 10^{-6}$  eV atm<sup>-1</sup> this would indicate an "effective pressure" of  $1740/11 = 160$  atmospheres. Although he expressed the argument in a slightly different form, in effect he compared this with the average pressure exerted by a force of 300 grams over the total diode surface of area  $71 \times 10^{-9}$  m<sup>2</sup>, the result being 420 atmospheres. The discrepancy between these two values of pressure was ascribed to the non-uniformity of stress distribution and also to the fact that, as Fulop had previously described<sup>(29)</sup>, the current density and luminous emission of the diode are non-uniform, being a minimum at the centre.

In fact the numerical agreement is probably better than Konidaris realised. Using the relation of Section 5 (a) and making allowance for the fact that glass is softer than sapphire or diamond, the pressure  $p_0$  at the centre of the probe has been calculated to be about 8500 atmospheres and the contact radius  $r_0 = 41$   $\mu$ m. The value for pressure is a good deal less than the estimated elastic limit of 14,000 atmospheres, and so one can be confident that no

damage was done to the diode. Since the junction depth of the diode is  $1.3 \mu\text{m}$  and the radius of its exposed surface  $150 \mu\text{m}$ , the calculation of  $41 \mu\text{m}$  for  $r_0$  indicates that the  $z$  value for the junction depth in the Fuchs relations is about  $0.032 r_0$  and that the radius extends to  $3.7 r_0$  at the edge of the diode. Using these figures the computer program for the 'hydrostatic pressure'  $P_{\text{hyd}}$  was set for  $z = 0.032 r_0$ , and from the print-out tabulated values of  $P_{\text{hyd}}$  were obtained from  $r = 0$  to  $r = 2.0 r_0$  at intervals of  $0.1 r_0$  and thereafter at wider intervals to  $r = 5.0 r_0$ .

The first point to be considered is that in the region of the probe contact where the pressure is very high the current must be substantially cut off. This is easily seen from the following calculations. If  $P_{\text{hyd}} = 2500$  atmos. then  $\Delta E_g = 27.5$  meV. Since Konidaris was working in the LE region the exponential is of the form  $\exp(-\Delta E_g/kT)$ , and for  $kT = 25$  meV  $\exp(-27.5/25) = 0.33$ , so that the current density is reduced to a third. At 5000 atmospheres the current density is about a tenth, and at the full pressure of 8500 atmospheres it is reduced to about 2.4



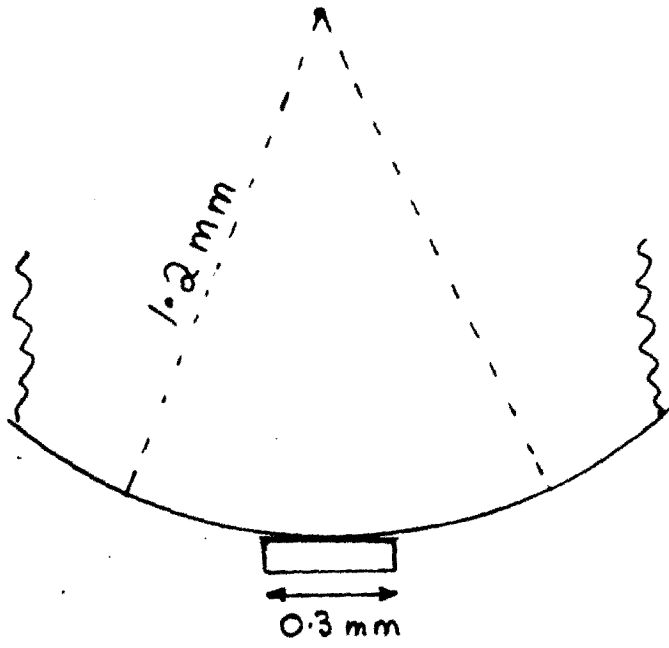


Fig.52

per cent; however, at 160 atmospheres the current density is up to 93 per cent of its original value. Thus where a large spectral shift might be expected, albeit from a very limited area, the current density is very low and correspondingly very little light is emitted. Conversely at the edge of the diode where the pressure, as given by the computer print-out, is only 20 atmospheres the spectral shift is insignificant.

However, the computer print-out shows that the effective pressure of 160 atmospheres which Konidaris measured takes place at a radius of about 50  $\mu\text{m}$ . One cannot be too sure of the light-gathering powers of the glass probe, but a diagram of its approximate dimensions and shape relative to the diode is shown in Fig 52. (Since Young's modulus for glass is almost the same as for GaAs/P, both materials yield equally and the contact area is approximately flat). From this diagram one can envisage the possibility that the light from the edge of the diode was so refracted by the probe that it did not enter the spectrometer; instead a broad annular area at

an average radial distance of about 50  $\mu\text{m}$  (just outside the contact radius) could very well contribute a large fraction of the total light collected, and it was the spectral shift of this light that was measured.

In the following sub-section the suggestion is made that it is not 'hydrostatic pressure' which is probably responsible for widening the energy gap but rather the pressure component  $p_z$  at right angles to the junction interface. This does not invalidate the above explanation for Konidaris's results because the distribution of  $p_z$  in the region of the probe is similar to  $p_{\text{hyd}}$ . (The difference arises at larger radial distances from the probe when  $p_z$  reduces rapidly to zero). For a  $p_z$  value of 160 atmospheres the computer print-out gives a value for the radial distance of about 40  $\mu\text{m}$ , ie just inside the edge of the probe contact area. This would suggest that the glass probe only picked up light from the contact area and on the whole this is a more satisfactory explanation.

A further point to be considered is that, from the light emission graph produced by Konidaris, it can be seen

that the light intensity was reduced by about 3 per cent, and this is consistent with the sort of current decrease that has been measured in the present research. The fact that he did not observe any current change is not altogether surprising in view of the changes that can occur with small fluctuations of temperature and voltage and the necessity for backing off the main current so as to measure any change directly.

Finally, it is appropriate in this sub-section to review briefly an experiment by S. Share, of the Harry Diamond Laboratories, Washington, D.C. The work, which in many respects resembles that of Konidaris and reinforces the conclusions outlined above, was reported in August 1973 and published a few months afterwards<sup>(11)</sup>, but the existence of the paper was only discovered very much later in 1983 during a computer search of the literature.

Share applied uniaxial stress on a  $\text{GaAs}_{0.6}\text{P}_{0.4}$  LED by squeezing it between two gold-plated copper anvils with a pressure change from 200 to 3000 atmospheres and measuring the light emitted from "a side of the diode that is

perpendicular to the junction plane". Except for the fact that the experiment was performed at a liquid nitrogen temperature of 77 K, the results were very similar to those of Konidaris, namely a spectral shift that indicated an increase of band gap from 1.974 to 1.981 eV and a decrease in luminous output. At the same time the current through the diode was monitored over a range from 0.1 to 10 mA in the LE region, and this showed that with an applied stress of nearly 3000 atmospheres there was a consistent current decrease of about 40 per cent (the precise percentage being difficult to assess from the published paper because of the cramped logarithmic scale); since the whole of the diode was under pressure this is consistent with the calculation quoted on p.72 that a pressure of 2500 atmospheres would cut down the current to about a third, allowance being made for a pressure coefficient at 77 K which is about a half that at room temperature. Although a number of complicating factors are discussed in the paper, the general conclusion of Share is that the major part of the effects observed is due to the

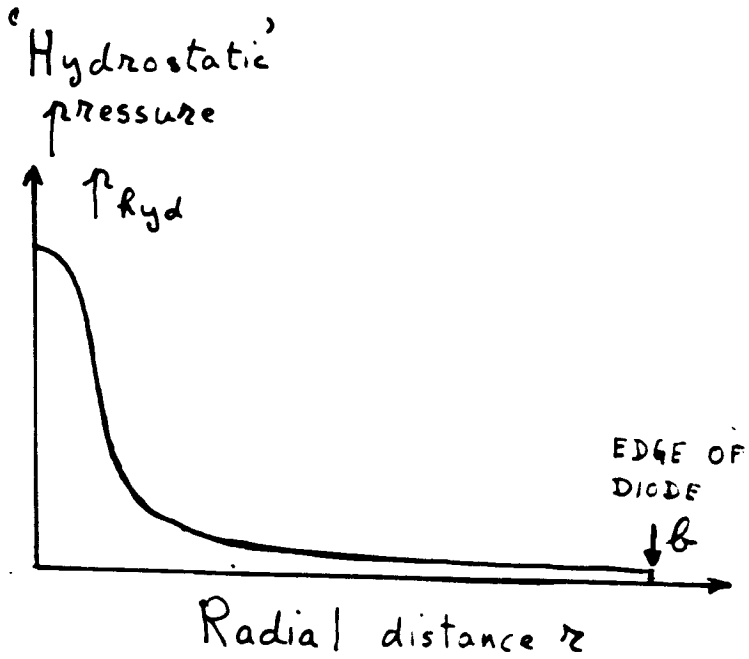


Fig.53. Pressure variation along the junction interface; ie at a  $z$  value of  $1.3 \mu\text{m}$ .

increase in band gap brought about by pressure and that this pressure is the uniaxial stress applied at right angles to the junction interface.

(c) Effect of pressure on diode current

In general the radial distribution of hydrostatic pressure along the junction interface of the diode up to the edge of the device at a distance  $b$  is shown in Fig 53, the information being taken from one of the curves of Fig 51 on p.69. The question of  $r_0, p_0$  and consequently the  $z$  value of the curve appropriate for the junction depth is discussed in an example later in this sub-section

Assuming that pressure widens the band gap  $E_G$ , as outlined in the previous sub-section, then any current element  $\delta I$  will be decreased to  $e^{-m} \delta I$  where  $m = \Delta E_G / kT$  in the LE region (or  $\Delta E_G / 2kT$  in the GR) and where for a pressure  $p$  in atmospheres  $\Delta E_G = 11 \times 10^{-6} p$  electron volt, since  $11 \times 10^{-6} \text{ eV atm}^{-1}$  is the pressure coefficient (28). Although, as has already been pointed in part (b) of this section, the current density is known not to be strictly constant (29), for the sake of simplicity let it be a

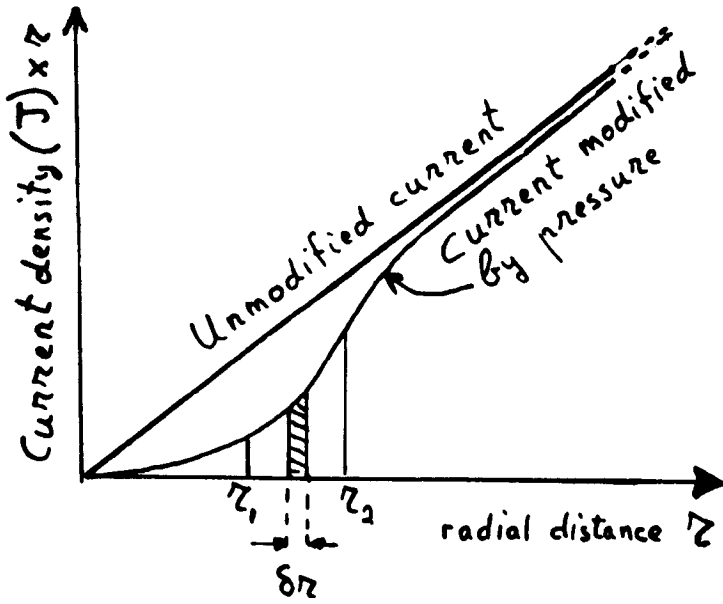


Fig.54

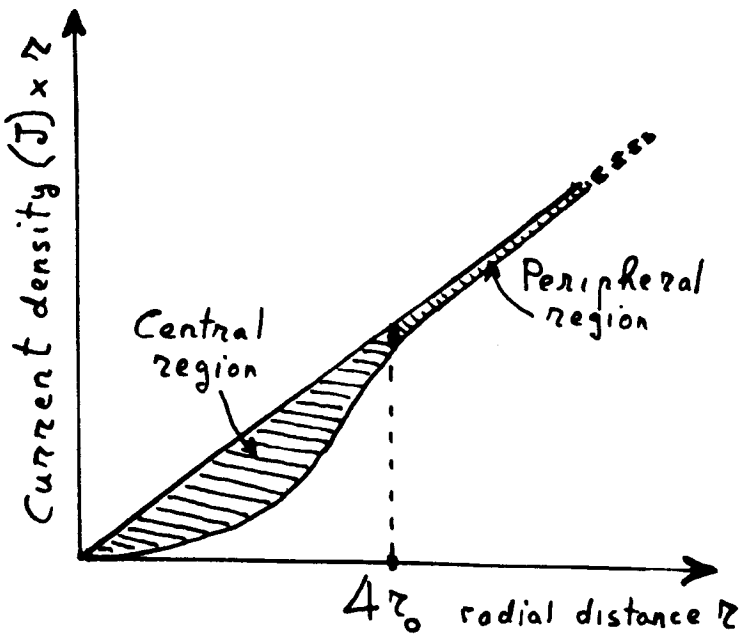


Fig.55



constant  $J$ . Then any current element  $\delta I$  is modified by pressure to  $\delta I'$  (see Fig 54) so that

$$\delta I' = J e^{-m} 2\pi r \delta r$$

and in the region  $r_1$  to  $r_2$  as shown in Fig 54

$$I'_{1,2} = 2\pi J \int_{r_1}^{r_2} e^{-m} r \, dr$$

The unmodified current in this region is

$$I_{1,2} = J\pi (r_2^2 - r_1^2) = I(r_2^2 - r_1^2)/b^2$$

where  $I$  is the total current through the diode.

The change in current  $|\Delta I_{1,2}| = I_{1,2} - I'_{1,2}$  and

therefore the change in current as a fraction of the whole current is given by

$$\frac{|\Delta I_{1,2}|}{I} = \frac{r_2^2 - r_1^2}{b^2} - \frac{2}{b^2} \int_{r_1}^{r_2} e^{-m} r \, dr.$$

For calculating the integral various methods can be adopted, including the use of a computer. However, a comparatively simple way is as follows. Fig 54 can be arbitrarily broken up into a 'central' region from  $r = 0$  to  $r = 4r_0$  and a 'peripheral' region from  $r = 4r_0$  to the boundary of the diode; this is illustrated in Fig 55. For the central region it is fairly straightforward to break

up the area under the curve into 20 strips and integrate by Simpson's Rule.

In the case of the peripheral region beyond  $r = 4r_0$  one can make the approximation that  $r^2 \gg r_0^2 \gg z^2$  and then the parameter  $u$  in the Fuchs relation on p.60 reduces to  $u = r$ . From this it is easily shown that the expression for  $p_{hyd}$  given on p.68 approximates to

$$p_{hyd} = \frac{2}{3} p_0 \frac{z}{r} \sigma = 0.247 \frac{z}{r} p_0$$

This has been verified by comparison with numerical values from the computer print-out. Furthermore, the pressure in the peripheral region is so low that  $e^{-m}$  approximates to  $1-m$ , and for the LE region where  $kT = 25$  meV

$$m = \frac{11 \times 10^{-6}}{25 \times 10^{-3}} \times 0.247 \frac{z}{r} p_0$$

$$= 1.09 \times 10^{-4} \frac{z}{r} p_0 \quad (p_0 \text{ being in atmospheres}). \text{ Hence}$$

$$\begin{aligned} \frac{|-\Delta I_{r,b}|}{I} &= \frac{b^2 - r^2}{b^2} = \frac{2}{b^2} \int_r^b (r - 1.09 \times 10^{-4} z p_0) dr \\ &= 2.18 \times 10^{-4} z (b - r) p_0 / b^2 \end{aligned}$$

From this the contribution of pressure in the peripheral region to the edge of the diode can be readily calculated.

This process can be done for the 100  $\mu\text{m}$  and the 500  $\mu\text{m}$  probe and the same pattern emerges; in fact it is more or less the same for all the probes over all the ranges of forces investigated. The example of the 500  $\mu\text{m}$  probe suffices. Given the junction depth of 1.3  $\mu\text{m}$ , four values of  $r_0$  of 13, 6.5, 2.6 and 1.3  $\mu\text{m}$  respectively were chosen, corresponding to values of  $z = 0.1r_0$  to  $1.0r_0$ , and the appropriate values of force  $F$  (in grams) and pressure  $p$  (in atmospheres) were calculated from the formulae of Section 5 (a) and Figs 25 and 26 (pp.36- 39) namely  $F = (0.28r_0)^3$  and  $p_0 = 1.04r_0 \times 10^3$ . Then the percentage values of  $|\Delta I|/I$  for the central and peripheral regions were calculated in the manner indicated above, and the whole set of results summarised in the following table ( $R = 500 \mu\text{m}$ ):

$r_0/\mu\text{m}$	$z$	$F/\text{grams}$	$p_0/10^4$ atmos	Percentage change of current		
				Central	Peripheral	Total
13	$0.1r_0$	48.2	1.35	1.52	1.60	3.12
6.5	$0.2r_0$	6.03	0.673	0.33	1.01	1.35
2.6	$0.5r_0$	0.386	0.269	0.039	0.45	0.49
1.3	$1.0r_0$	0.048	0.135	0.007	0.23	0.24

It is interesting to compare how the contribution of the

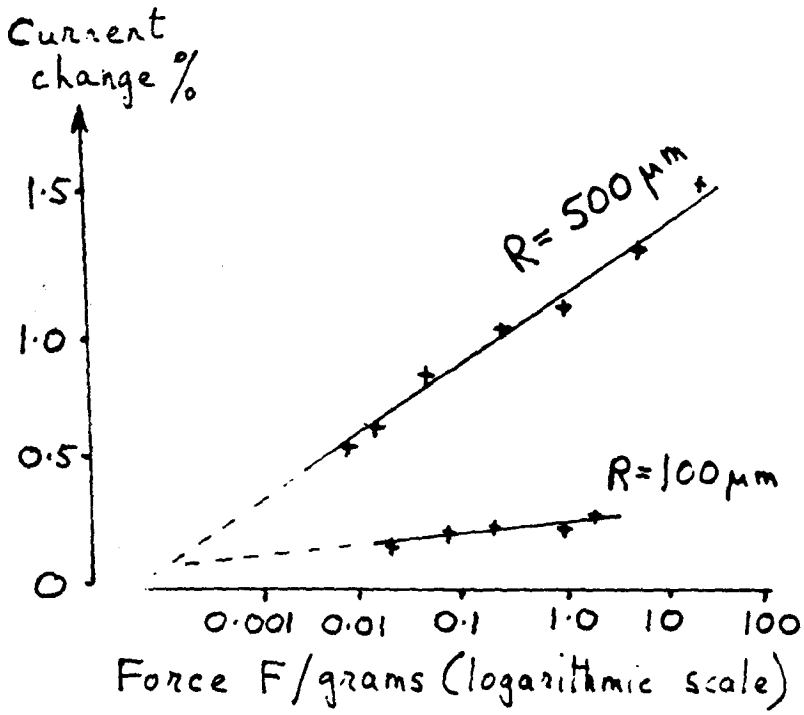


Fig.56. I = 1 mA

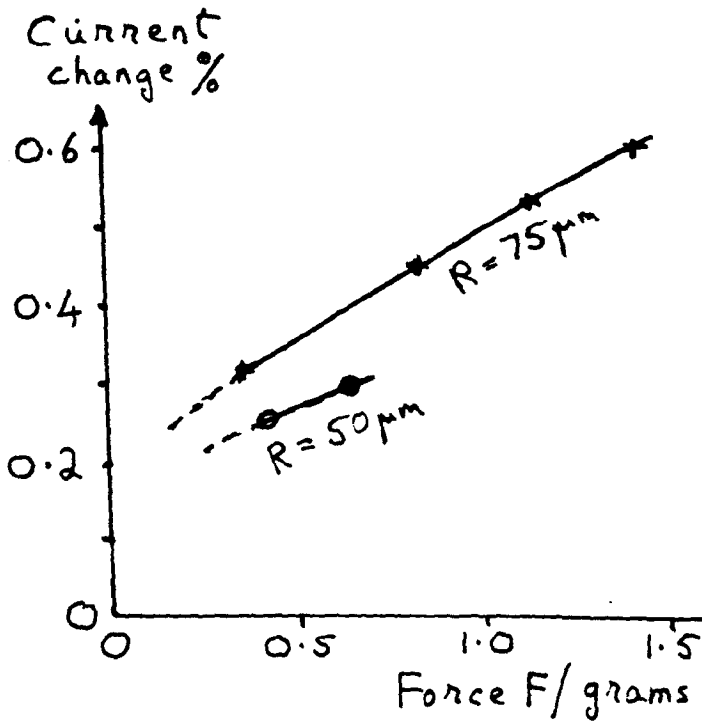


Fig.57. I = 10 mA

central and peripheral regions vary with a ten-fold increase of  $p_0$  or  $r_0$  (or a thousand-fold increase in  $F$ ); from the appropriate formulae one would expect that, as a very rough approximation, the peripheral percentage would vary linearly with  $r_0$  whereas the central percentage would depend on the area of contact, ie on  $r_0^2$ . This is seen to be the case.

In order to relate the calculations to the experimental data one can consider Fig 56 which shows a set of readings for the 500  $\mu\text{m}$  probe taken from Fig 41 of Section 6(b), p.54, and in which the ordinate scale has been changed to percentage change in current. From the tabulated values on p.80 it can be seen that in Fig 56 it is only at the top end of the pressure (near to the elastic limit) where there is any sort of agreement. As has already been mentioned on p.56, this situation was a puzzle in the early days of the research; Fig 57 shows a set of results that were recorded way back in 1977 for the 75  $\mu\text{m}$  diamond probe (again with the ordinates converted to percentage current change) where extrapolation of the

graph back to zero force apparently gives a current decrease which is about half that for the maximum force.

From the table on p.80 the conclusion is that pressure could very well play a significant role when it is fairly high (approaching the elastic limit) and that its effect is very roughly a linear one. Consequently, some other factor must be operating, and this shows up markedly when the contact pressure of the probe is very low. The theory advanced in the next section is that the moment the probe touches the surface of the diode, no matter how lightly, heat is conducted to the probe away from the junction interface so that the lowering of the temperature causes a decrease in current. Of course, this effect mainly manifests itself in the LE region where the power dissipation is sufficient to raise the diode and its sink significantly above room temperature. Nevertheless it is particularly relevant to this research in that light emission is the important aspect of an LED and the majority of the measurements have been made in this region. The question of the GR region will be discussed

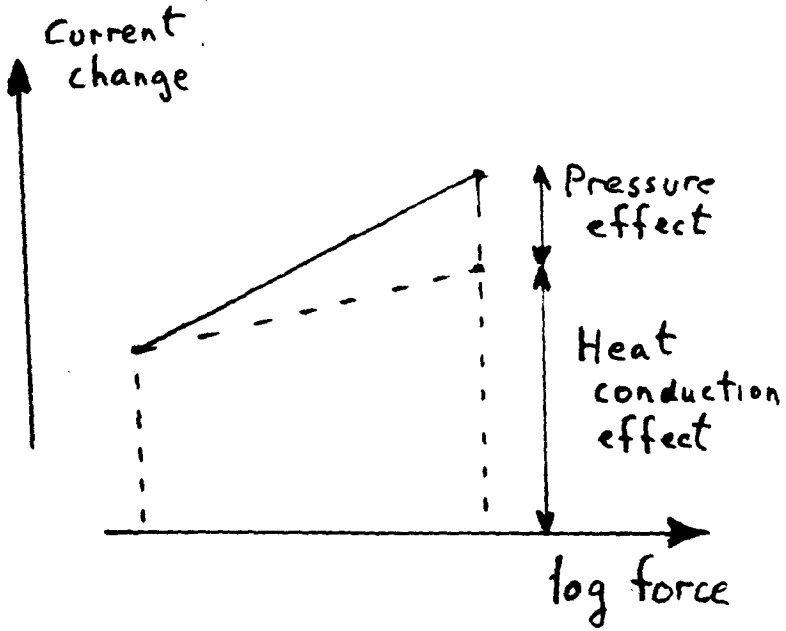


Fig.58

in the next sub-section and in Section 9.

It will be shown in the next section that this temperature effect is not expected to alter very much when the contact pressure is made much larger, so that as a very rough approximation its contribution is the same at high pressure. Hence, if one subtracts the heat conduction effect from an experimental graph of general pattern such as is shown in Fig 58, one is left with a pressure effect which, as will be shown in Section 9, is a good deal less than the percentage calculated from the hydrostatic pressure. A possible explanation for this is that it is not the overall effective hydrostatic pressure that causes the increase in band gap but rather the stress component  $p_z$  in the direction of current flow across the junction interface; this hypothesis has already been advanced in the previous sub-section dealing with the two spectral shift experiments where the applied stress was essentially uniaxial. The percentage current changes for  $p_z$  are substantially less than those for  $p_{hyd}$ , and calculated values for  $p_z$  are summarised in the next sub-section.



(d) Effect of the uniaxial stress component  $p_z$ 

The theory that it is  $p_z$  rather than  $p_{hyd}$  which is the relevant stress comes about because the Fuchs relation for  $p_z$  tails off very rapidly with radial distance (see Fig 49, p.64) so that at  $r = 2r_0$ ,  $p_z = 0.0005p_0$  when  $z = 0.2r_0$  and  $p_z = 0.026p_0$  when  $z = 1.0r_0$ . Hence for practical purposes the contribution of the peripheral region is negligible and only the central region up to  $r = 2r_0$  needs to be considered.

The theory is reinforced by consideration of the table on p.80 referring to  $p_{hyd}$  for a probe of 500  $\mu\text{m}$  radius. If probes of much smaller radius  $R$  are used, say 100  $\mu\text{m}$  or less, but the same pressure  $p_0$  maintained then the  $r_0$  values will be reduced in proportion to  $R$  and the percentage figures for the central region as given in this table will be correspondingly reduced by a factor of  $1/R^2$ . However the peripheral values will be unaltered since in a region that is well outside the contact area the pressure must be the same for a given  $p_0$ ; in fact this can also be seen from the equation of  $|\Delta I_{r,b}|/I$  quoted on p.79.

This is a very important point because it implies that with a probe of radius much smaller than  $500 \mu\text{m}$  the percentage current change due to  $p_{\text{hyd}}$  would still be very much the same owing to the contribution of the peripheral region. Yet all the experimental evidence emphatically points to the contrary; the curve for constant  $p_0$  shown on Fig 44 of Section 6(b), p.55, indicates quite clearly that the electrical change is roughly proportional to probe radius. In fact one of the features which has emerged from the present research is that it is important to vary the probe radius quite considerably, and in particular to use probes with as broad a curvature as possible in order to get correspondingly larger electrical readings that are easier to measure.

In order to calculate the effect of  $p_z$  Simpson's Rule was applied in the same manner as for  $p_{\text{hyd}}$ , but with 10 intervals instead of 20 since  $r$  needs only to be taken to  $2r_0$ ; the percentage current changes for the four forces of 48, 6.03, 0.386 and 0.048 grams on the  $500 \mu\text{m}$  probe, corresponding to  $z = 0.1, 0.2, 0.5$  and  $1.0 r_0$ , are

Current change %  
(logarithmic scale)

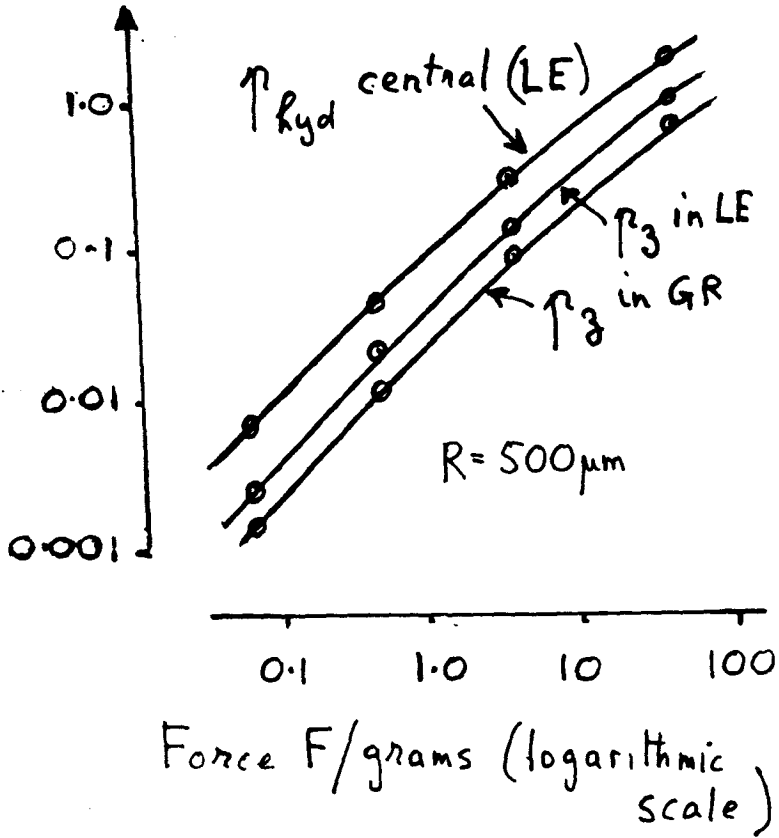


Fig.59

0.80, 0.16, 0.018 and 0.0024 per cent respectively. These figures can be compared with the central region for  $p_{hyd}$  as given in the table on p. 80, and it can be seen that they follow the same pattern but are approximately half the latter.

The calculations for  $p_z$  and for  $p_{hyd}$  have been made on the basis that in the LE region the pressure effect on the band gap operates as  $\Delta E_g/nkT$  where  $n = 1$  although this is not strictly true since  $n$  varies from diode to diode and is usually slightly more than 1. In the GR region  $n$  is theoretically 2 and for most diodes it is fairly close to this. Using the same Simpson technique the percentage current changes in the GR due to  $p_z$  for the 500  $\mu m$  probe have been calculated, and the values are 0.64, 0.081, 0.011 and 0.0013 per cent respectively.

A log-log graph of the calculated percentage current changes against force is shown in Fig 59, and for good measure the values for the central region of  $p_{hyd}$  (the LE only) have been included. It is perhaps surprising that the figures for the GR are not all that different from

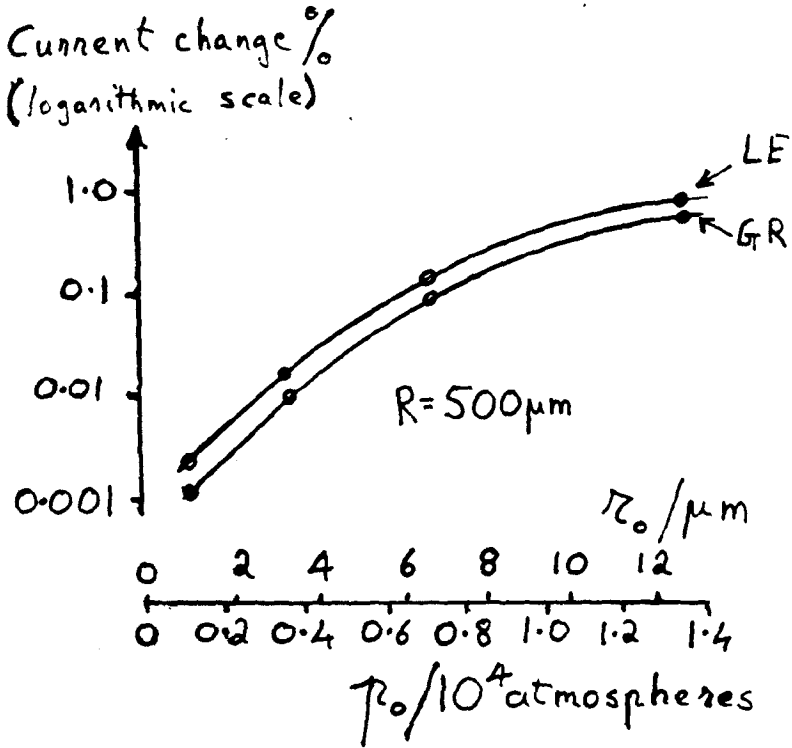


Fig.60. Calculated current change brought about by  $p_z$

those for the LE region since at first sight the change in the exponential might be expected to give a fairly large decrease. The reason is that it is only in a very tiny central area where the exponential really operates; the stress drops off so steeply with radial distance that the exponential factor rapidly approximates to a linear one. From the gradient of the log-log diagram an approximate relation of the form  $\Delta I/I \approx F^{0.7}$  can be seen to exist for the upper portions of each of the three graphs; this is an empirical relation covering stresses up to the elastic limit and probably has no theoretical significance but the numerical result will be used in the discussion of Section 9 (b).

Finally, for the range of values of the force  $F$  the corresponding values of the pressure  $p_0$  and resulting radius  $r_0$  can be read off from the 500  $\mu\text{m}$  graphs of Figs 25 and 26 in Section 5(b), pp.38-39, and the percentage current change brought about by  $p_2$  in the LE and GR regions plotted against  $p_0$  and  $r_0$  (Fig 60); the quantities  $p_0$  and  $r_0$  are of course directly related to one another.

The two curves in Fig 60 are useful in that they enable straightforward calculations to be made for any force on any probe knowing the values of  $p_0$  and  $r_0$  for the particular situation. An example will illustrate this. In Fig 40 of Section 6(a), p.52, experimental results are displayed for a force of 3 grams on the 200  $\mu\text{m}$  sapphire probe, where  $p_0 = 0.98 \times 10^4$  atmospheres and  $r_0 = 4.0 \mu\text{m}$ . In Fig 60 the  $\Delta I/I$  value in the GR region for  $p_0 = 0.98 \times 10^4$  atmospheres is 0.32 per cent, but this refers to the 500  $\mu\text{m}$  probe and a contact radius of 10  $\mu\text{m}$ . If the contact radius is only 4.0  $\mu\text{m}$  for the 200  $\mu\text{m}$  probe then the current change brought about by stress that is concentrated around the contact area must be scaled down by the factor  $(4.0/10)^2$  so that the resulting percentage is  $0.32 \times (4.0/10)^2 = 0.051$  per cent. The same calculation can be applied to Fig 39 of Section 6(a), p.52, where the force is 0.8 gram on a 75  $\mu\text{m}$  diamond probe, and the result is 0.015 per cent. These two values, both of which refer to the GR region, will be used in the discussions of Section 9 (a).

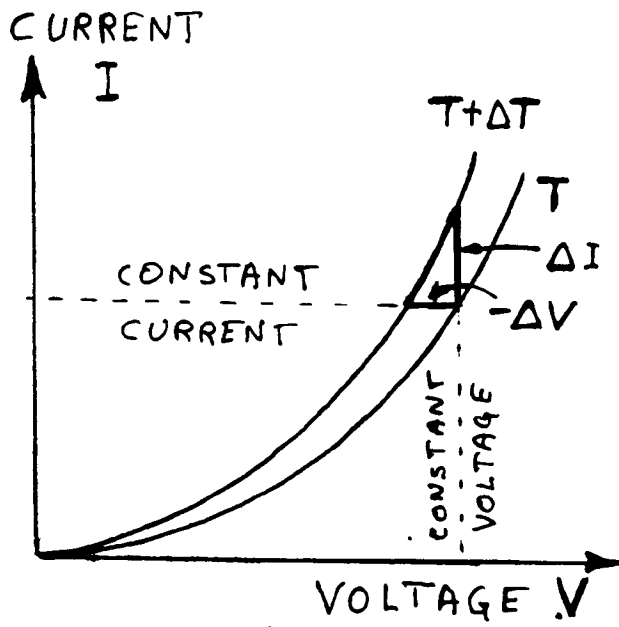


Fig.61



## 8 TEMPERATURE EFFECT

### (a) Theoretical temperature coefficient

The first step in determining the temperature coefficient of an LED was to make an estimate of the expected effect by a theoretical analysis and then to confirm it by measurement with a suitable circuit.

The results of Section 4 show that  $I = I_0 \exp(qV/nkT)$  where  $n$  is approximately 1 in the LE and 2 in the GR region. In addition there is the basic theory<sup>(30)</sup> that

$$\text{in the LE, } I_0 \propto n_i^2 \propto \exp(-E_G/kT)$$

$$\text{and in the GR, } I_0 \propto n_i \propto \exp(-E_G/2kT)$$

$$\text{Thus in the LE, } I \propto \exp(qV - E_G)/kT$$

$$\text{in the GR, } I \propto \exp(qV - E_G)/2kT$$

From Section 3 (a) it is known that  $E_G = 1.92$  eV, and from Section 4 (a) that the voltage  $V$  decreases from about 1.7 volt down to about 0.8 volt over a current range of 10 mA to 1 nA; hence the term  $(qV - E_G)$  is always negative, and for a fixed voltage the current  $I$  increases with temperature  $T$  (Fig 61). In the present research it has been found much more convenient to maintain a constant

current and measure the voltage change which, as indicated in Fig 61, would be a negative  $\Delta V$  if  $\Delta I$  were positive for a positive  $\Delta T$ . The situation is similar to that already considered in Section 6 (a) in connection with Fig 38 (p.50) and, as pointed out in that section, a full discussion of the theory is given in Appendix C.

Thus if  $I$  is kept constant, then in both the GR and in the LE region

$$(qV - E_G)/kT = \text{constant.}$$

Differentiating gives 
$$\frac{dV}{dT} = \frac{V - E_G/q}{T} + \frac{1}{q} \frac{dE_G}{dT} = \frac{|-\Delta V|}{\Delta T}$$

An estimate of  $dE_G/dT$  can be made from the values quoted for GaAs and GaP<sup>(31)</sup> namely  $-5.0$  and  $-5.4 \times 10^{-4}$  eV K<sup>-1</sup> respectively. Taking the average for GaAs<sub>0.6</sub>P<sub>0.4</sub> gives

$$dE_G/q dT = -0.5(2) \times 10^{-3} \text{ volt K}^{-1}$$

Assuming room temperature 300 K then, for  $(V - E_G/q)/T$ , a p.d. of 1.62V in the LE gives  $-0.3/300 = -10^{-3}$  V K<sup>-1</sup>, and

$$1.32V \text{ in the GR gives } -0.6/300 = -2 \times 10^{-3} \text{ V K}^{-1}.$$

This gives  $\Delta V/\Delta T$  as  $-1.5 \times 10^{-3}$  and  $-2.5 \times 10^{-3}$  V K<sup>-1</sup>, respectively, and for lower voltages further down in the

GR region the values would obviously be slightly larger.

(b) Measurement of temperature coefficient

From the theoretical estimate of about  $2 \text{ mV K}^{-1}$  made in the previous sub-section, it is obvious that measuring the current-voltage characteristics at two temperatures 20 K apart would only give about 40 mV difference and would be difficult to determine without extreme precision in the measurements. Instead, it was decided to use the constant current Wheatstone bridge of Fig 104 (p.163) in Appendix E and on balancing the bridge at one temperature to read the galvanometer voltage at another temperature.

Using very simple apparatus this proved to be a fairly straightforward measurement. A large, tall beaker was lined at the bottom with crushed ice, and the LED lowered to within a centimetre or two from the ice layer. After about ten minutes the galvanometer deflection steadied, showing that thermal equilibrium had been reached, and a  $50^{\circ}\text{C}$  thermometer with its bulb close to the LED recorded a temperature in the region of  $6$  to  $8^{\circ}\text{C}$ . The LED was lifted out, and again the galvanometer drift showed that

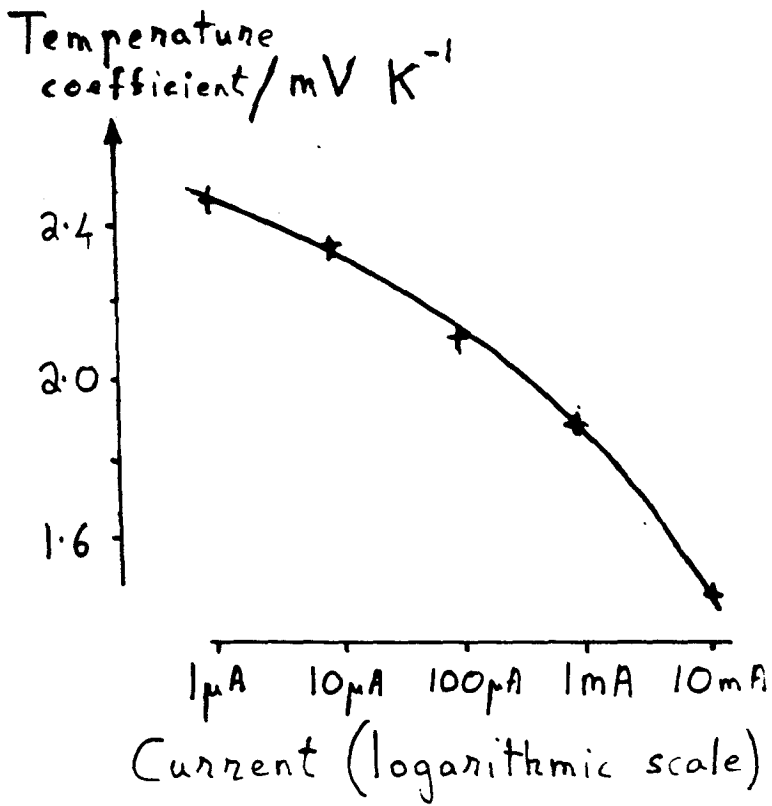


Fig.62

after about ten minutes it had settled down to a room temperature of about  $24^{\circ}\text{C}$ . The difference in voltage registered on the galvanometer was about 30 to 40 mV for currents ranging from 10 mA in the LE to  $2\ \mu\text{A}$  in the GR region.

Three diodes were tested and all showed approximately the same spread of values for temperature coefficient. A typical set of results for one of these is shown in Fig 62 and from this it can be seen that the experimental determination agrees fairly closely with the theoretical calculation of the previous sub-section, both in the value of the temperature coefficient and the fact that it rises gradually over a very wide range of currents as one proceeds from the LE to the GR region.

Another feature of this technique is that, by using a constant current through the diode and determining the out-of-balance voltage across the bridge with a millivoltmeter of virtually infinite impedance, the measurement is simple and direct in that no correcting factors are necessary. Since the results are ultimately required as

a fractional increase in current per degree rise in temperature the relation of Section 4(b) is needed whereby

$$\Delta I/I = q|-\Delta V|/nkT$$

Thus simultaneously with the temperature measurements the current-voltage characteristics of the diode must be determined so that the value of  $nkT/q$  in the LE and GR regions can be calculated and, also, an estimate made of the transition current between the two regions. In the LE most diodes have a value for  $nkT/q$  of about 35 mV and hence for a temperature coefficient of  $1.75 \text{ mV K}^{-1}$   $\Delta I/I$  is about 5 per cent per degree. In the GR region it is about the same, or perhaps slightly less (say 4 per cent per degree), because although the voltage rise is greater the value of  $nkT/q$  also increases by a similar amount.

#### (c) Estimate of working temperature

In making a rough estimate of the temperature at which the LED is working it is important to bear in mind that it is designed to operate at approximately 20 mW (about 12 mA 1.7 volt) and that a heat sink is imperative. The actual diode is in the form of a flat cylinder about 300  $\mu\text{m}$  in

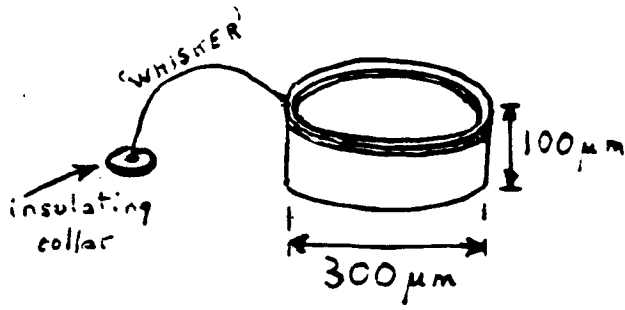


Fig.63

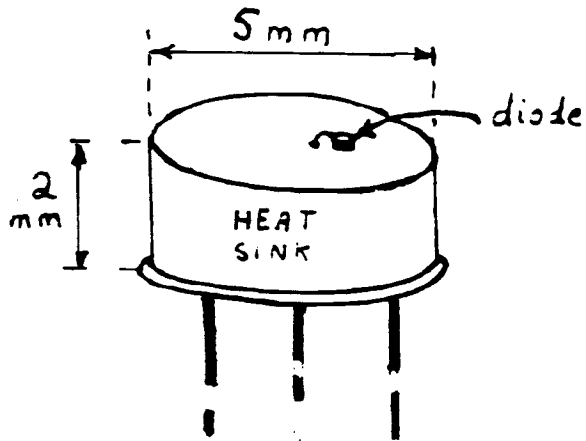


Fig.64

diameter and 100  $\mu\text{m}$  deep (Fig 63), and if it were isolated it would lose heat almost entirely by radiation. By applying Stefan's relation for a black-body radiator, namely power = Stefan's constant  $\times$  area  $\times (T^4 - T_0^4)$ , a calculation of the temperature  $T$  compared with a room temperature  $T_0$  of about 300 K gives a result of about 1100 K or 800°C. Consequently, the LED is mounted on a heat sink in the form of an alloy cap approximately 5 mm in diameter and 2 mm deep (Fig 64) giving a total area of about  $50 \times 10^{-6} \text{ m}^2$ . Assuming that the surface of the sink is a 100 per cent black-body radiator so that the full value of Stefan's constant of  $5.7 \times 10^{-8} \text{ W m}^2 \text{ K}^{-4}$  can be applied, then at 20 mW dissipation  $T^4 - T_0^4 = 70 \times 10^8$ ; hence for  $T_0$  of 300 K,  $T = [(70 + 81) \times 10^8]^{1/4} = 350 \text{ K}$ . Thus the sink is designed to be about 50 K above room temperature when the diode is operating at full power.

At 1 mW,  $T^4 - T_0^4 = 3.5 \times 10^8$  and therefore  $T = [(3.5 + 81) \times 10^8]^{1/4} = 303.19 \text{ K}$  or 3.19 K above room temperature. Obviously in this latter case  $(T^4 - 300^4)$  can be approximated to  $4 \times 300^3 \Delta T = 1.08 \times 10^8 \Delta T$ , where



$\Delta T$  is a temperature difference that is small compared with 300 K. Then at 1 mW,  $\Delta T = (3.5 \times 10^8) \div (1.08 \times 10^8) = 3.24$  K, which is close to 3.19 K. On this basis it can be assumed that below 1 mW the temperature difference varies linearly with the power and that the conversion factor is 3.2 K per mW. If the sink surface is not a 100 per cent black body then this factor would be higher; however, at the same time there must be additional cooling due to convection and possibly some conduction down the electrical leads, and these latter would reduce the factor. For the sake of simplicity it is assumed that these latter effects, both of which are approximately linear with temperature difference, roughly cancel out the reduced black-body factor, and the figure of 3.2 K per mW still stands as a reasonable estimate.

The above figure does not take into account the temperature drop from the junction interface through the LED to the heat sink. The figures for the thermal conductivity of GaAs and GaP are quoted <sup>(32)</sup> as 37 and 110 W m<sup>-1</sup> K<sup>-1</sup> respectively; a simple way of estimating

for  $\text{GaAs}_{0.6}\text{P}_{0.4}$  would be to average these figures taking into account the larger fraction of As, and this gives  $66 \text{ W m}^{-1} \text{ K}^{-1}$ . Then with the dimensions of the LED shown in Fig 63, for a power of 1 mW the temperature difference is given by

$$10^{-3} = \frac{66\pi (150 \times 10^{-6})^2}{100 \times 10^6} \delta\theta$$

so that  $\delta\theta = 0.021 \text{ K}$ . Obviously this is very small compared with 3.2 K for 1mW, and although this temperature drop through the LED plays a significant role in the heat flow hypothesis considered in the next sub-section, its influence in connection with the temperature of the heat sink relative to that of the junction is negligible.

A final point to be considered is that, if in the LE region the temperature is as much as 50 K above ambient conditions, then the value of  $kT$  as measured from the I-V characteristics should not be the theoretical 25 meV for 300 K but that for 350 K, ie approximately 30 meV. Thus the figure of 35 meV quoted on p.93 and derived from the measurements of Section 4 (a) (see p.29) is not unexpectedly high.

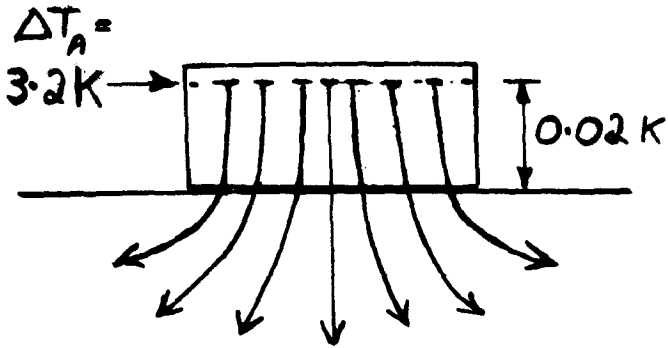


Fig.65. Situation at  $1\text{ mW}$  power.  
Heat mainly conducted to the sink.  
 $\Delta T_A$  = temperature above ambient.

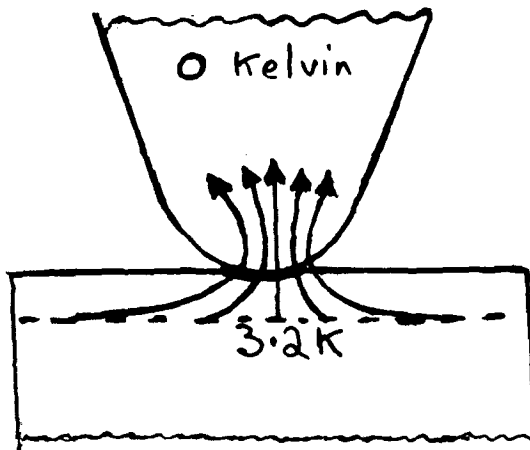


Fig.66. Heat dissipation switched  
to the probe.

(d) Heat flow hypothesis

From the previous sub-section it is estimated that the heat generated in the junction is conducted to the sink as shown in Fig 65. The temperatures indicated on the diagram refer to the excess temperature above the surroundings and are for a power of one milliwatt; for powers other than 1 mW the temperature must be proportioned, although at 10 mW and above the linearity breaks down. Also at 10 mW the luminosity of the diode is fairly high so that a significant amount of power must be radiated from the top surface.

When a probe is suddenly applied (Fig 66) nearly all the heat flow is switched to the probe because the latter is now a heat sink 3.2 K below the junction temperature compared with 0.02 K for the sink, and yet the conducting paths to the probe and to the sink are comparable in length (100  $\mu\text{m}$ ). Since the junction depth  $h$  is very small (1.3  $\mu\text{m}$ ) a simple model of the heat paths would be a radial inward flow in a cylinder of depth  $h$  to a narrow cylinder of radius  $r_0$ , the contact radius of the probe (Fig 67). In fact an intuitive (or indeed artistic)

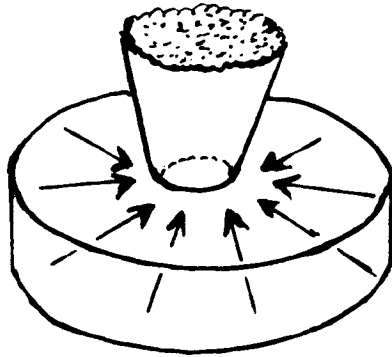


Fig.67. Flow of heat towards  
probe contact area

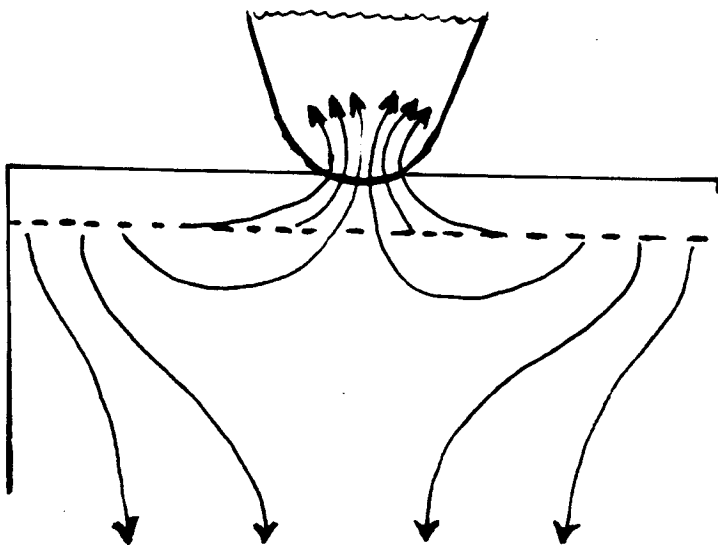


Fig.68

impression of the heat flow is more probably as shown in Fig 68, but nevertheless the simple model of Fig 67 is plausibly a fair approximation. For the moment, any temperature drop in the narrow contact region of the sapphire probe is ignored, although subsequently this will be taken into account.

On the basis of this model, let the heat developed in an annular ring of radius  $r$  and thickness  $\delta r$  be  $\delta H$ . Then  $-\delta H = 10^{-3} W 2r \delta r / b^2$  where  $b$  is the radius of the diode and the  $10^{-3}$  factor is inserted so that  $W$ , the total power of the diode, can be expressed in milliwatts. It can easily be shown from elementary theory that:-

$$-\delta H = \frac{2\pi kh}{\ln(r/r_0)} \delta \theta \quad \text{where } \delta \theta \text{ is}$$

the temperature between the annular ring of radius  $r$  and the cylindrical sink of radius  $r_0$ ,  $k$  the thermal conductivity and  $h$  the depth of the slice as shown in Fig 67.

Equating  $-\delta H$  gives:-

$$r \ln(r/r_0) \delta r = \frac{\pi kh b^2}{10^{-3} W} \delta \theta$$

In Section 6 (c) the assumption has been made that the current density across the junction interface is

constant, although Fulop has shown that this is not strictly true (29) . The same approximation is again made here so that it can be assumed that heat is more or less generated uniformly over all the junction interface; hence integration will give the sum of all the heat flow within a radius  $r$ , and this will add up to a total temperature difference  $\theta$  between the inner sink and radius  $r$ .

Integration of the above equation leads to

$$\left[ \frac{1}{2} r^2 \ln(r/r_0) - \frac{1}{4} r^2 \right]_{r_0}^r = \frac{\pi k h b^2}{10^{-3} W} \theta$$

$$\text{and therefore } \theta = \frac{W}{2\pi 10^3 k h b^2} \left[ r^2 \ln\left(\frac{r}{r_0}\right) - \left(\frac{r^2 - r_0^2}{2}\right) \right]$$

It is to be noted that  $\theta$  is the excess above room temperature and that in the derived relation  $\theta$  is zero for  $r \ll r_0$ , a result which is to be expected since the probe is assumed for the moment to be at room temperature.

Without the probe the junction excess temperature is  $3.2 \text{ K mW}^{-1}$  so that now with the application of the probe the excess temperature  $\Delta\theta = 3.2 - \theta$ . If numerical values that have already been quoted in the previous sub-section are inserted for  $K$ ,  $h$  and  $b^2$  we get

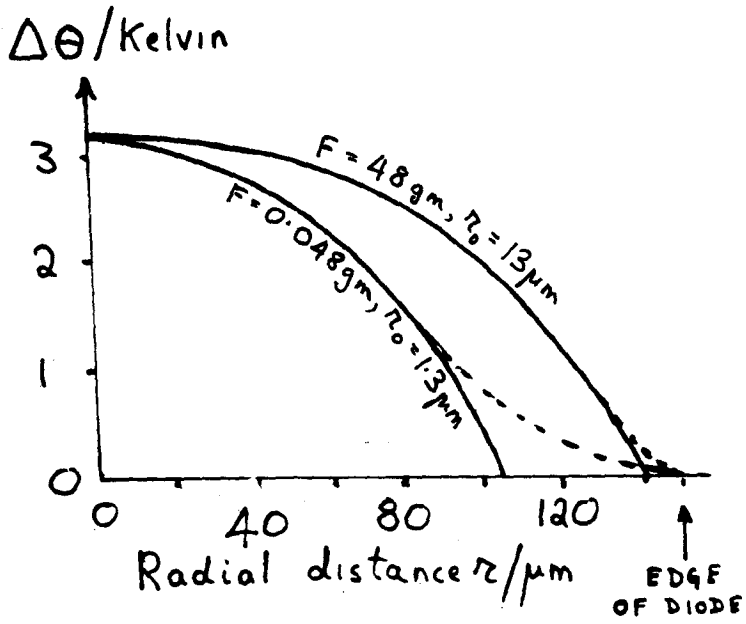


Fig.69



$$\Delta\theta = W\{3.2 - 4.12 \times 10^7 [2r^2 \ln(r/r_0) - (r^2 - r_0^2)]\}$$

In order to test this theory the example of the 500  $\mu\text{m}$  probe already discussed at length in Section 7 (c) will be considered; in particular the two extreme cases of a maximum force of 48 grams and a minimum of 0.048 grams will illustrate the situation, the corresponding values of  $r_0$  being 13 and 1.3  $\mu\text{m}$  respectively.

Tabulated values of  $\Delta\theta$  for the two cases were easily calculated from the above relations and the distribution of temperature plotted against radial distance  $r$ , as shown in Fig 69. Of course the temperatures should tail off asymptotically near the the edge (shown as dotted curves) rather than end abruptly, but this is a defect in the simplifying assumptions that are made in setting up the model. In general the distribution of temperature fits in with the ideas illustrated in Fig 68, namely that at the diode edge there is no cooling by the probe and the heat continues to flow down the sink. Also there is not a great deal of difference between the two curves despite the enormous difference in the probe forces (by a factor

of a thousand), but this is because the change in  $r_0$  is only a factor of ten and because  $r_0$  occurs principally in the logarithmic term which is a slowly changing function.

However, as already mentioned (p.98), there is still a further modification to be made, namely the fact that the radial inward flow of heat to the probe is not to a thin cylindrical sink of zero excess temperature but rather to a narrow 'neck' of material where the semiconductor and sapphire are in contact. The 500  $\mu\text{m}$  probe is fairly large and being set in a metal holder has a total heat capacity comparable to the actual sink of the LED. Of course, heat capacity will only affect transient and not steady-state conditions, but the time constant involved would appear to be more than a minute and this is shown by the following observation:- as already recorded in Section 6 (a), when the probe touches the LED there is an immediate deflection of the galvanometer brought about by the combined effects of pressure and sudden cooling, and this is followed by a slow drift in the opposite direction which lasts for over a minute and must be due to the probe taking in heat until

equilibrium is reached. The thermal conductivity of sapphire<sup>(33)</sup> is not particularly high, being about  $34 \text{ W m}^{-1} \text{ K}^{-1}$ , and this 'throttling' of the heat flow through the contact region must result in a temperature drop between this region and the main body of the sapphire and its metal holder. It is only possible to make a speculative guess, but it is suggested that it could be 2.5 K for the large force of 48 grams and 2.2 K for the one of 0.048 gm.

In making this speculative guess it should be noted that, although the contact area for the smaller force is a good deal less than that for the larger one, there is a very narrow gap between the flat LED surface and the rounded surface of the sapphire and that this gap extends a long way beyond the actual area of contact; hence there must be quite an amount of heat transfer across this gap, and effectively the contact areas are much more nearly equal than the two values of  $r_0$  would otherwise suggest. In fact because the heat flow with the smaller force is less owing to its narrower neck the actual temperature drop in this case could very well be slightly less. What

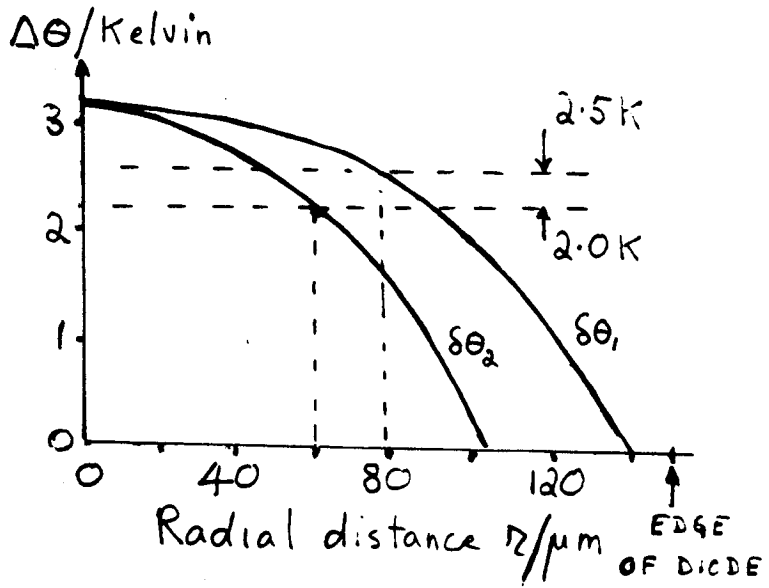


Fig.70

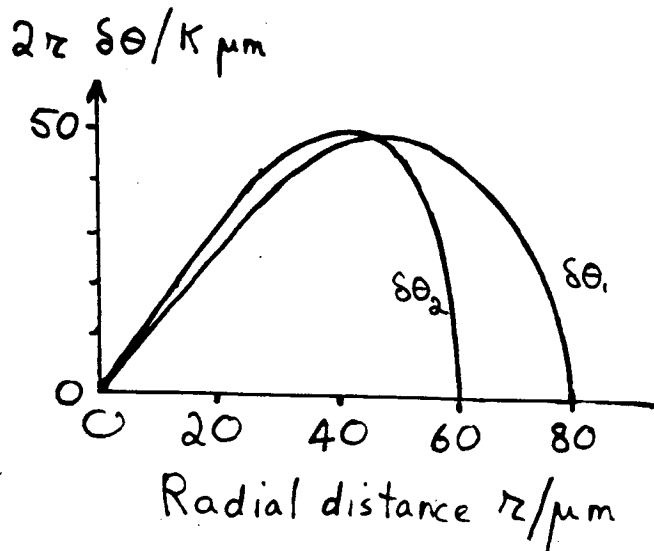


Fig.71

is certain is that there must be significant temperature drops across each neck, but they cannot exceed in value the maximum temperature difference of 3.2 K that has been theoretically calculated and indicated in Figs 68 and 69. Assuming for the moment that the temperature drops are in fact as suggested, then all the temperatures shown in Fig 69 must be reduced by the appropriate amount; this is best illustrated by drawing lines 2.5 and 2.2 K up from zero and making these the new axes (Fig 70).

In order to calculate the average cooling of the junction the values ( $\Delta\theta = 2.5$ ) and ( $\Delta\theta = 2.2$ ) in Fig 70 (called  $\delta\theta_1$  and  $\delta\theta_2$ ) are multiplied by  $2r$  and plotted against  $r$  as shown in Fig 71. Numerical integration is accomplished by the simple process of counting squares under the curves, and then division by the diode radius ( $150 \mu\text{m}$ ) squared gives the two averages, which turn out to be 0.10 and 0.075 K respectively. These calculations are for a power of 1 mW and are directly proportional to the power. Since the readings for the  $500 \mu\text{m}$  probe were taken with a fixed current of 1 mA, the voltage being 1.55 V,

the power is 1.55 mW, and so the average cooling of the junction must be scaled up to 0.16 and 0.12 K. Given a value of 5 per cent per degree in the LE region as deduced in part (b) of this section, this gives a current change for the 48 and 0.048 gram forces of 0.8 and 0.6 per cent respectively, so that the difference is 0.2 per cent. This last figure is needed in the next section (p. 116).

At this point in the proceedings a confession must be made that the foregoing calculations have been performed for various hypothetical temperature drops between 2.0 and 2.7 K, and the values ultimately selected fit in with the calculations to be discussed in Section 9 (a). Admittedly this could lead to the accusation that the theory has been 'accommodated' to the experimental data, but the fact remains that the temperature drops lie well within the range of 3.2 K and therefore the assumption is a feasible one.

This arbitrary assumption is probably the least satisfactory aspect of what must anyway be regarded as a speculative theory. However the evidence presented in

other parts of this thesis definitely points to the fact that heat flow almost certainly plays a significant role in the experiments performed. Though there may be defects in the details of the theory outlined in this section, nevertheless the underlying concept is surely correct. The calculations show that for the probe of 500  $\mu\text{m}$  radius current changes of 0.8 and 0.6 per cent in the LE region are of the right order for forces which are very different in magnitude and which cover a range from the elastic limit to very small stresses. These percentage values will be used in the detailed calculations that are made in the following pages of Section 9 (a).

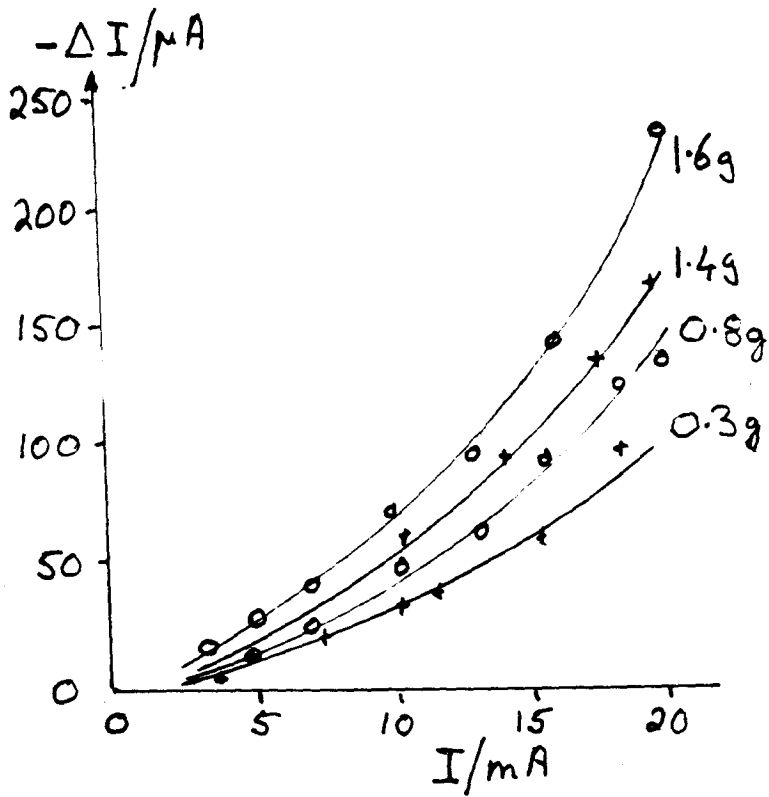


Fig.72.  $75 \mu m$  diamond probe

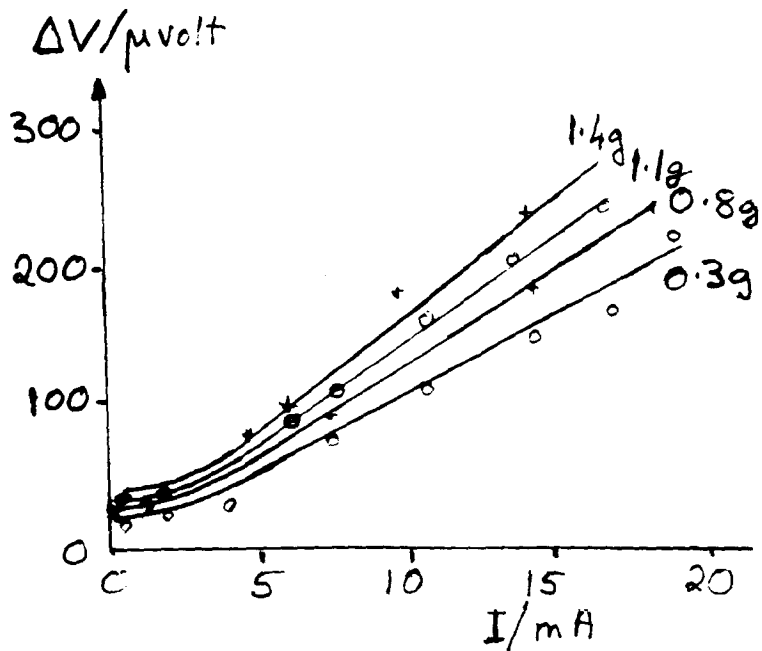


Fig.73.  $75 \mu m$  diamond probe



## 9 FINAL STAGES

### (a) Re-assessment of early measurements

In the light of the pressure and heat flow theories outlined in the foregoing sections the measurements that were taken fairly early on in the research can now be interpreted with a reasonable degree of satisfaction. These measurements were for the most part in the LE region primarily because it had previously been reported<sup>(1,7)</sup> that no change was detectable in that region; however, there was also the advantage that the small changes which were in fact observed were easier to measure than the corresponding ones in the GR region, this being particularly the case when in the early stages the largest probe available was the diamond one of radius 75  $\mu\text{m}$ . Three sets of readings, which are listed below as (i), (ii) and (iii), have already been quoted in the previous sections and will now be discussed as follows.

(i) Figs 35 and 37 (pp.48-50). These graphs, both of which refer to the 75  $\mu\text{m}$  diamond probe, are here reproduced for convenience as Figs 72 and 73; they were of impor-

tance in that they verified experimentally the relation of the a.c. resistance  $R_{ac}$  whereby the direct measurement of negative current change  $-\Delta I$  by one circuit technique corresponded with the positive voltage change  $\Delta V$  using another technique. The fact that the curves in Fig 72 are very close to parabolic indicates that there is a linear relation between  $-\Delta I/I$  and  $I$ , and this is reflected in Fig 73 since

$$|-\Delta I|/I = q\Delta V/nkT$$

Over the range of currents investigated, namely 2 to 20 mA the voltage only changes from about 1.55 to 1.65 V so that the power is very nearly proportional to current, and in this range there is a considerable temperature excess (relative to room temperature) which is approximately proportional to power. With the top force of 1.4 grams giving a pressure that is near the elastic limit and with a maximum current of 15 mA, the comparatively large galvanometer reading of 300  $\mu V$ , which corresponds to a current change of about 1 per cent, is for the most part due to cooling by the probe, and by comparison the pressure

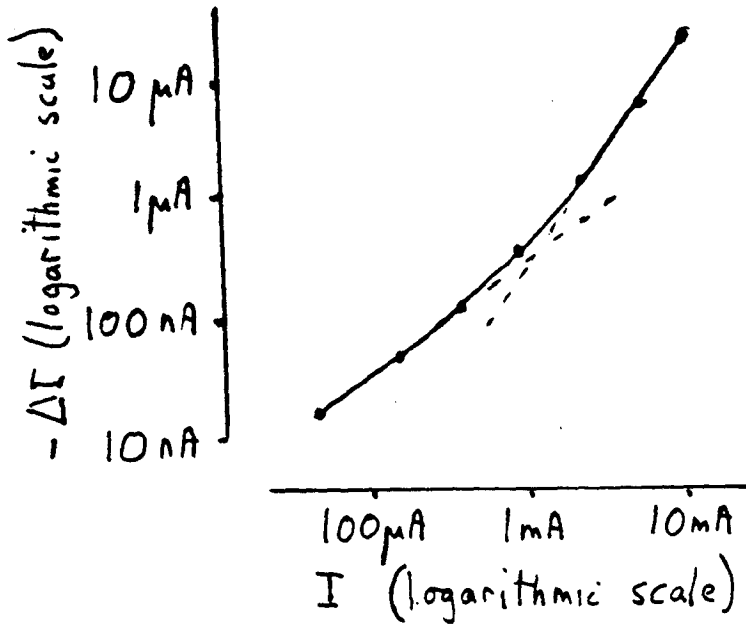


Fig.74. 0.8 gram on 75  $\mu m$  diamond probe;  
 $p_0 = 1.3 \times 10^4$  atm.

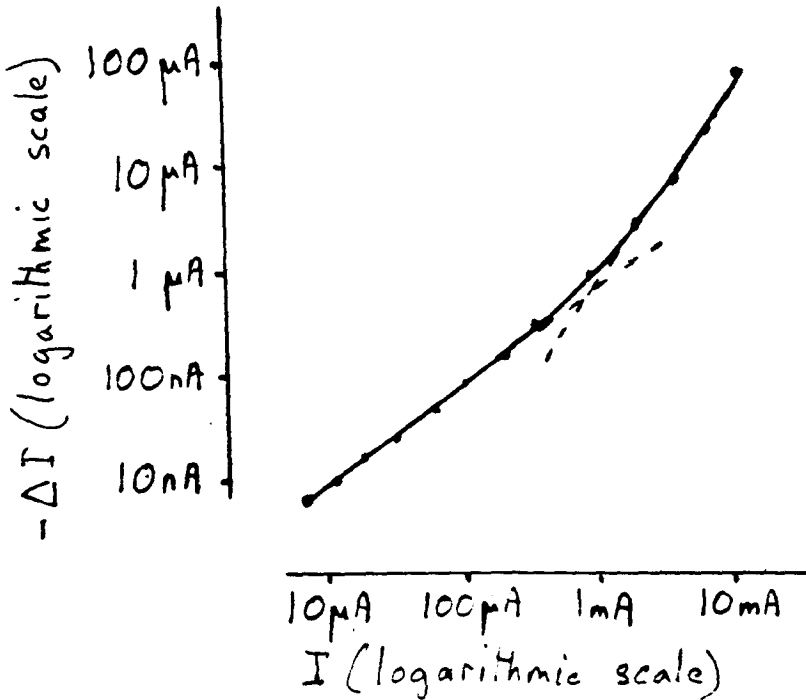


Fig.75. 3.0 grams on 200  $\mu m$  sapphire probe;  
 $p_0 = 0.98 \times 10^4$  atm.

effect is approximately a tenth of this.

However there is a further feature of Fig 73 that is highly significant, namely the fact that, although the straight line can be extrapolated back to the origin, nevertheless at a fairly low current of about 100  $\mu\text{A}$  there is a definite 'intercept' which for the largest force is about 0.1 per cent in  $\Delta I$ . When this was recorded (April 1977), it was largely ignored because the less sensitive galvanometer was being used and not much confidence was ascribed to the accuracy of the readings at the bottom end of the range. Nevertheless, in the light of the theories that have been subsequently developed, it can now be seen that this intercept is a measure of the residual pressure effect when the diode current is sufficiently low for the heating to be insignificant. The figure of about 0.1 per cent agrees quite well with the more accurately determined value of 0.10 per cent that is quoted in the next paragraph for the 200  $\mu\text{m}$  sapphire probe.

(ii) Figs 39 and 40 (p.52). These curves are reproduced here as Figs 74 and 75 and show that the range of readings

was extended to the GR region even in the early stages of the research, using a constant force of 0.8 gram on the 75  $\mu\text{m}$  probe and going down to about 50  $\mu\text{A}$ ; subsequently with a constant force of 300 grams on the 200  $\mu\text{m}$  probe it was possible to obtain results down to about 10  $\mu\text{A}$ . As reported in Section 6 (a), in both graphs the slope in the LE region is very close to 2 and in the GR region it is about 1. Once more the logarithmic slope in the LE region verifies that  $-\Delta I/I$  varies as I (ie the predominating temperature effect), but in the GR region (where the temperature excess must be very small) the slope of 1 indicates that  $-\Delta I/I$  is constant; since the pressure is constant, an obvious interpretation of this is that it is a true measure of the pressure effect. The changes of current, as measured directly from the GR parts of Fig 74 and Fig 75 are 0.03 and 0.10 per cent respectively.

The  $p_0$  values for these two cases are quite high, and it has already been pointed out in Section 7 (d), p.84, that the percentage change due to  $p_{\text{hyd}}$  in the 'peripheral' region alone would be more than ten times the above

Facing  
p.110

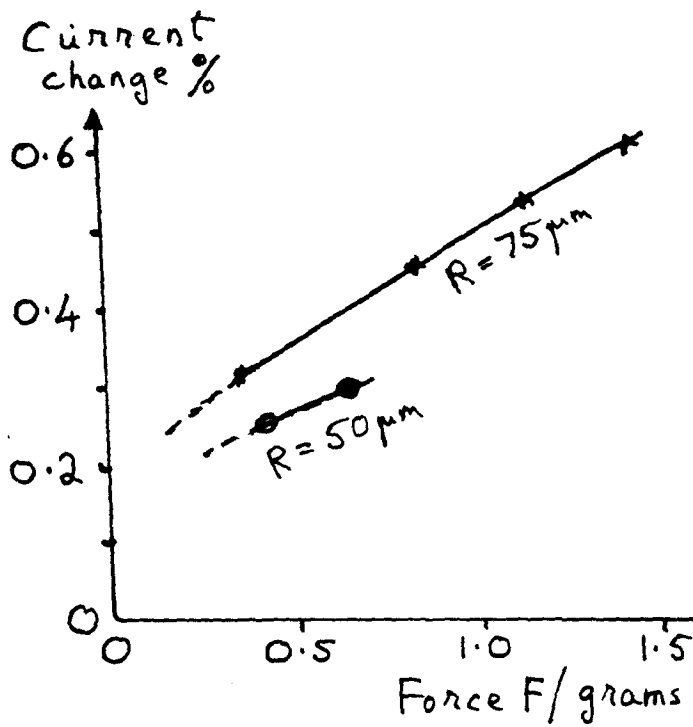


Fig.76. I = 10 mA

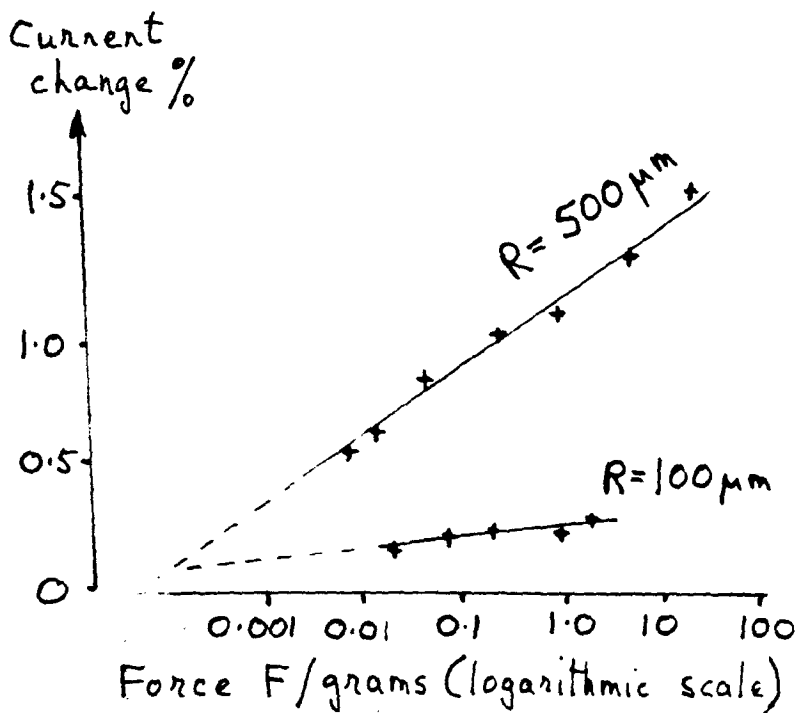


Fig.77. I = 1 mA

figures. On the other hand if the effect is due to uniaxial stress  $p_z$ , then as calculated in Section 7 (d), p.88, the current changes would theoretically be 0.015 and 0.051 per cent respectively. Admittedly there is a discrepancy here of  $\times 2$ , but the measurements in the GR region were not easy to make and some experimental error must be accepted. However, even in the GR region there could be a slight temperature effect, and it is suggested that this extra effect might account for the experimental value being somewhat high.

(iii) Figs 45 and 41 (pp. 56 and 54). These graphs refer to a wide variation of forces on a range of probes. In reproducing them here as Figs 76 and 77 the ordinate scales have been converted to percentage current changes. Fig 76 does not represent further experimental data since the readings have been taken from Fig 73 at a constant current of 10 mA; also shown are a couple of measurements taken very early on with a 50  $\mu\text{m}$  diamond probe, but only the 75  $\mu\text{m}$  graph will be discussed here. The explanation for Fig 76 has already been briefly mentioned in Section 7

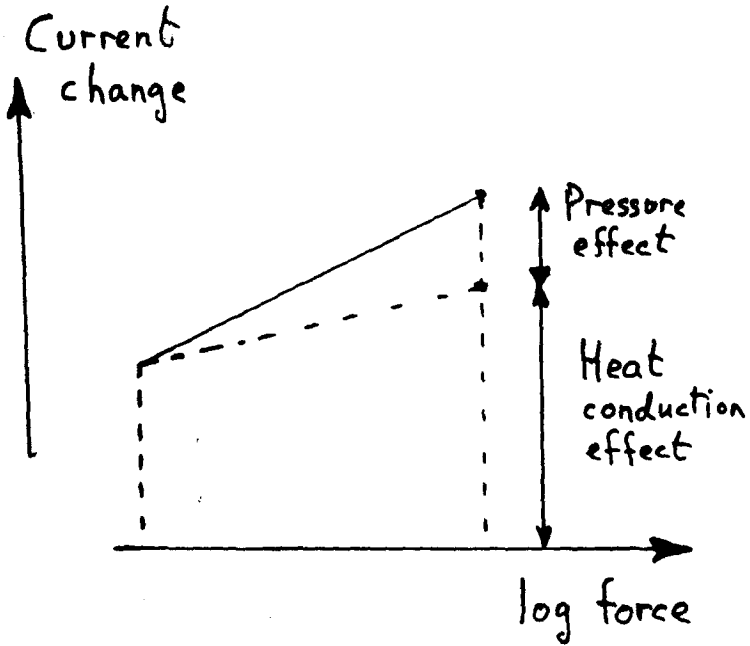


Fig.78

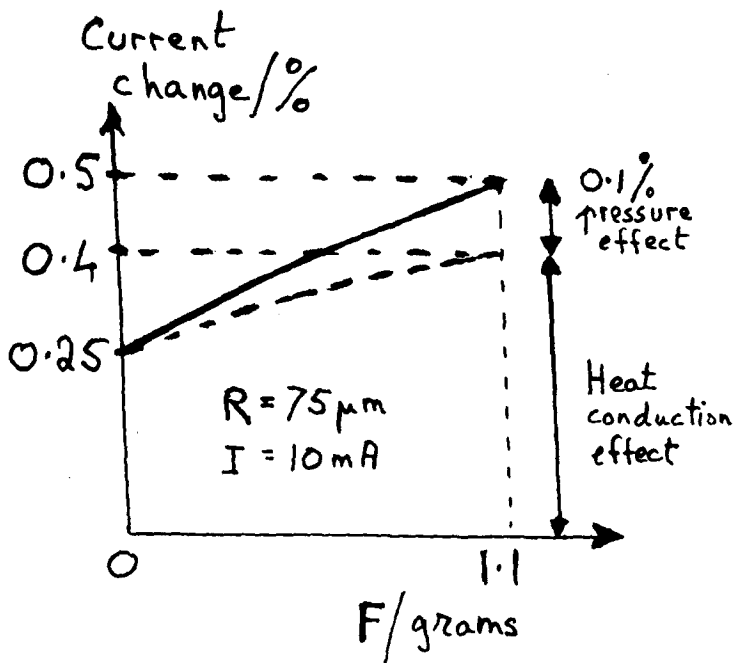


Fig.79. Data taken from Fig.76.



(p.83) with reference to Fig 58, and this latter diagram is also repeated here as Fig 78. With a current of 10 mA the readings of Fig 76 were taken when the LED was glowing bright red, and from Section 8 (c), p.94, the power rating of 16 mW would indicate a temperature of about 40 K above ambient conditions. It is surmised that at this high temperature the heat conduction effect will be quite large and could be as much as 0.25 per cent for a low force exerting negligible pressure and 0.4 per cent with a force of 1.1 gram on the probe. Consequently the situation is as shown in Fig 79 leaving 0.1 per cent as the pressure contribution of the 1.1 gram force, which is near the elastic limit. This would bring the estimate into line with the evidence of Fig 73 (p.106) that the percentage current change levels out at about 0.1 per cent for currents below 0.5 mA.

However for the readings of Fig 77 numerical data of a more precise nature are available since, in the case of a current of 1 mA, heat flow theory has been quantitatively estimated. In Section 8 (d), p.105, the calculation is

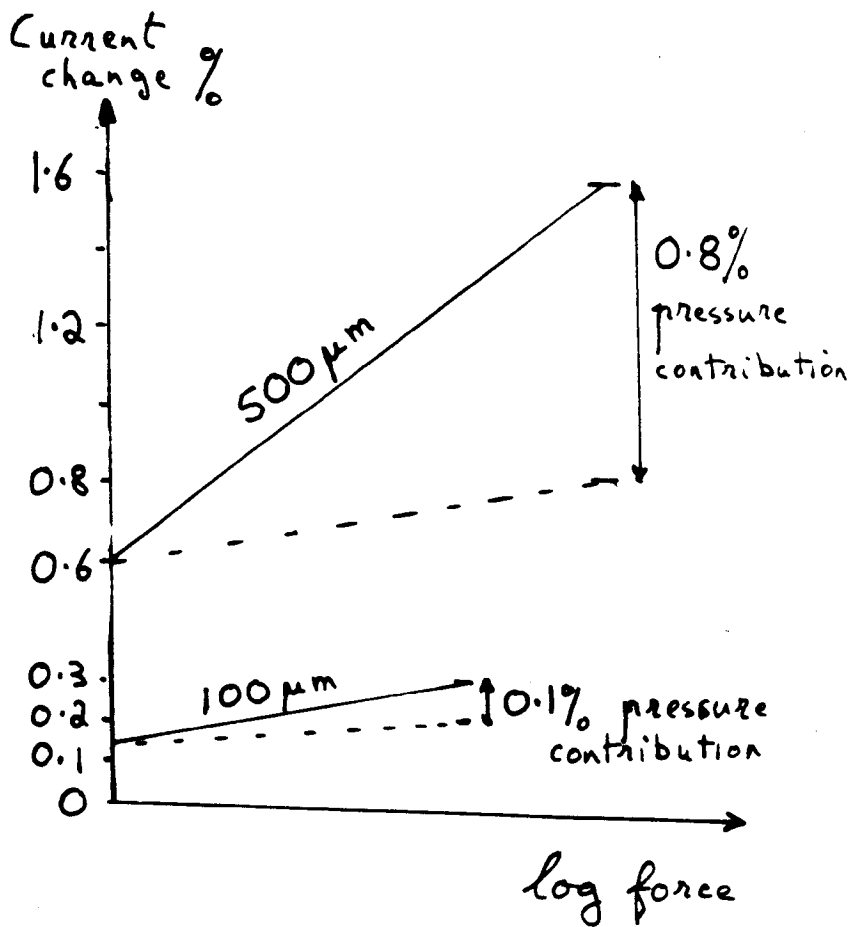


Fig.80

made that for the 500  $\mu\text{m}$  probe the heat flow contributions are 0.8 and 0.6 per cent at the two extreme ends of the pressure range; for the 100  $\mu\text{m}$  probe the corresponding figures are 0.2 and 0.15 per cent respectively. The application of these figures to the 500 and 100  $\mu\text{m}$  probes is displayed in Fig 80, and from this it can be seen that the pressure contributions at large forces near to the elastic limit are 0.8 and 0.1 per cent respectively for the two probes. The figure of 0.1 per cent for the 100  $\mu\text{m}$  sapphire probe ties in well with the readings for the 75 one of Fig 73 (p.106), the two probes being comparable, and also with the value of 0.1 per cent for 3 grams on the 200  $\mu\text{m}$  probe discussed in connection with Fig 75 (p.108), the pressure here being somewhat below the elastic limit.

The pressure value of 0.8 per cent current change for the 500  $\mu\text{m}$  probe agrees well with the value quoted in Section 7 (d), pp.85-86, when discussing the theoretical contribution that the uniaxial stress component  $p_z$  is likely to make with a force of 48 grams on that particular probe. However it has already been admitted in Section

8(d) that the heat flow figures have been deliberately selected in order to give this close agreement with the theoretical pressure effect, and in the next sub-section evidence is reported to confirm these pressure figures by adopting an experimental technique that minimises the temperature effect.

(b) Further electrical measurements under stress

It could be argued that the interpretation advanced in the previous sub-section is wrong in that all the current changes could be ascribed solely to temperature and that mechanical stress plays an insignificant part. However this can be countered by the evidence of Figs 73, 74 and 75 showing a residual effect in the GR region where the power dissipation is so low that there can be little or no temperature effect. More importantly there is the evidence supplied by the spectral shift measurements of Konidaris and of Share, and it is from the former's arrangement that the idea arose for a modification to the technique of applying stress by a probe. Konidaris pressed his glass probe lightly against the LED operating at maximum power,

and thermal equilibrium was established before determination of the initial wavelength; he then increased the force to maximum and measured the wavelength again, assuming that the thermal equilibrium was scarcely disturbed. Incidentally Share followed the same procedure.

This technique of a light force of about a gram followed by a force of 50 grams was employed with the 500  $\mu\text{m}$  probe by the method explained at the end of Appendix A (Fig 97). When the initial force of a gram was applied, there was an immediate deflection of the galvanometer in the 'cooling' direction followed by a slow drift backwards in the 'heating' direction which lasted for over a minute; the explanation for this, namely absorption of heat by the probe, has already been discussed in Section 8 (d), p 101. When thermal equilibrium had been established, as shown by the galvanometer no longer drifting significantly, the considerable extra force of 50 grams was then added to the probe without disturbing its contact with the diode other than that it pressed more deeply into the surface. The large extra pressure produced a better contact so that

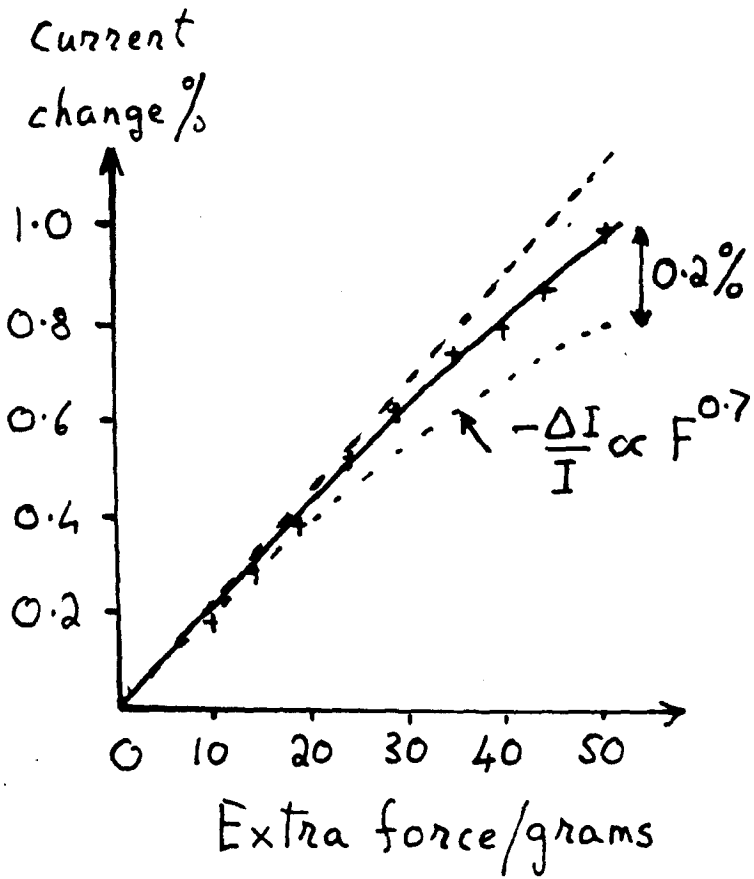


Fig.81. Probe radius 500  $\mu\text{m}$ ;  
diode current  $I = 1 \text{ mA}$

further heat flow from the LED resulted, but the increased flow was smaller than the initial one caused by a gram, as shown by the fact that the subsequent drift backwards was shorter (less than a minute). When the force of 50 grams was suddenly lifted, there was an immediate and approximately equal deflection of the galvanometer in the opposite (heating) direction. Incidentally the heating and cooling directions of the galvanometer were easily verified by bringing up a hot soldering iron close to the diode.

Working in the LE region with a current of 1 mA the deflections on the galvanometer that were observed on suddenly applying and lifting the extra force were averaged out and plotted for a range of forces from 50 grams down to 10 grams. The deflections were measured in microvolts and the readings converted to percentage change of current using a conversion factor of 100 uV equivalent to 0.28 per cent. Fig 81 shows the results for the 500 um probe, and it can be seen that the graph bends gently from a straight (dotted) line. From Section 7(d) on p.87 there is experimental evidence that an empirical relation exists

of the form  $-\Delta I/I$  varies as  $F^{0.7}$ , and this would be a graph of slightly greater curvature which is also shown as dotted on Fig 81; this latter curve has been drawn on the calculated basis that a force of 50 grams gives 0.8 per cent current change, as determined in Section 7 (d), p.86.

At the 50 gram value the experimental reading is almost exactly 1.0 per cent so that there is 0.2 per cent difference between the theoretically calculated and the experimental current changes. From Section 8 (d), p.104, this 0.2 per cent is the estimated difference between an initial heat flow with a low force and that with a force of 50 grams (or 48 grams to be precise). Again one is drawing on heat flow calculations of doubtful validity; but in the case of Fig 81 the initial heat flow effect has been eliminated by the revised experimental technique, and one is only left with an extra flow that is a much smaller quantity. In any event the difference between Fig 81 and Fig 77 is so striking that one is inevitably drawn to the conclusion that the former diagram (81) represents the pressure effect standing in its own right with only a



minor heat flow superimposed. Although the diodes used in Figs 81 and 77 were different, the device in the latter case having been damaged in experimentation, the evidence now points strongly to the fact that the pressure effect of 50 grams on the 500  $\mu\text{m}$  probe produces about 0.8 per cent change in the LE region.

The experiment of Fig 81 was designed with the earlier results of Fig 77 very much in mind and hence the readings were taken with a constant current of 1 mA, which is well within the LE range (the LED glows significantly). Also, attention was concentrated on the 500  $\mu\text{m}$  probe since, as has already been pointed out, this was the largest probe that could be safely used without fear of damaging the diode (see Appendix A, p.150); all the evidence pointed to the fact that the broader the curvature the greater the electrical change, and since the change was of the order of 1 per cent or less it was obviously important to use as large a probe as possible. Thus in the light of all this the theoretical calculations for pressure and temperature were mostly based on the 500  $\mu\text{m}$  probe.

In the final stages of the laboratory work a further experiment was performed in which the technique of a small contacting force followed by the main stressing force was adhered to, and thus the heat flow problem in the LE region (and in the GR, if it existed) was kept to a minimum. The extra force was a constant 50 grams so that there was a large pressure bordering on the elastic limit, and the current was varied from 10 mA in the LE region to 0.1  $\mu$ A well down in the GR region. In this experiment it was found that the galvanometer (voltage) deflection  $V_G$  seemed to be constant over the whole range of current. There was some spread of results; one had to be very quick in reading the galvanometer since it drifted off immediately after deflection due to draughts etc. The spread became more troublesome in the GR region, but nevertheless by repeated observations both on loading and unloading it became clear that the average deflection was 250  $\mu$ V and that this was more or less constant over the complete current range.

It had been expected that the voltage deflection would

have been slightly greater in the LE region from 10 mA down to 500-100  $\mu$ A due to an extra, though small, heat flow effect on application of the main stressing force, but this was not discernible. One explanation is that this extra effect exists in the GR region as well, even though the temperature excess is extremely small, and that it is constant. This possibility has already been advanced in the previous sub-section, p.110, in connection with the discrepancy between theory and experiment that is found with Figs 74 and 75.

For this particular diode the current - voltage characteristics were measured, and the values of  $nkT$  in the LE and GR regions were found to be 31 and 55 meV with a transition at approximately 60  $\mu$ A. On this basis the percentage current change for a deflection of 250  $\mu$ V is  $25/31 = 0.81$  per cent and  $25/55 = 0.45$  per cent in the LE and GR regions respectively. In the case of the former figure the agreement with other measurements for the 500  $\mu$ m probe is very good, and as regards the theory in Section 7 (d), p.86, the calculated value of 0.80 per cent

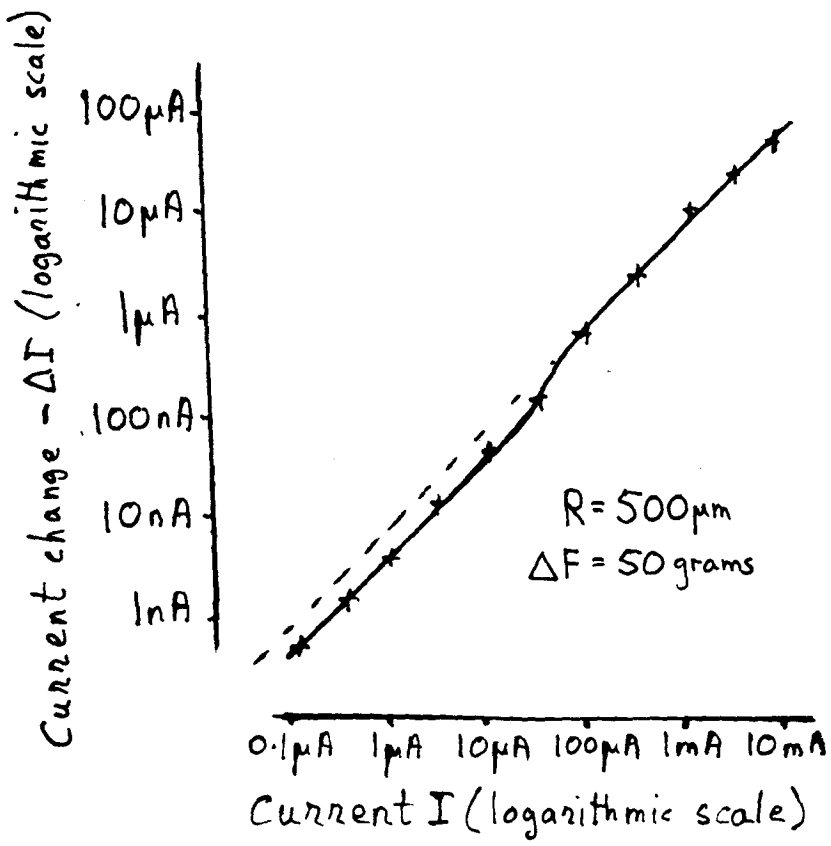


Fig.82

for  $p_z$  fits well - perhaps fortuitously. For the GR region the corresponding  $p_z$  calculation is 0.64 per cent and so the agreement is only fair.

It should be mentioned that during the course of the readings the fluctuation was  $\pm 50 \mu\text{V}$ ; but this seemed to be random, and with repeated observations it appeared to be about  $250 \mu\text{V}$  right throughout the very wide current range. When plotted logarithmically as in Fig 82 the experimental error does not really show up (an advantage of logarithmic presentation), and indeed the transition from the LE to the GR region is not particularly marked. When the experiment was devised and reported<sup>(34)</sup> the concept of avoiding a heat flow was well understood, but it was only at this stage that the significance of the change of a.c. resistance  $R_{ac}$  from the LE to the GR region was fully appreciated and hence that, even though the voltage deflection might be substantially constant, the equivalent current change would decrease with increasing  $R_{ac}$ .

The fact that the logarithmic presentation of Fig 82 shows a slope of 1 in the LE region and not 2, as in Figs

74 -75 (p.108), indicates conclusively that the technique of adding the main stressing force to a small nominal one effectively eliminates any significant heat flow effect.

On the whole this experiment proved to be a satisfactory conclusion to the previous work with the 500  $\mu\text{m}$  probe (and indeed with the other smaller probes) and was one more piece of evidence that the uniaxial stress component  $p_z$  plays its appropriate part both in the LE and the GR region.

10 REVIEW OF PAST WORK

In summing up the results reported in this thesis it is important to appreciate the climate of opinion that prevailed at the outset of the research with regard to the effect of pressure stress on diodes. The predominant figure was W. Ridner, of the Raytheon Research Division, Waltham, Mass., who working mainly with germanium stressed with very fine diamond probes of 10, 17 and 20  $\mu\text{m}$  radius using quite large forces up to 11 grams (2,3,4). Enormous current increases were recorded of the order of x30 for reversible effects and x250 for non-reversible ones both in forward bias and in reverse bias. The question of elastic reversibility is to some extent glossed over, as is the matter as to whether permanent damage had or had not been done; thus with forces of 5-10 grams on a 20  $\mu\text{m}$  diamond stylus it was reported that indentation occurred without visible cracks although heat treatment and subsequent etching showed that plastic deformation had taken place. The electrical changes were somewhat vaguely attributed to the creation of strain-induced generation/

recombination centres.

Round about the same time in 1964 Y. Matukura <sup>(5)</sup> in Japan was performing similar experiments on diodes of germanium and silicon using a 20  $\mu\text{m}$  sapphire probe with forces up to 10 grams. Again very large increases in current of the order of  $\times 100$  were reported, both for forward bias and also in reverse bias (though the reverse changes were somewhat smaller) and an explanation based on dislocation theory was advanced. In addition T. Imai <sup>(6)</sup> worked on germanium tunnel diodes with a fine steel needle and also with a rather naïve arrangement of pressing with a flat plate whose surface had been sprinkled with 300 mesh carborundum powder. Once more the matter of reversibility is vague:- "By the removal of the applied stress the diode currents return nearly to its (sic) initial value, thus the stress-induced current change is almost reversible with a critical value which varies from specimen to specimen". The electrical changes are for the most part ascribed to piezo effects.

In the above cases where the probes were always very



fine the contact radius  $r_0$  never exceeded  $1 \mu\text{m}$  and therefore the junctions had to be approximately a mere  $1 \mu\text{m}$  deep since stress falls off very rapidly with depth units of  $r_0$ . With the LED's used in the present research (and by Konidaris) the shallow depth is of necessity a feature of the light-emitting design; but it does mean that without encapsulation the device is susceptible to temperature-induced fluctuations brought about by draughts, and this was particularly noticeable in the GR region where it was difficult to make sensitive electrical measurements.

The work of Konidaris with a fine diamond probe  $25 \mu\text{m}$  in radius loaded with forces up to 10 grams was obviously an extension of the researches of Ridner and the Japanese, and his results (large positive change in the GR current) are in line with the earlier experiments. As has already been pointed out in Section 2 (p.12) the explanation of the results is based on the theory that pressure builds up elastic energy  $E(r)$  and that it is the highly anisotropic distribution of pressure, leading to large values of the gradient  $dE/dr$ , which causes the change in current. In

this theory  $E$  varies as  $p$  and therefore it is the pressure gradient  $dp/dr$  and not the pressure  $p$  which is the controlling parameter. Although there may be severe damage in an extremely small area in the immediate vicinity of the probe contact, the  $dp/dr$  factor extends beyond this to the edge of the diode, and thus the effect is distributed over most of the junction where  $dp/dr$  is significant but where  $p$  is very small and well below the elastic limit. This latter point accounts for the current change being reversible and for any negative current change due to the pressure  $p$  being insignificant. Konidaris ascribes his effect as being due to the generation of extra recombination centres, thus accounting for his observations as being confined to the GR region only; in this respect it could be argued that it should equally occur in the LE region as well, but is likely to have been masked by the much larger current in that region.

However, in the experiment of Share  $dp/dr$  is zero, and in his results one sees what happens when the uniaxial stress  $P_z$  takes control. Incidentally Share was primarily

looking at the light output, and hence his negative change in current is in the LE region. It would have been interesting if Share had extended his electrical measurements to the GR region, and also at room temperature as well as 77 K. Where Share and Konidaris are in agreement is in the latter's experiment with the large glass probe of radius 1.1 mm. This has already been discussed at considerable length in Section 7 (b), in which the present worker has attempted to improve the numerical correlation between the change in wavelength and that in energy gap, as postulated by Konidaris, and the results are fairly satisfactory.

The present worker's own researches have of necessity been done with probes, but the much broader curvature has ensured that the situation is close to the spectroscopic arrangement of Konidaris and to Share in general. No measurement of the spectral change has been attempted (one can rely on the results of Konidaris in this respect), but the recorded current changes are in agreement with those of Share in the LE region and extend to the GR since in both regions the same mechanism is presumed to apply,

namely an increase in the energy gap  $E_G$ .

Finally, it is appropriate at this stage to consider briefly the theory of the change in energy gap that is brought about by pressure. The main criteria for pressure effects on basic semiconductors such as Ge, Si, GaAs and GaP were reviewed critically as far back as 1961 in a paper by W. Paul, of Harvard University, (35) and the principles involved do not appear to have changed very much over the intervening years. The thrust of more recent research seems to be in tidying up details, the investigation of more novel materials such as the II-VI compounds and the development of devices with a highly specialised purpose; for example, a recent paper from the Soviet Union (36) reports on the pressure effect on energy gap of a silicon carbide (Schottky diode) LED which has been developed as an optoelectronic strain gauge for use under very large mechanical loads at high temperatures.

Probably the most fundamental, and indeed the simplest, approach is by way of bond theory in that pressure results in a decrease in lattice constant which in turn implies a

reduced bond length and hence an increased bond strength. Since the energy gap is, in the words of Paul "the difference between a bonding and an anti-bonding configuration" a greater bond strength should result in a corresponding increase in energy gap. As Paul points out<sup>(35)</sup>, there is well established evidence that for Ge and Si there is a correlation between a decrease in lattice constant and a decrease in relative permittivity ("dielectric constant") from which it can be inferred that there is an increased separation between the conduction and valence band edges. Nevertheless, although Ge has a positive pressure coefficient of band gap change, for Si the coefficient is anomalous in being negative, so that other factors must be involved. One possibility may reside in the difference between the (111) crystal direction for Ge as compared with the (100) for Si, and another is the fact that both materials have indirect energy gaps for which the situation at the extrema of the band edges is rather complex.

In the case of GaAs, which should be a more straightforward material inasmuch as it is a direct gap type, Paul

points out that the very marked increase in electrical resistivity with pressure is a direct consequence of an increase in energy gap. A paper that deals exclusively with GaAs (28), and is quoted by Konidaris, is one by G.E. Fenner, of the General Electric Research Laboratory, New York, who worked with GaAs lasers. The experimental evidence is similar to that of Konidaris (7) and Share (11) in that he observed a decrease in wavelength when pressure was applied. Fenner maintains that the wavelength shift is primarily due to a change in relative permittivity and that this in turn implies an increase in energy gap.

The situation for GaP is somewhat different and is discussed fairly fully by Paul. Unlike GaAs, but like Si, it is a material with an indirect gap and like Si again it has an anomalous (small) negative pressure coefficient. However, when GaP ( $E_G = 2.24$  eV) is added in a smaller proportion with GaAs ( $E_G = 1.35$  eV) the resulting mixture has a direct energy gap which is approximately the appropriate average value; on this basis  $\text{GaAs}_{0.6}\text{P}_{0.4}$  material should theoretically have an  $E_G$  value of 1.71 eV, and this

compares reasonably well with the experimentally determined figure of 1.92 eV found in this research (see p.16), a value which is in agreement with that of Konidaris (7) as measured by his spectroscopic technique.

It is in the above manner that the problem of estimating the pressure coefficient for  $\text{GaAs}_{0.6}\text{P}_{0.4}$  can be tackled. For GaAs alone Paul (35) and Wolf (17) both quote a range of  $9$  to  $12 \times 10^{-6}$  eV atmosphere<sup>-1</sup>; the range is probably due to the fact that a lower figure is associated with a lower temperature (eg a laser cooled with liquid nitrogen) and the upper figure is the likely one for room temperature. Fenner's measurement (28) of  $10.9 \times 10^{-6}$  eV atm<sup>-1</sup> is for a GaAs laser cooled with dry ice. Konidaris uses this reference as his source (7) for a value of  $11 \times 10^{-6}$  eV atm<sup>-1</sup>, and in fact this number has been assumed in the present research; however Fenner only reports on GaAs and not a GaAs/P mixture, and the following reasoning has been devised for applying the same value to the LED under investigation.

Firstly, extrapolation of Fenner's figure for GaAs to

a room temperature value of  $12 \times 10^{-6} \text{ eV atm}^{-1}$  has been assumed, and applying this to an energy gap value of 1.35 eV gives a fractional coefficient change of  $8.89 \times 10^{-6} \text{ atm}^{-1}$ .

Secondly, all the authorities are agreed that the pressure coefficient for GaP is small (and negative) and is about  $-1.7 \times 10^{-6} \text{ eV atm}^{-1}$  so that, as a fraction of the energy gap of 2.24 eV, this comes to  $-0.76 \times 10^{-6} \text{ atm}^{-1}$ . Then for a 60/40 GaAs/P mixture, 60 per cent of one fraction less 40 per cent of the other gives an overall fractional change of  $5.00 \times 10^{-6} \text{ atm}^{-1}$ , and on applying this to a band gap of 1.92 eV one arrives at a pressure coefficient of  $9.6 \times 10^{-6} \text{ eV atm}^{-1}$ . In view of the uncertainties involved in this estimate and the equally great uncertainties in the figure for Young's modulus (which affects the calculations for pressure distribution) a decision was made early on in this research to slightly upgrade the pressure coefficient to  $11 \times 10^{-6} \text{ eV atm}^{-1}$ , thus maintaining the same value as used by Konidaris in his spectroscopic work.



11 CONCLUSION

A general conclusion of the present research is that it has been a fundamental mistake in the past to use fine probes whereby even very small forces can produce catastrophic damage which is not truly reversible. It is better to employ probes of much larger curvature because the necessary stresses can still be easily achieved with forces of tens or hundreds of grams, and at the same time the contact area is very much more extensive so that the electrical changes to be measured are correspondingly increased; in addition the enlarged radius of contact ensures that devices with deeper junction layers can be investigated. There is no difficulty in obtaining large sapphire probes at a relatively cheap price<sup>(10)</sup>, their curvature and elastic constants being quoted by the manufacturers. For probes of very large curvature it is also possible to make them locally out of glass, as did Konidaris, or use other readily available materials such as ball bearings.

Of course, the availability of a device with the

emission of bright light from a shallow layer has greatly facilitated the problem of determining the elastic limit, and the estimate of a probable upper limit for this value has been a significant feature of the present research. It has also been shown that the reverse bias characteristics are substantially different from what had previously been recorded, and the suggestion is made that further research in this field, particularly the temperature dependence, could profitably be undertaken; the characteristic has been shown to be very susceptible to the influence of light. In the forward direction the importance of temperature has been emphasized.

As regards the effect of pressure the overall situation is perhaps less clear cut. The simple theory and the more elaborate development of the Fuchs equations for the distribution of stress provide a framework, but one is always aware that the detailed calculations depend on a knowledge of such quantities as Young's modulus and Poisson's ratio, and for complex substances like  $\text{GaAs}_{1-x}\text{P}_x$  accurate values for such quantities do not seem to be

available. Although pressure has an effect in the LE region, it is overshadowed by temperature. In the GR region one would expect the pressure to predominate, and this has been verified experimentally; but the effect is small and is somewhat reduced compared with the LE because the change in band gap is governed by the  $\Delta E_G/2kT$  term whereas in the LE region it is  $\Delta E_G/kT$ .

Of the two main effects - pressure and temperature - the former has been more satisfactorily analysed, particularly from a theoretical point of view, although an element of doubt has been cast on one of the Fuchs equations, namely that for  $p_t$ . It was originally thought that the stress effect was brought about by the overall 'hydrostatic' pressure  $P_{hyd}$ , and  $P_{hyd}$  contains the  $p_t$  component. However, as the pressure theory was being developed and matched with the experimental data that had already been accumulated for a range of probes and forces, it became clear that if pressure does play a part then it is the uniaxial stress component  $p_z$  which is responsible. Also the Fuchs equation for  $p_z$  seems to fit in well with

numerical data quoted in engineering text-books for ball bearings so that calculation based on  $p_z$  can be assumed to be reliable. On the whole the pressure effects ascribed to  $p_z$  have matched in well with the experimental results despite the fact that the current changes associated with pressure are very small and only reach 0.8 per cent in the LE region for the broadest probe of 500  $\mu\text{m}$  when loaded to the elastic limit with a force of 50 grams.

In the LE region where the diode is at least a few degrees above room conditions the temperature effect certainly predominates over that of pressure. Here however the analysis is a good deal less satisfactory because Herr Fuchs is no longer available to set up the relevant equations, and with the present worker's very limited ability in the field of applied mathematics the model of the heat flow is simplistic, to say the least. Also the thermal conductivity of the diode material is not accurately known.

As regards the overall aims of the research it has already been pointed out in the introduction that an

improvement in pressure transducer devices would be a worthwhile gain, and that this was emphasized some years ago by C. A. Hogarth in the context of the somewhat different topic of heterojunctions<sup>(8)</sup>, his exact words being: "Certain special structures may well find advantage in pressure transducers and strain gauge applications where a smaller dependence of gain factor on temperature may be achieved than with silicon devices". The present research clearly indicates that such a device is not forthcoming by the application of a probe on an LED of the type under investigation.

However, despite all the reservations expressed above, it is felt that the results of the research have been worthwhile in that a more coherent pattern has emerged from what had previously been a confused situation. In addition, the practical difficulty of loading a probe onto a device has been satisfactorily overcome; apparatus is now available for a whole series of probes carrying a very wide range of weights from a few milligrams to hundreds of grams. In parallel with this the problem of measuring

small changes in current has been solved, and it is suggested that the technique of passing a constant current through a device and measuring across a bridge the small change of voltage brought about by some external factor is one that could be employed in other experimental situations.

Given that these mechanical and electrical facilities have now been developed, it is suggested that further research could proceed with silicon and germanium diodes. These could be fairly large devices with junction layers much deeper than  $1 \mu\text{m}$  so as to be less susceptible to draughts, and they could be investigated with probes of broad curvature carrying heavy loads. Naturally enough, it would be essential to work well within the elastic limit. The physical constants such as elasticity, thermal conductivity, etc, are well established for silicon and germanium so that the results could be interpreted with a good degree of confidence. An interesting feature is that though silicon and germanium have negative temperature coefficients for band gap of  $-2.3$  and  $-3.7 \times 10^{-4} \text{ eV K}^{-1}$

respectively<sup>(37)</sup>, the pressure coefficients are of opposite sign. Thus the figure for germanium is positive, being  $7.3 \times 10^{-6} \text{ eV atmosphere}^{-1}$  (37), so that like GaAs/P, for which the value is  $11 \times 10^{-6} \text{ eV atm}^{-1}$ , the probe stress and any cooling effect will add up; on the other hand the pressure coefficient for silicon is negative and is rather low, being  $-2.0 \times 10^{-6} \text{ eV atm}^{-1}$  (37), so that any experiment would present a challenge but a worthwhile one in view of the overwhelming importance of the material.

In fact on looking back over a span of twenty years to the work with spherically tipped probes for the stressing of silicon and germanium, the two semiconductor materials that have made such an impact on modern technology, it would appear that the results have not been particularly consistent and yet the discrepancies do not seem to have been ironed out. No doubt such a line would nowadays be regarded as dated and a bit of a 'loose end', but it would be interesting if it could be tied up.

---

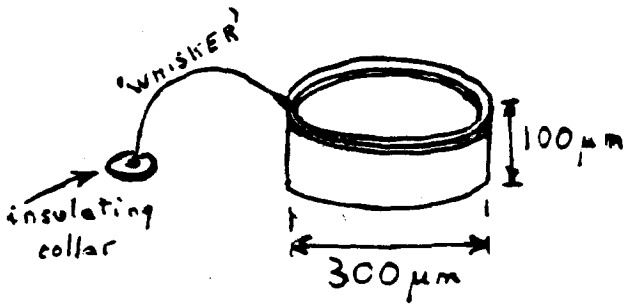


Fig.83. Repeat of Fig.1

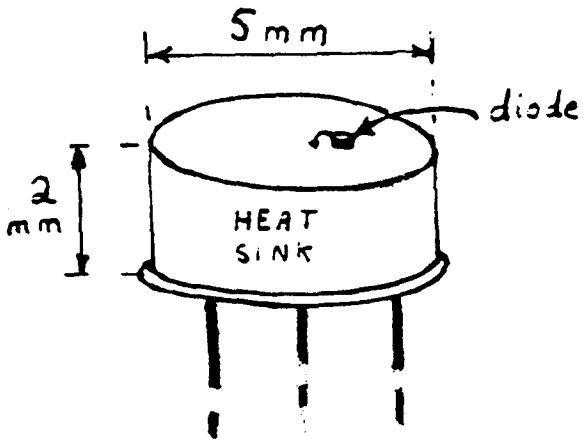


Fig.84. Repeat of Fig.2



APPENDIX A: Method of applying stress

The semiconductor details of the LEDs supplied by Standard Telecommunication Laboratories Ltd have been described by Konidaris (1,7), and from his accounts the main points to be noted are as follows. Starting with an n-type Se doped ( $10^{17} \text{ cm}^{-3}$ ) epitaxial layer of  $\text{GaAs}_{0.6}\text{P}_{0.4}$  grown from the vapour phase upon an n+ GaAs slice, a heavily doped p-type layer is obtained by Zn diffusion so that a planar junction at a very shallow depth of about  $1.3 \mu\text{m}$  is formed. Around the edge of the top layer a very narrow Al contact is evaporated, leaving a bare circular area of the p-region of diameter  $0.3 \text{ mm}$  to emit radiation; the short diffusion length ( $0.3 \mu\text{m}$ )<sup>(38)</sup> of the minority carrier ensures that the radiation originates in the junction, or very close to it.

The main features of the shape and physical size of the diode and the heat sink upon which it is mounted are shown as Figs 1 and 2 of Section 2 (and also in Section 8 in connection with the analysis of heat flow) and are once more repeated here for convenience as Figs 83 and 84. The

Facing  
p.140

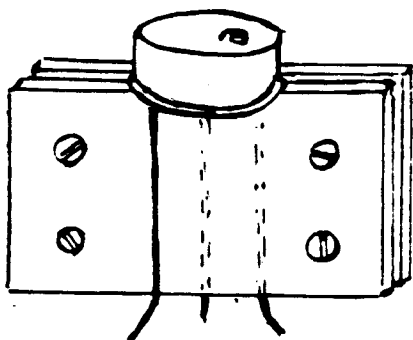


Fig.85. Repeat of Fig.3

heat sink consists of an alloy cap filled on the underside with insulating material into which three stout leads of diameter 0.43 mm are firmly embedded. One of the leads terminates in an insulating collar that is set in the alloy cap, and from this a final connection to the narrow Al ring is made via a very fine wire or 'whisker'. This whisker proved to be extremely fragile and broke off very readily when touched so that it was always a source of anxiety when stressing operations were in progress. Of the two other leads, one makes an electrical connection to the alloy cap and the other is a dummy that terminates in the insulating material. Since the three stout leads are arranged in a triangular pattern under the alloy cap, in the present research one of the live ones and the dummy were gripped between a pair of insulating plates bolted tightly together (Fig 85) so that the whole device was well secured to the plastic plates, and at the same time electrical connections could easily be made to the external circuit.

The diamond and sapphire probes were rod-shaped jewels

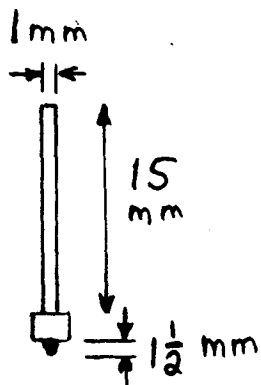


Fig.86

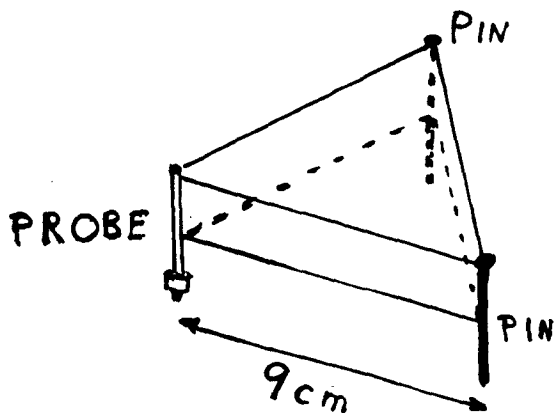


Fig.87. Weight distributed  
equally on two pins and probe.

with their ends rounded off to the appropriate curvature and were fixed in metal holders about 1 mm in diameter and 15 mm long so that about 1.5 mm of the jewel protruded (Fig 86). Using 2 mm (model aeroplane) balsa sheets as the constructional material, hollow frames were made up, consisting of an equilateral triangle of side 9 cm with stiffening walls stuck to the edges, and to the apex of each frame a probe and two dressmaking pins were firmly cemented with "Araldite" (Fig 87). Each triangular frame was separately weighed (about 3 grams), and in each case the centre of mass was found to coincide almost exactly with the centroid of the triangle so that the force applied by the probe and the two pins was about a gram apiece. By placing an extra mass at the centroid, the force exerted at each of the three supports could be increased to an amount equal to one third of the total weight of the arrangement, and this force could be as much as 100 grams if necessary.

The triangular frame was arranged with the two pins resting on rigid blocks made of fairly hard wood, and

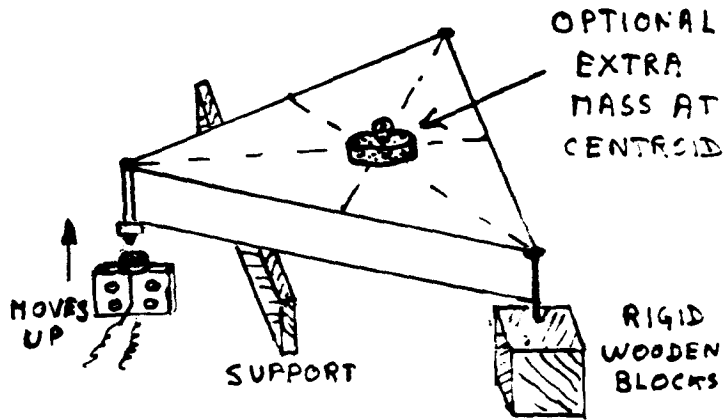


Fig.88

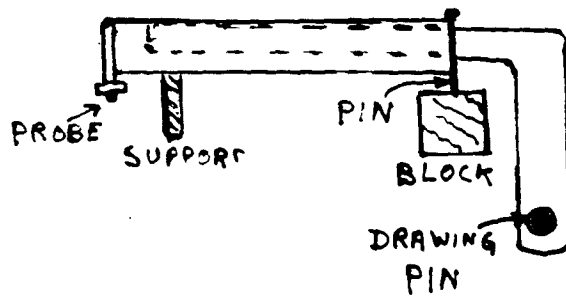


Fig.59

the end with the sapphire probe was held up by a wooden support as shown in Fig 88. The plastic plates with the diode and its sink could then be manoeuvred upwards (by a suitable mechanism to be described) until the centre of the diode itself engaged the sapphire probe and gently lifted the frame a millimetre or so off the support, the axis of rotation being the line between the points of the two pins resting on the rigid blocks. Thus by this means the probe exerted on to the centre of the diode a force equal to one third of the total weight of the triangular frame.

Although large forces could be safely applied by the broad probes, in the case of a fine diamond probe even a gram was excessive. Under these circumstances, the 3 gram weight of the triangular frame was balanced out by inserting an extra L-shaped piece of balsa wood (Fig 89); the weight and centre of gravity of this extra piece were varied by sticking in a drawing pin (or two, if necessary) as shown. Thus the situation could be adjusted until it was barely in stable equilibrium, and on removing

the temporary support (by lowering it with a suitable mechanism) the whole arrangement oscillated gently with a long period on the points of the two dressmaking pins. Then a very small extra weight of, say, 10 mgm at the centroid would produce a force of 3.3 mgm on the probe. Thus altogether the range of possible forces was from a few milligrams to a hundred or more grams.

When the plastic plates holding the LED were raised so as to engage the diode with the probe, the problem was to adjust the position of the plates very carefully beforehand and to ensure that the centre of the diode was coincident with the probe just prior to contact being made. Obviously a micrometer type of stage was necessary with lateral movements that could be controlled to a few thousandths of a millimetre. Because of the complexity of these adjustments and the problem of lifting the diode, it was decided to build up a fairly large and robust stage and to scale down the movements by appropriate geometrical reduction; to this end the constructional material of "Meccano" proved to be very suitable.



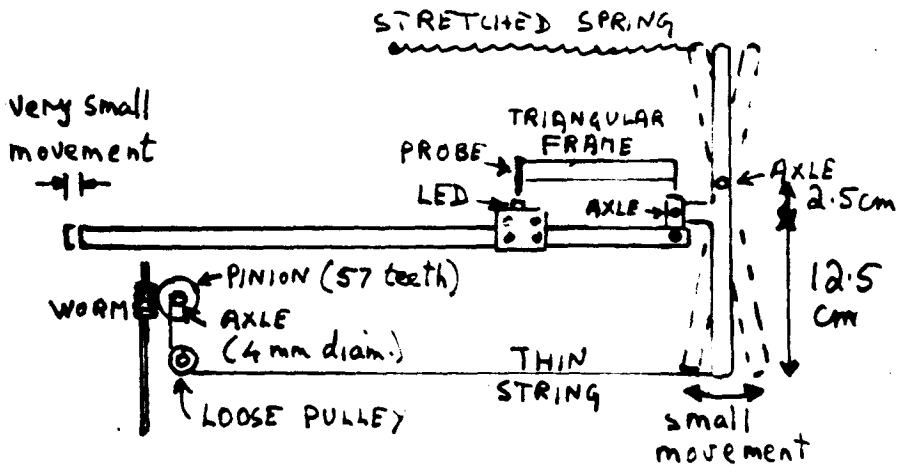


Fig. 90

In this mechanical stage the dimensions are all based on the unit of half an inch spacing between bolt holes, and in converting to centimetres a simple scale of 2.5 cm to the inch has been adopted. Fig 90 shows the plastic plates holding the LED bolted onto a long rigid arm; this arm can be displaced a very small amount in the direction of its length by a slight rotation of the vertical lever of velocity ratio 2.5 to 12.5 (ie 1:5), and this rotation is effected by winding a thin string onto an axle 4 mm in diameter that is turned by a worm and gear of 57 teeth. One revolution of the worm rotates the gear by approximately 0.11 radian, and this shifts the string on the axle by about 0.22 mm; with the 1:5 reduction on the lever the plastic plates are moved by 0.044 mm or 44  $\mu\text{m}$ . The overall reduction factor could have been made greater, but in practice it was found to be satisfactory. By pulling hard with a tightly stretched spring, backlash in the movement was more or less completely eliminated, and a fraction of a turn on the worm gave the finite amount of displacement that was necessary for the final adjustment

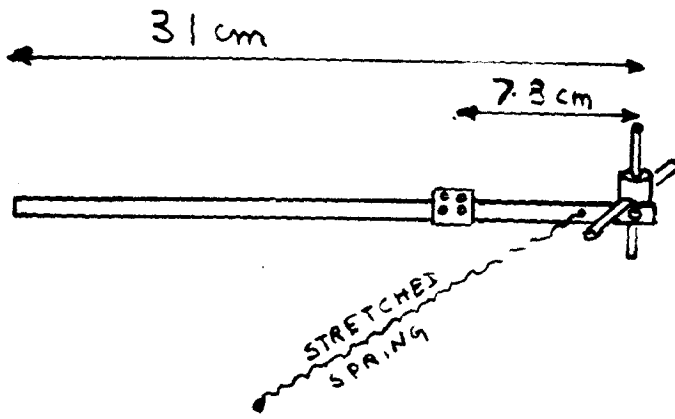


Fig.91

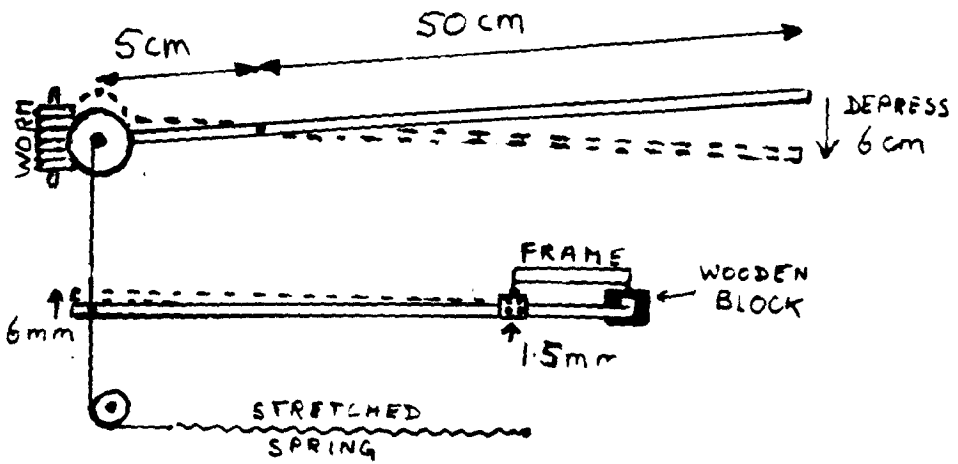


Fig.92

of the LED relative to the probe.

Fig 91 shows that the long arm can also be moved in a horizontal plane at right angles to the plane of the diagram. What is shown is yet another spring for taking out any play on the vertical axle about which the long arm rotates and also the velocity ratio of 7.8 to 31 (1:4) of the long arm. The dimension of 7.8 cm comes about because it is the length from apex to base of the triangular frame holding the probe; the significance of this is explained below.

The vertical adjustment is also effected by means of a worm, 57-tooth gear, etc, and is similar to the mechanism shown in Fig 90 except that it operates in a different plane; it is illustrated in Fig 92. However, there is a further detail in that the 57-tooth gear is shown to be mounted on the end of a long arm of velocity ratio 5:50 (ie 1:10), and on depression of this arm by about 6 cm at the 'handle' end the gear is lifted vertically 6mm. This displacement is translated by the string to the long arm holding the LED, and the latter is thereby raised by

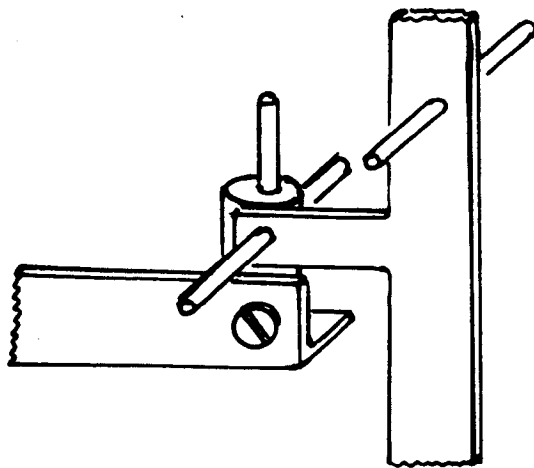


Fig.93

about 1.5 mm, which is sufficient to engage the LED with the probe and lift the loaded triangular frame by a millimetre or slightly less from its temporary support. An important detail is the use of a cylindrical 'coupling' ("Meccano" part 63) shown in Fig 93, which permits universal rotation, care being taken to eliminate slackness in the various bearings by pulling with tightly stretched springs in the three directions of space. The triangular balsa-wood frame was initially located on the rigid wooden supports so that the line between the dress-making pins was extremely close to the line of the upper horizontal bearing of the "Meccano" coupling. Thus after the final adjustments had been made for the alignment of the diode relative to the probe, the rocking of the frame upwards resulted in a very small change ( $5\ \mu\text{m}$  or less) in the alignment because the the frame is large (7.8 cm from apex to base) compared with the vertical displacement of the probe of less than a millimetre.

For viewing the contact of the LED with the probe two low-power travelling microscopes were used. Being of

Facing  
p.147

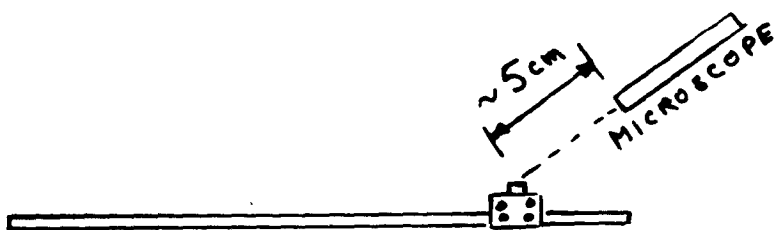


Fig.94 Front elevation

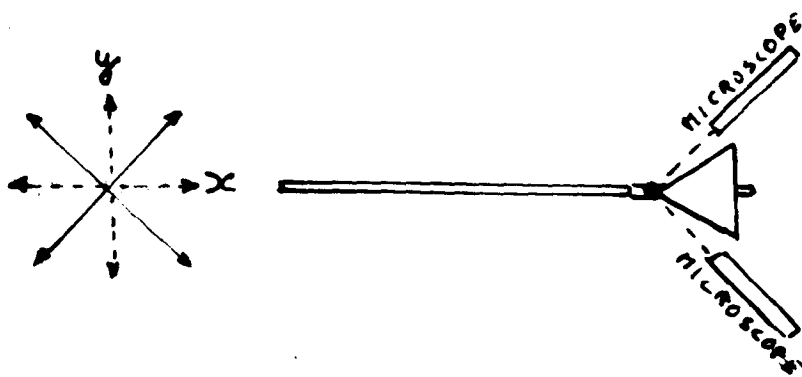


Fig.95. Plan; x and y movements coupled together

low power the difference between the objective lens and the object was fairly long (about 5 cm) as shown in Fig 94, and by orientating the barrel of a microscope so that it pointed downwards at about  $45^\circ$  a clear view of the top face of the diode and the lower end of the probe was obtained. Adjustments to a microscope were easily effected because it had micrometer movements in the horizontal and vertical directions, and the barrel could be moved longitudinally by a rack and pinion. By positioning the two microscopes at right angles to one another (Fig 95) alternate views in two orthogonal directions were possible.

It was obviously convenient to displace the diode laterally at right angles to the line of sight of a microscope so that adjustments in position as seen through one microscope did not affect subsequent adjustments as seen through the other. To this end the worms operating the orthogonal horizontal displacements (shown as x and y in Fig 95) were coupled together by a pulley system which, when operated by a handle, rotated the worms simultaneously at equal speeds. The resultant displacement was then



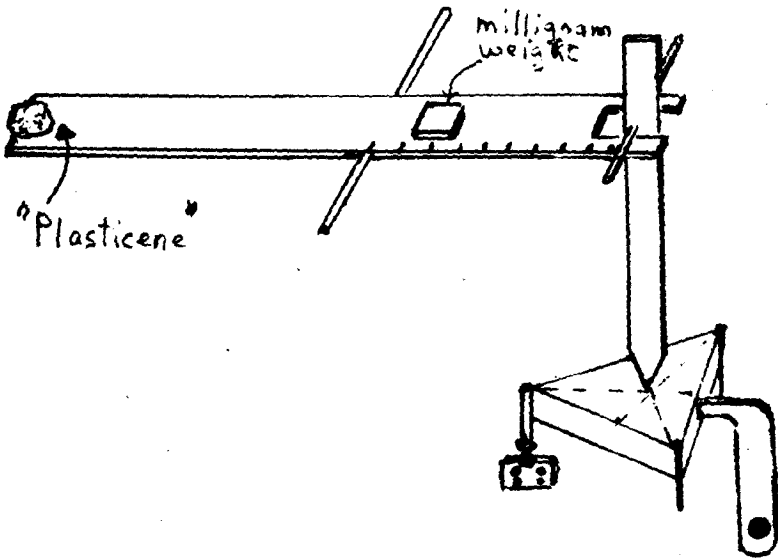


Fig.96

at  $45^\circ$  to the direction of the long arm, and by reversing one of the pulleys the movement was changed to the other  $45^\circ$  direction. In devising the pulley system the opportunity was taken to iron out the discrepancy between the 1:5 velocity ratio of the y-shift and the 1:4 of the x-shift, and overall the reduction factor was slightly increased, giving greater sensitivity to the adjustments.

Finally, for loading the balsa-wood frame the easiest way was to place a weight on its centroid, but for very small forces, when the frame had been balanced as shown in Fig 89, a useful device was made up as follows. The device (Fig 96) was a balsa-wood strip about 20 cm in length with a long pin cemented in the middle so that it rested on smooth supports; the short pin cemented at the end carried a thin, loosely hanging arm as shown. When balanced with a small piece of "Plasticene" on the end of the strip the centre of gravity was such that the whole arrangement was only just in stable equilibrium. Then a temporary support was placed in position by a lever mechanism and a very small weight, usually 100 mgm, was positioned on the strip

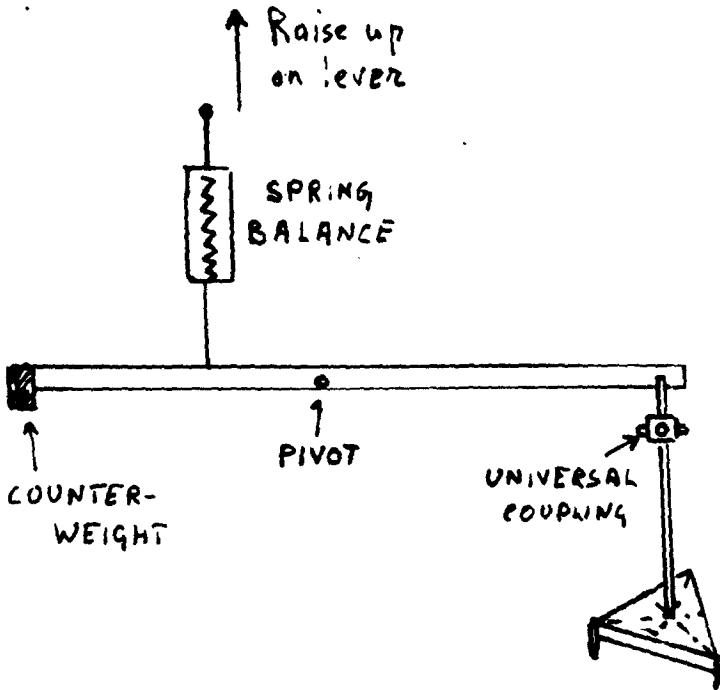


Fig.97

(which was marked out with a scale of ten) at a suitable spot for producing the force required. On gently lowering the temporary support, the hanging arm engaged with the centroid of the triangular frame, thereby loading the probe.

This idea was subsequently developed for much greater forces of the order of 10-100 grams for probes of larger radius. The parts were of "Meccano" and the unbalanced force was applied by raising a spring balance on a lever arm as shown in Fig 97. This device proved to be very useful for later measurements when a different technique for loading a probe was required; a small force was applied initially so that the probe was in light contact with the diode, and then on raising the lever the spring balance was rapidly stretched thus giving rise to a much larger force without disturbing the contact between the probe and diode.

The final point to be discussed in this Appendix is the reason why only the probes going up to a maximum radius of 500  $\mu\text{m}$  were used in this research despite the

Facing  
p.150

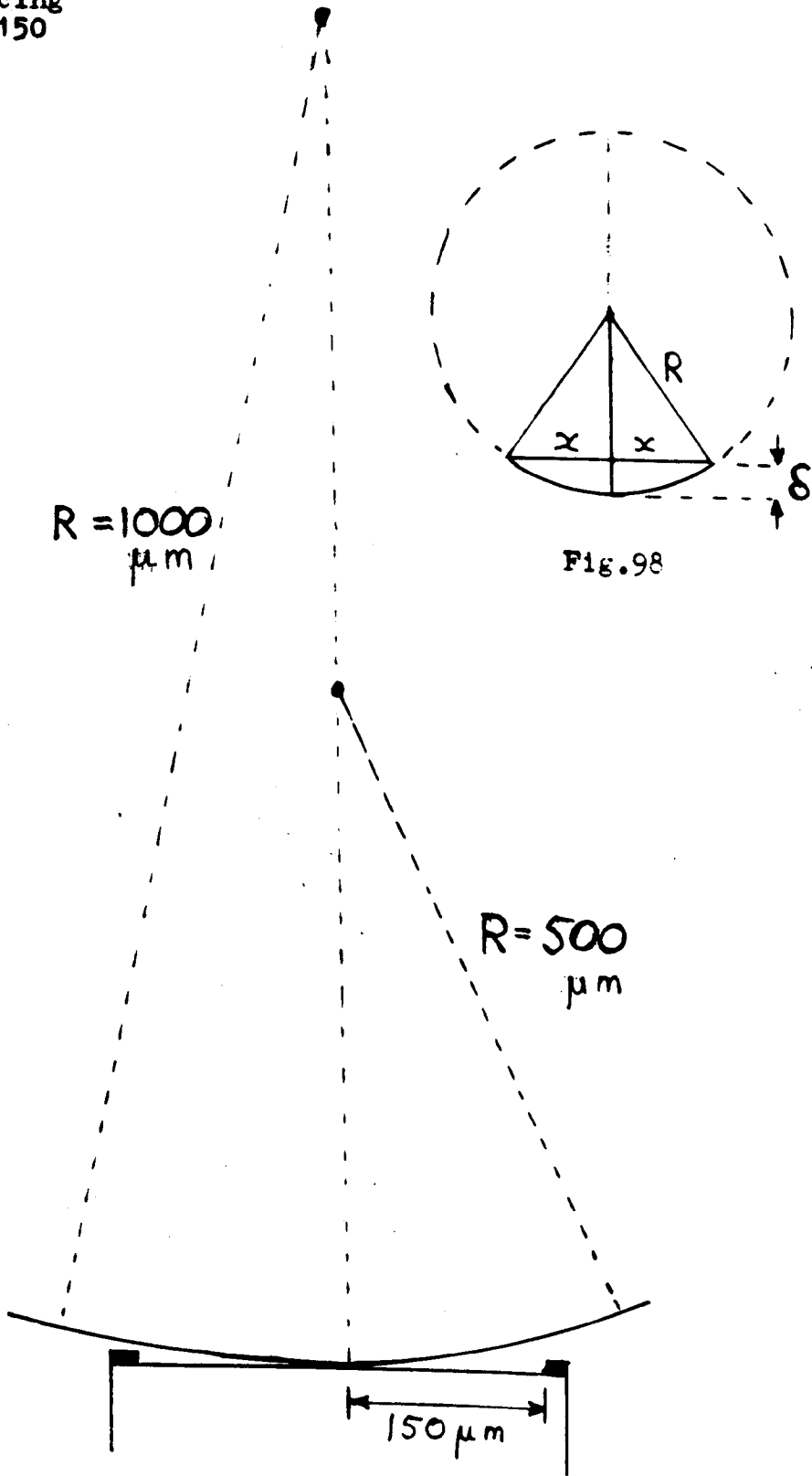


Fig. 99

fact that two larger sapphire probes (750 and 1000  $\mu\text{m}$  radius respectively) were available; reference has been made to this in Section 6 (b), p.55.

Once more the 'spherometer relation', as illustrated in Fig 98 is required. The exact relation is  $(2R-\delta)\delta = x^2$  and when  $\delta \ll 2R$  this reduces to a very good approximation  $\delta = x^2/2R$ . The radius of the exposed surface of the diode that emits radiation is 150  $\mu\text{m}$ , and so when  $x = 150 \mu\text{m}$  and  $R = 500 \mu\text{m}$  then  $\delta = 22.5 \mu\text{m}$ ; for  $R = 1000 \mu\text{m}$  the corresponding value of  $\delta$  is 11.25  $\mu\text{m}$ . The narrow aluminium ring contact around the edge of the diode (Fig 83) is extremely shallow in depth, and measurement by a travelling microscope with a limited sensitivity of 0.01 mm (10  $\mu\text{m}$ ) gave an estimate that showed it to be somewhat less than 10  $\mu\text{m}$  but of that order. Thus a probe of radius 500  $\mu\text{m}$  would certainly not touch the ring contact, but with a 1000  $\mu\text{m}$  probe the clearance would be tight; this is illustrated in Fig 99, which is approximately to scale and shows the 1000  $\mu\text{m}$  curvature on the left and the 500  $\mu\text{m}$  one on the right.

The main problem arises with the fine wire, or 'whisker', connection which, as already stated, was extremely fragile. In fact in one instance a number of diodes sent in a packet from Standard Telecommunication Laboratories Ltd did not survive the hazards of the Post Office service despite careful packing and had to be sent back for repairs to the whiskers; subsequently a number were broken during the course of the research. With a 1000  $\mu\text{m}$  radius it would be necessary to offset the probe to the side of the diode away from the wire in order to be absolutely safe; not only was this difficult to adjust because the line of sight of the microscopes (see Figs 94 and 95) did not permit accurate location of the centre of a large probe, but also it was considered to be undesirable in as much as the theory of stress depended on the probe contact being reasonably central.

APPENDIX B:- Current-voltage characteristics of the diode

The precise relation for the diode, both in the GR and in the LE region, is  $I = I_0 [\exp(qV/nkT) - 1]$ , but in order to estimate  $I_0$  one naturally looks at the GR region where as has already been shown in Section 4(a) the experimental value of  $n$  is approximately 2, making  $nkT/q = 50$  mvolt. In Fig 19 (p.30) of Section 4 the smallest value of  $I$  that could be measured is 10 pA, for which the value of  $V$  is about 0.45 volt; this gives  $\exp(qV/nkT) = \exp 9.0 = 8100$ , and hence  $I_0 = 1.2 \times 10^{-15}$  amp. In Fig 16 (p.29) which shows a characteristic taken much earlier in the research with a less sensitive technique, the corresponding value of  $I_0$  is  $5 \times 10^{-15}$  amp. In general the diodes tended to range between  $5 \times 10^{-15}$  and  $5 \times 10^{-16}$  amp so that  $10^{-15}$  amp is probably a realistic average.

Since all the research on the LEDs in forward bias was undertaken with voltages greater than 0.5V, ie  $\exp(qV/nkT)$  greater than  $10^4$ , it is obvious that for practical purposes the  $-1$  term in the diode relation can be completely disregarded and that the formula can be



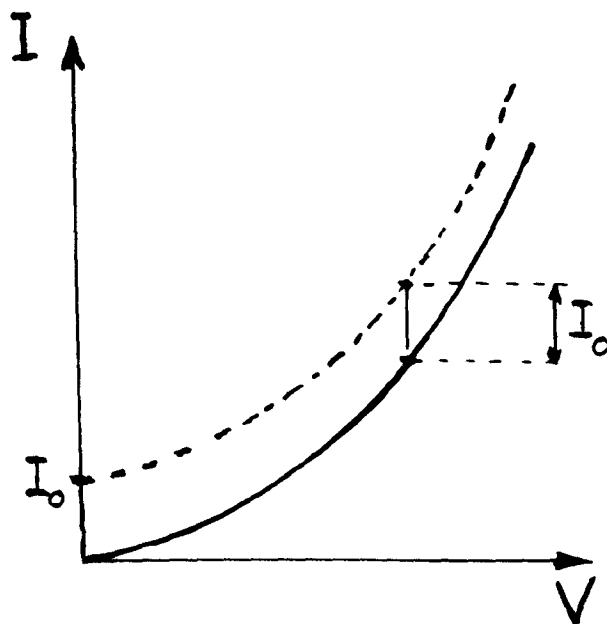


Fig.100

approximated to  $I = I_0 \exp(qV/nkT)$ . This is illustrated on an exaggerated scale in Fig 100, in which the dotted curve shows the departure of the approximate relation from the true one at low voltages.

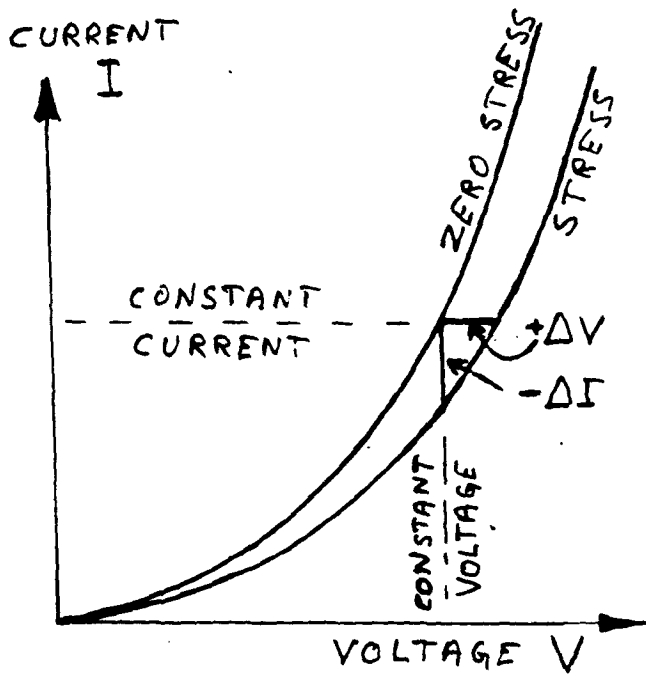


Fig.101

APPENDIX C:- Change of characteristics under stress

In Section 6 (a) an important distinction is made, on the one hand, holding the diode at a constant voltage and measuring the change in current when stress is applied and, on the other hand, operating the diode at a constant current and determining the change in p.d. across it brought about by stress. Obviously the former is the desired effect to be measured, but in practice the latter technique proved to be the more feasible. Exactly the same problem arises in Section 8 where the physical change is not stress but temperature, and this is discussed further in Appendix D.

The situation is illustrated in Fig 101 which shows a negative change  $-\Delta I$  in current when the diode is stressed at a constant voltage; this would imply an increase in impedance of the diode and therefore, with a constant current, the p.d should show a positive increase  $\Delta V$ . In the experimental account the current change is written as  $|\Delta I|$ , but in this Appendix, which is essentially of a mathematical nature, it will be assumed to be  $\Delta I$  and

the minus sign should emerge in the equations. At this stage the only assumption made is that the diode is operating at a potential above 0.5 volt so that it is following the approximation of a simple exponential relation as deduced in the previous Appendix. What is not assumed, and is yet to be shown, is that the two curves are sufficiently close together for them to have virtually the same slope in the region of electrical change; if this were so, then one could assume that the ratio  $\Delta I / \Delta V =$  the slope  $dI/dV$  of the zero stress curve and that this slope  $= 1/R_{ac}$  where  $R_{ac}$  is the a.c. resistance of the unstressed diode at the electrical point under consideration.

At constant voltage  $V$  we have:-

$$\text{with zero stress } I = I_0 \exp(qV/nkT)$$

$$\text{and under stress } I' = I'_0 \exp(qV/nkT) = I + \Delta I$$

$$\text{Therefore } I'_0/I_0 = 1 + \Delta I/I \quad \text{eq (i)}$$

At constant current  $I$  we have:-

$$\text{with zero stress } I = I_0 \exp(qV/nkT)$$

$$\text{and under stress } I = I'_0 \exp[q(V + \Delta V)/nkT]$$

Therefore  $I_0'/I_0 = \exp(-q \Delta V/nkT)$

$$= 1 - (q \Delta V/nkT) + \frac{1}{2}(q \Delta V/nkT)^2 - \dots \quad \text{eq (ii)}$$

Equating (i) and (ii) gives

$$-\frac{\Delta I}{I} = \frac{q \Delta V}{nkT} \left( 1 - \frac{1}{2} \frac{q \Delta V}{nkT} + \dots \right) \quad \text{and hence}$$

$$-\frac{\Delta I}{\Delta V} = I \frac{q}{nkT} \left( 1 - \frac{1}{2} \frac{q \Delta V}{nkT} + \dots \right) \quad \text{eq (iii)}$$

But  $I = I_0 \exp(qV/nkT)$ ; and on differentiation

$$\frac{dI}{dV} = I \frac{q}{nkT} \quad \left( \text{or } \frac{dI}{I} = \frac{q dV}{nkT} \right) \quad \text{eq (iv)}$$

Substitution of eq (iv) in eq (iii) gives the approximate relation (neglecting second-order terms)

$$-\frac{\Delta I}{\Delta V} = \frac{dI}{dV} \left( 1 - \frac{1}{2} \frac{q \Delta V}{nkT} \right) \quad \text{eq (v)}$$

In the readings shown in Fig 77 (p.110) the maximum value of the current change  $\Delta I/I$  is 1.6 per cent. Hence from eq (iv) it is permissible to substitute the term  $q \Delta V/nkT$  in eq (v) by  $\Delta I/I$  since this only involves a second-order approximation; and at the same time, if one reverts to the form  $|\Delta I|$ , then eq (v) becomes

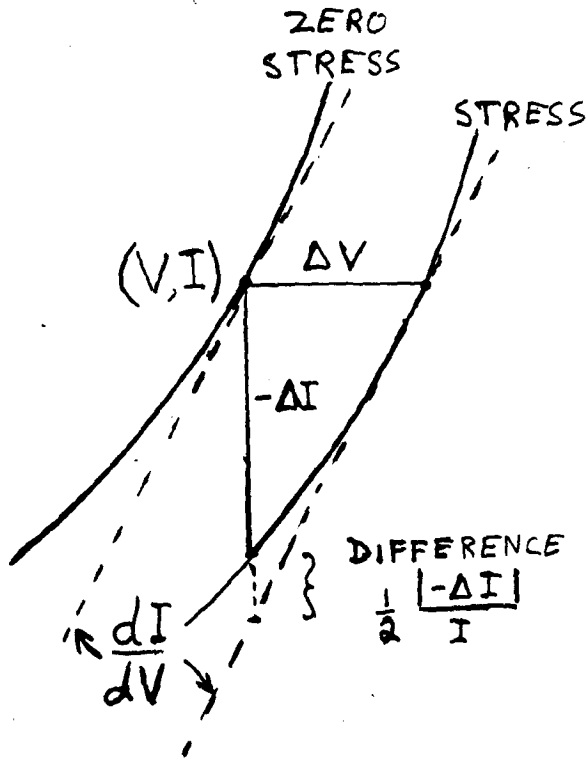


Fig.102. Enlargement of Fig.101

$$\frac{|-\Delta I|}{\Delta V} = \frac{dI}{dV} \left( 1 - \frac{1}{2} \frac{|-\Delta I|}{I} \right)$$

Thus  $|-\Delta I|/\Delta V$  is only slightly smaller than  $dI/dV$ , and the difference is shown geometrically on an exaggerated scale in Fig 102.

For a current change of 1.6 per cent the difference is only 0.8 per cent. However in general the agreement is even better because in the more important readings shown in Figs 81 and 82 (pp. 115 and 120) the maximum values of current change are 1.0 and 0.8 per cent respectively and hence the approximations involved do not exceed 0.5 per cent.



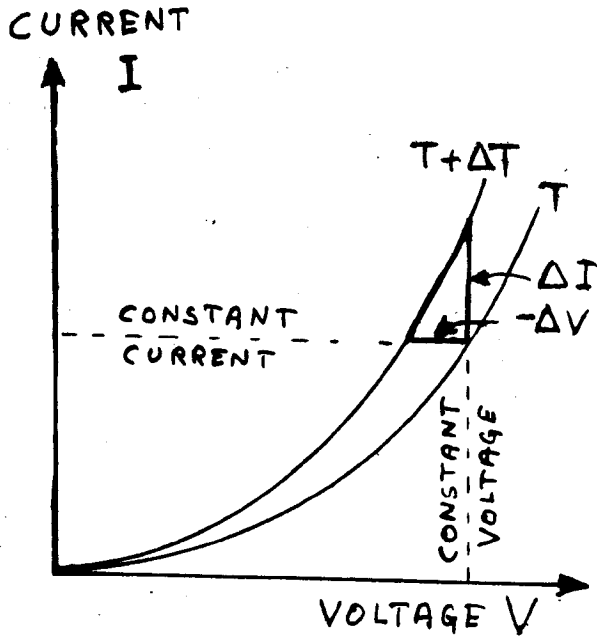


Fig.103

APPENDIX D:- Change of characteristics with temperature

In the case of temperature change discussed in Section 8(a) and (b) an increase in temperature  $\Delta T$  causes an increase in current  $\Delta I$  or a corresponding negative change  $-\Delta V$  in voltage (Fig 103). Thus the situation is not unlike that considered in Appendix C except that in the latter case the signs are the other way round. With the imposition of stress under constant current conditions the voltage change did not exceed 600  $\mu V$ , but in measuring the temperature coefficient the rise of about 20 K produced a voltage change of 30-40 mV. Hence at first sight it might seem that this comparatively large voltage might invalidate the approximation that  $\Delta I/\Delta V = dI/dV$ . In fact virtually no approximation is involved, as can be seen from the following analysis.

From Section 8 (a) the basic relation is

$$I \propto \exp\{(qV - E_G)/nkT\}$$

If the current  $I$  is kept constant and the temperature changed to  $T + \Delta T$  then this becomes

$$I \propto \exp\{[q(V + \Delta V) - (E_G + \Delta E_G)]/nk(T + \Delta T)\}$$

In equating I the exponential disappears and we obtain

$$\frac{\Delta V}{\Delta T} = \frac{V - E_G/q}{T} + \frac{1}{q} \frac{\Delta E_G}{\Delta T} \quad \text{eq (1)}$$

As quoted in Section 8 (a), p.90, the value of  $\Delta E_G/\Delta T$  for GaAs/P is a constant and presumably remains more or less fixed over the experimental temperature range. The interesting fact that emerges from eq (i) is that there is a straight-line relation between  $\Delta V$  and  $\Delta T$ . This proved to be an unexpected bonus in the research, not only because the constant current technique was so much easier to manage electrically, but also because a comparatively large temperature range of nearly 20 K could be used without fear of losing accuracy due to non-linearity. Thus a somewhat crude method of maintaining an environment at a constant temperature and measurement with a 50°C thermometer was feasible, and yet the resulting value of  $\Delta V/\Delta T$  was the same as the true temperature coefficient  $dV/dT$ .

There also arises the problem of connecting the voltage coefficient with the fractional current change  $dI/I dT$ . So long as stress is not imposed, the energy gap  $E_G$  can

only change with temperature; thus, in the basic relation above, namely  $I \propto \exp[qV - E_G]/nkT$ ,  $I$  is a function of  $V$  and  $T$  solely and can be written as  $I(V,T)$ . Hence the well-known partial differential relation can be quoted as:

$$dI = \frac{\partial I}{\partial V} dV + \frac{\partial I}{\partial T} dT$$

At constant current  $I$ ,  $dI = 0$  and then

$$\frac{\partial I}{\partial T} = - \left( \frac{dV}{dT} \right)_I \frac{\partial I}{\partial V}$$

But at constant voltage  $V$   $\frac{\partial I}{\partial T} = \left( \frac{dI}{dT} \right)_V$

and at constant temperature  $T$   $\frac{\partial I}{\partial V} = \left( \frac{dI}{dV} \right)_T$

Hence  $\left( \frac{dI}{dT} \right)_V = - \left( \frac{dV}{dT} \right)_I \left( \frac{dI}{dV} \right)_T$

The minus sign is to be expected because the slope  $dI/dV$  ( $= qI/nkT$ ) of the constant temperature characteristic is positive and so is the current temperature coefficient at constant voltage, namely  $\frac{dI}{dT}$ ; but the slope of  $dV/dT$  against  $I$  should be negative (and was so in the experimental measurements, as is shown in Fig 62, p.92). Thus the conversion relation

$$\frac{dI}{I dT} = \frac{q}{nkT} \frac{dV}{dT}$$

could be used without involving any approximation, the only theoretical error being an extremely small one due to a possible variation in  $dE_G/dT$  in the temperature range measured (about 6-8°C to 24°C).

Finally one must consider the general case of applying stress with a probe such that, in addition to the pressure effect, there can be a change of temperature which will also alter the current-voltage characteristics. The temperature change is small and the relevant current change is always less than 1 per cent, as is the corresponding percentage for pressure. Hence by the Superposition Principle the effects should be independent of one another and it is permissible to measure their combination by the voltage change  $\Delta V$  at constant current.

APPENDIX E:- Circuitry and galvanometer deflection

In Section 6 (a) it is emphasized that by taking the same stress readings both with the 'constant voltage' circuit of Fig 34 (p.47) and with the 'constant current' one of Fig 36 (p.49) a preliminary start on the electrical effects of stress was made, and it was verified that  $-\Delta I$  and  $\Delta V$  were related by the a.c. resistance  $R_{ac}$  of the diode. In both circuits the measurements were not strictly taken with a constant voltage across the LED or a constant current through it since the galvanometer deflection, measured either as a current  $I_G$  or a voltage  $V_G$ , inevitably disturbed the arrangement. In fact if  $R_G$  is the galvanometer resistance, then correcting factors had to be applied as follows:

$$\text{in Fig 34, } (-) \Delta I = I_G (1 + R_G/R_{ac})$$

$$\text{in Fig 36, } \Delta V = V_G (1 + R_{ac}/R_G)$$

Although these two factors appear at first sight to be different, they are in principle the same. The former circuit requires current sensitivity, and for low values of  $R_{ac}$  the galvanometer was shunted; in the ideal case

Facing  
p.163

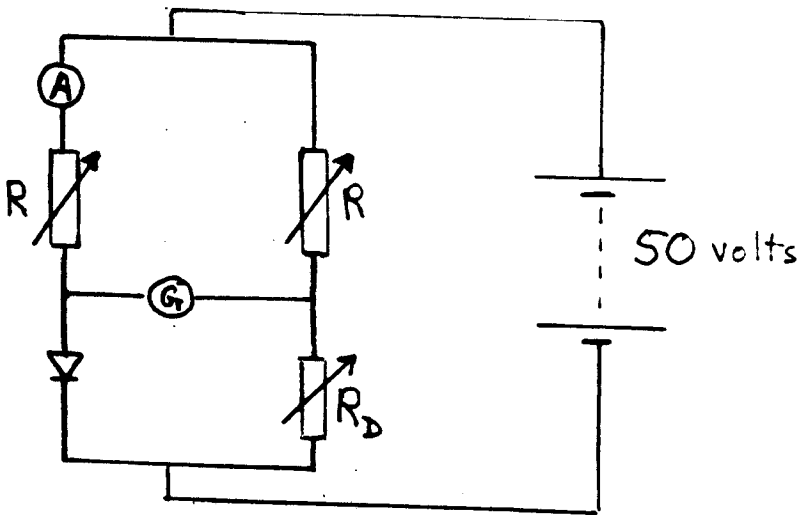


Fig.104

of  $R_G = 0$  then  $(-) \Delta I = I_G$ . In the latter circuit the galvanometer should be of high impedance and comparable at least with  $R_{ac}$ ; ideally  $R_G$  should be infinite and then  $\Delta V = V_G$ .

As regards the a.c. (and d.c.) resistance of the LED, the values are discussed in Section 4 (b), and it can be seen from Figs 22 and 23 (p.32) that  $R_{ac}$  varies more or less inversely as the current, ranging from approximately 3 ohms at 10 mA to 50 k ohms at 1  $\mu$ A. These values can be compared with the resistance of 1 k ohms for the "Galvamp" used for the early measurements; later on the experimental technique was much improved by the purchase of a "Levell" meter with a resistance of 100 k ohms for most of the ranges and 1 M ohms for its more sensitive scales.

It can be readily seen that the circuits of Figs 34 and 36 (pp.47,49) resemble a bridge, and subsequently it was decided to operate with a conventional Wheatstone bridge as shown in Fig 104. The fixed supply of 50 volts was a "Coutant" power pack which is specially designed to give an extremely constant voltage, and the ammeter



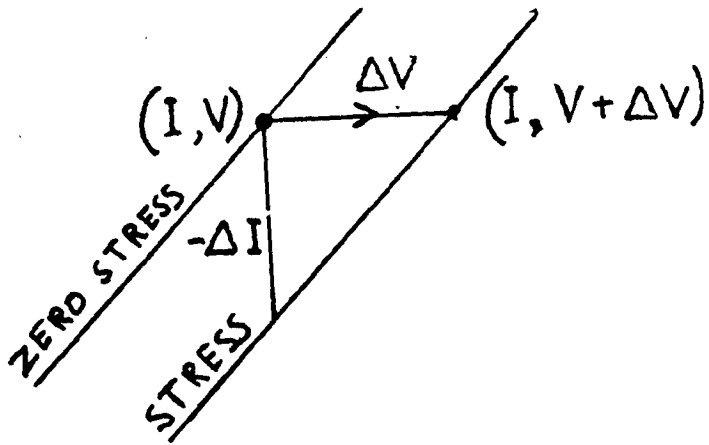


Fig.105 (a)

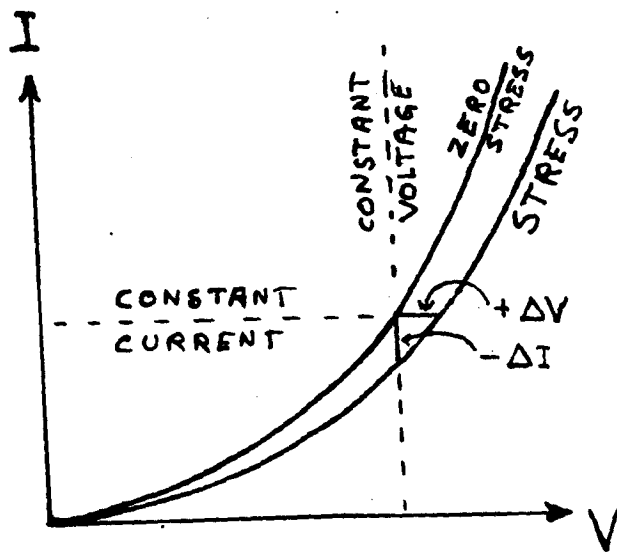


Fig.105 (b)

was an "AVO" or a "Griffin" 10/1.0  $\mu$ A electronic meter. Because the supply of 50 volts was very much greater than the diode voltage of about 1.5 V or less, the two large resistances  $R$  were correspondingly much greater than the d.c. resistance  $R_{dc}$  of the diode, thus ensuring virtually a constant current through the diode. By keeping the two branches of the bridge equal, the resistor  $R_D$  was adjusted to the value of  $R_{dc}$ , and the bridge balanced. On applying stress the galvanometer deflection  $V_G$  (or  $I_G$ ) was recorded but as previously a correcting factor due to galvanometer drain had to be applied; an analysis of this factor is as follows.

Fig 105 (a), which is an enlarged version of Fig 38 (p 50) or Fig 105 (b), shows the relevant electrical changes  $-\Delta I$  or  $\Delta V$  of the diode under stress. With a constant voltage the application of stress causes the resistance of the diode to increase, and this results in a decrease of current  $-\Delta I$ . In the alternative situation of a constant current  $I$  through the diode (see Fig 106) the increase in resistance causes the potential at the point A to rise

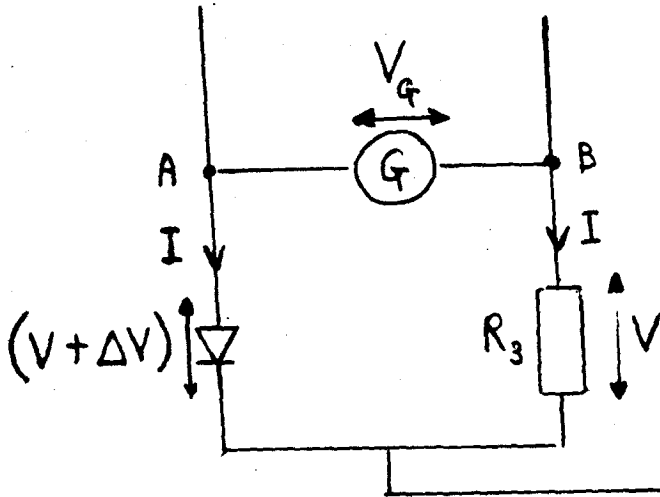


Fig.106. Galvo of infinite impedance

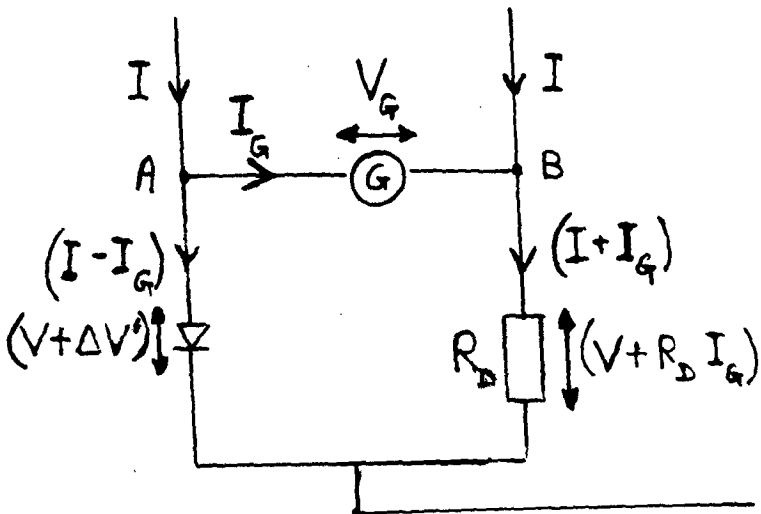


Fig.107. Galvo of finite impedance

with respect to the point B, and if the galvanometer had an infinite impedance this increase would be directly measured as  $V_G$ .

In practice the galvanometer takes a small current  $I_G$  (Fig 107) so that the current through the LED is slightly reduced to  $(I - I_G)$  and the potential rises by a smaller amount  $\Delta V'$ . However, because of the exponential  $I - V$  characteristic of the LED,  $V$  varies as  $\ln I$  and the very small change to  $\ln (I - I_G)$  will not appreciably alter the previously unstressed p.d. of  $V$  across the diode; the extra p.d. of  $\Delta V'$  comes about only by virtue of the changed electrical characteristic under stress. This is an important point because for the fixed resistor  $R_D$  the situation is different; this component has a linear characteristic and therefore the increase of current  $I_G$  will cause the potential at B to rise to  $(V + R_D I_G)$ . From the situation illustrated in Fig 107 we get

$$V + \Delta V' = V_G + V + R_D I_G$$

and therefore  $\Delta V' = V_G + R_D I_G$

The switch from the unstressed characteristic to the

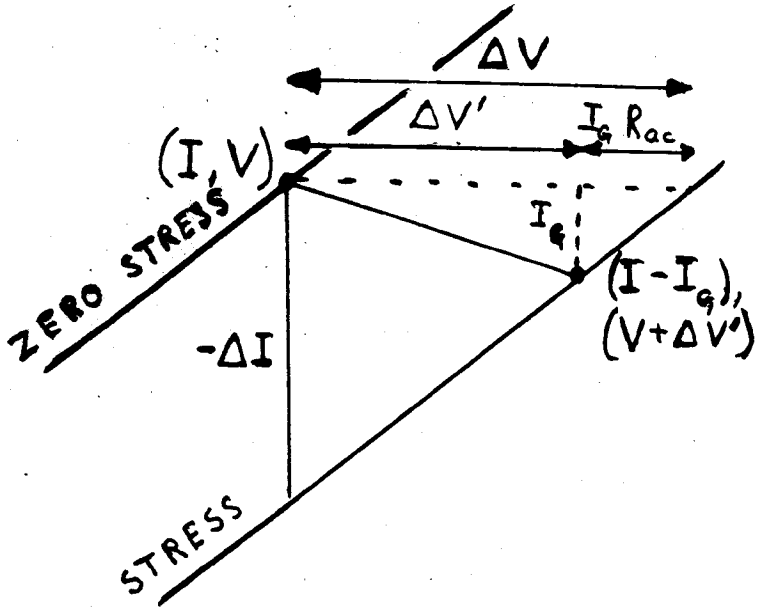


Fig.108

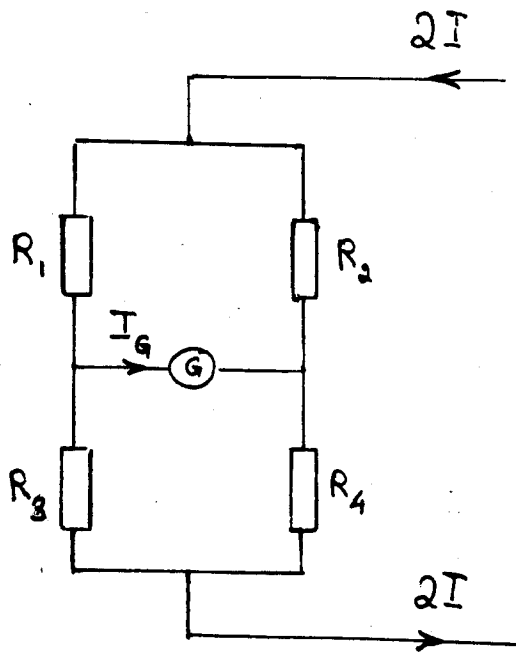


Fig.109

stressed one is shown in Fig 108. In this diagram the two characteristics are very close to one another and are presumed to be parallel, as discussed in Appendix C.

Since the slope is  $1/R_{ac}$ ,  $\Delta V' = \Delta V - I_G R_{ac}$

Equating  $\Delta V'$  gives  $\Delta V - I_G R_{ac} = V_G + I_G R_D$

and substitution of  $I_G = V_G/R_G$  results in

$$\Delta V = V_G \left( 1 + \frac{R_D + R_{ac}}{R_G} \right)$$

From  $\Delta V = |-\Delta I|/R_{ac}$  alternative relations are

$$|-\Delta I| = \frac{V_G}{R_{ac}} \left( 1 + \frac{R_D + R_{ac}}{R_G} \right)$$

$$|-\Delta I| = \frac{I_G}{R_{ac}} (R_G + R_D + R_{ac})$$

It is interesting to check this result by considering a Wheatstone bridge made up of four pure resistances as shown in Fig 109. Assuming the well-known relation

$$I_G = 2I \left[ \frac{R_2 R_3 - R_1 R_4}{R_G (R_1 + R_2 + R_3 + R_4) + (R_1 + R_2)(R_3 + R_4)} \right]$$

if the resistors are now adjusted to the situation of Fig 109 then  $R_1 = R_2 = R$ ,  $R_3 = R_D + \Delta R$  and  $R_4 = R_D$ , where  $\Delta R$  is the hypothetical increase of resistance in the

diode due to stress. Since  $\Delta R \ll R_D$  the two branches of the bridge are virtually the same and the current of  $2I$  splits equally down each branch; also because  $R_D \ll R$ , the currents remain constant. We then have

$$I_G = I \left[ \frac{R \Delta R}{R_G (R + R_D + \Delta R/2) + R(2R_D + \Delta R)} \right]$$

Because  $\Delta R \ll R_D$  and  $R_D \ll R$

approximation gives  $I_G = I \Delta R / (R_G + 2R_D)$

and therefore  $\Delta V = I_G (R_G + 2R_D)$  since  $\Delta V = I \Delta R$ .

For the diode this corresponds to

$$\Delta V = I_G (R_G + R_D + R_{ac})$$

because the exponential characteristic of the diode is such that its resistance manifests itself as  $R_{ac}$  when the balance changes by a small amount. Once again we can substitute  $\Delta V = |-\Delta I| / R_{ac}$  so that

$$|-\Delta I| = \frac{I_G}{R_{ac}} (R_G + R_D + R_{ac})$$

$$|-\Delta I| = \frac{V_G}{R_{ac}} \left( 1 + \frac{R_D + R_{ac}}{R_G} \right)$$

ie, the same as already derived from first principles.

These galvanometer correction factors are different

from those quoted on p.162 for the earlier circuits in that an extra term  $R_D$  now appears, and this comes about because in the Wheatstone bridge circuit the resistor  $R_D$  must be included to balance the d.c. resistance of the unstressed diode,  $R_D$  being equal to  $R_{dc}$ . In Section 4 (b) Figs 20-23 (pp.31-32) it can be seen that  $R_{dc}$  is roughly 50 to 25 times larger than  $R_{ac}$  and ranges from 160 ohms at 10 mA to 1.25 M ohms at 1  $\mu$ A. Thus the Wheatstone bridge circuit of Fig 104 (p.163) is inherently less sensitive than the one used earlier in the research, namely Fig 36 (p.49). This would be a disadvantage if the original galvanometer of impedance 1000 ohms were being used, but the reduction in sensitivity was no longer a problem when the "Levell" meter with an impedance of 1 M ohm on its most sensitive ranges was available. In general the relation

$$|-\Delta I| = \frac{V_G}{R_{ac}} \left( 1 + \frac{R_D + R_{ac}}{R_G} \right)$$

could be approximated to

$$|-\Delta I| = \frac{V_G}{R_{ac}} \left( 1 + \frac{R_D}{R_G} \right)$$



In addition, with the "Levell" meter on its maximum sensitivity the term  $R_D/R_G$  was normally a good deal less than unity for diode currents greater than  $30 \mu\text{A}$ , and in these circumstances it could also be neglected.

---

## REFERENCES

- (1) W. Fulop and S. Konidaris, SSE, 19, 313 (1976)
- (2) W. Ridner, J App Phys, 33, 2479 (1962)
- (3) W. Ridner and I. Braun, J App Phys, 34, 1958 (1963)
- (4) W. Bernard, W. Ridner and H. Roth, J App Phys, 35,  
1860 (1964)
- (5) Y. Matakura, Jap J App Phys, 3, 516 (1964)
- (6) T. Imai, Jap J App Phys, 4, 102 (1965)
- (7) W. Fulop and S. Konidaris, Phys Letters, 44A, 349  
(1973)
- (8) C.A. Hogarth, "Proc Int Conf Phys Semicond, Hetero-  
junction Layer Structures, I, Budapest, 1970". Hung  
Acad Sci, Budapest, I-V (1971)
- (9) S. Konidaris and W. Fulop, SSE, 17, 863 (1974)
- (10) Agate Products Ltd, 2/4 Quintin Avenue, Merton Park,  
London, SW 20 8LD
- (11) S. Share, J App Phys, 45, 77 (1974)
- (12) S. Konidaris, PhD Thesis, Brunel Univ (1973)
- (13) Private discussion with Dr W. Fulop (1984)
- (14) W.B. Morton and L.J. Close, Phil Mag 43, 320 (1922)

- (15) G. Berndt, Zeitschr Tech Physik, 3, 14 (1922)
- (16) C.Lipson and R.C.Juvinall, "Handbook of Stress and Strength" 45 and 51 (Collier-Macmillan, 1963)
- (17) H.F.Wolf, "Semiconductors", 129 (Wiley, 1971)
- (18) Manufacturer's quote; see ref 10
- (19) W.A.Brantley and D.A.Harrison, "Proc Eleventh Ann Reliability Phys Conf, Las Vegas, Nev, USA, 1973" (IEEE, 1973)
- (20) P.G.Eliseev and A.V.Khaidarov, Kvantovaya Elektron, Moskva, USSR, 2, No 1, 127 (1975). Translated in Sov J Quantum Electron (USA), 6 No 1, 73 (1975)
- (21) G.W.C.Kaye and T.H.Laby, "Tables Phys Chem Const" 13th Ed, 33 (Longman, 1966)
- (22) *ibid*, 34
- (23) Private communication to Dr W. Fulop (1979)
- (24) S. Fuchs, Physik Zeitschr, 14, 1282 (1913)
- (25) H. Hertz, "Gesammelte Werke" I (Leipzig, 1895)
- (26) A.E.A.Love, "A Treatise on the Mathematical Theory of Elasticity" 4th Ed, 198 (Cambridge, 1952)

- (27) F.H.Newman and V.H.L.Searle "The General Properties of Matter" 4th Ed, 143 (Arnold, 1948)
- (28) G.E.Fenner, J App Phys, 34, 2955 (1963)
- (29) W. Fulop, SSE, 14, 77 (1970)
- (30) S.M.Sze, "Physics of Semiconductor Devices" 2nd Ed, 92 (Wiley, 1981)
- (31) "CRC Handbook of Chemistry and Physics" 58th Ed, (1977) E-104 (CRC Press Inc, 2255 Palm Beach Lakes Bld, West Palm Beach, Florida 33409)
- (32) ibid, E-101
- (33) ibid, E-5 and E-17
- (34) Private communication to Dr W. Fulop (1981)
- (35) W.Paul, J App Phys, 34, 2955 (1961)
- (36) L.A.Kosyachenko, E.F.Kukhto and V.M.Sklyarchuk, Fiz Tek Poluprovodn (USSR), 17, No 11, 1935 (1983); Sov Phys Semicond.(USA), 17, No 11, 1237 (1983)
- (37) "CRC Handbook of Chemistry and Physics" 58th Ed, E-104 (1977)
- (38) W. Fulop and S. Konidaris, SSE, 15, 923 (1972)